REGULATION OF REPLICATION FORK REVERSAL BY RADX AND RAD51

By

Archana Krishnamoorthy

Dissertation
Submitted to the Faculty of the
Graduate School of Vanderbilt University
in partial fulfillment of the requirements
for the degree of

DOCTOR OF PHILOSOPHY
In
Biochemistry

January 31, 2021
Nashville, Tennessee

Approved

Dr. Walter Chazin

Dr. David Cortez

Dr. Jennifer Pietenpol

Dr. Ian Macara

Dr. Yi Ren

To Amma, Appa, and Aravind.

This work would've been impossible without your love, support, and endless sacrifice.

ACKNOWLEDGMENTS

I'm grateful to my advisor, Dr. David Cortez, for his support, motivation, and encouragement through the years. Your brilliance and passion for science has been a privilege to witness and I hope I continue to carry forward at least a fraction of your wisdom. Your uncanny ability to identify the right experimental design and your meticulous approach to science has helped shape my perspective on research. My project has not been straightforward and I appreciate your patience while I wrangled with my data. I'm particularly grateful for all of your scientific and non-scientific advice. Dave – I will fondly remember our arguments about data at lab meetings, your "optimism", and all the fun we had while writing my paper. Thank you for listening to my complaints/rants without taking offense and I'm glad that I can always count on you to have my back. Also, you should be really proud of your strong GIF/emoji game; maybe you aren't as old (school) as I thought.

I'm extremely grateful for the support from my thesis committee members: Drs. Chazin, Macara, Ren, and Pietenpol. My committee meetings were always an ego boost and helped me feel better about myself as a scientist. Dr. Chazin – thanks for all the advice and the team RADX meetings, always great to hear your structural insights. Dr. Macara – I have always admired your ability to ask the most prescient questions, thank you for all the encouragement. Dr. Pietenpol – I learned a lot during our joint lab meetings and I always look forward to hearing your translational perspective. Dr. Ren – thanks for all the support and advice. Thank you also to Drs. James Dewar and Jared Nordman for their advice and guidance during my postdoc search.

A significant amount of my time in Nashville was spent in the lab and I would like to thank the former and current Cortez lab members for making it fun to come in to work. All of them have helped improve this body of work immeasurably. Kavi – Thank you for the random walks, chocolate breaks, discussions on Indian food, and all the science shenanigans. Madison and Sarah – I have really enjoyed discussing science, gossip, and rants with you. Extra thanks to Kavi, Sarah, and Madison for supplementing my writing days with donuts and chocolates. Courtney – Thank you for teaching me all things telomere biology. I admire your intellect and I'm sorry if I fueled your hatred for fork reversal with my lab meetings. Wenpeng – Thank you for the rides to the airport and all the science discussions. Jorge – I wish I could be half as cheery as you, thank you for the jigsaw puzzle sessions and cakes. Taha – Thank you for your help with the RADX

project, I have benefited from your extensive knowledge of literature. To all the new members of the lab – Samika, Matthew, and Atharv, I cannot wait to hear about your accomplishments in the future. Thanks also to Huzefa and Vaughn for the lab meeting rants, escape rooms, and science. Finally, I would be remiss if I ended this section without thanking the CRISPR and western ninja, Nancy, for her technical support and encouragement.

Thanks to Dr. Alessandro Vindigni for collaborating on my project and for hosting me in his lab for a week while I learned Electron Microscopy (EM). I'm grateful to Jessica Jackson for helping me with EM. To his other lab members – Annabel, Stephanie, Emily, and Alice, I look forward to reading your work in the future.

I would like to extend my gratitude to Dr. Brian Robertson, my Master's advisor, for his continued friendship and mentorship. Thank you, Brian, for simply being a phone call away and for being my unofficial guardian. I could not have survived my first few years in the US without you. To all my friends and professors in the Biology department at MTSU, especially Paola, Anna, and Dr. Sadler, thank you for your taking pity on me and teaching me the ropes of research and leadership.

Growing up in a household with very modest means, education was my liberation. Thank you, Amma and Appa, for instilling in me the importance of persistence and for encouraging me to pursue my goals without letting culture/society dictate your choices. Every time I was rejected from grad school (4x!) and for all the "failures" and setbacks I've had while in grad school, your motivation and kind words helped me overcome those challenges. Appa, I'm sorry I didn't win any competitive fellowships or awards – things just didn't work out. Amma, our morning phone calls were something that I looked forward to everyday. Thank you both, for having more faith in me than I have had in myself. Your sacrifices made it possible for me to be here and I consider myself very fortunate to be your daughter. Lastly, Amma and Appa, I'm so proud of how you have handled the pandemic and isolation. I miss you both so much and I hope we get to see each other soon.

To my brother, Aravind, thank you for always being there for me through everything. Your infinite wisdom on all things grad school and life always kept me grounded and has never failed to brighten a bad day. Thank you for teaching me to define my own success. For being the voice of reason during grad school slumps, endless memes, food pics, edits, long phone calls, vacations, and arguments – I'm truly grateful and I could not have asked for a better brother. Thank you for

being my role model, I will never cease to be amazed by you. I look forward to more Disneyworld trips, planetarium visits, designing your lab logo, and dancing at your wedding.

When I grow up (heh), I hope to be fortunate enough to pay my training and education forward. I know how it feels to be an 18-year-old waiting endlessly outside labs for an opportunity to do science. To those girls whose life circumstances prevent them from realizing their educational dreams, I hope I can afford to provide you an opportunity one day.

Finally, to all those family members and friends I have lost along the way, I wish you had more time. To my grandpa, Rahul, Pavani, Raju chithappa, Chinna athimber, Periya athimber, and Megha – I hope you are in a better place.

TABLE OF CONTENTS

LIST OF TABLES

LIST OF FIGURES

LIST OF ABBREVIATIONS

3HB	3 Helix Bundle
53BP1	p53 Binding Protein 1
ABRO1	Abraxas Brother Protein 1
ADP	Adenosine Di Phosphate
ALT	Alternative Lengthening of Telomeres
AND-1	Acidic Nucleoplasmic DNA binding protein
APIM	AlkB homolog 2 PCNA-interaction motif
ATM	Ataxia Telangiectasia Mutated
ATP	Adenosine Tri Phosphate
ATR	ATM and Rad3 related
BIR	Break induced Replication
BLM	Bloom Syndrome Protein
BOD1L	Biorientation of chromosomes in cell division protein 1-like 1
BRCA1	Breast Cancer 1
BRCA2	Breast Cancer 2
BrdU	5-Bromo 2'-deoxyuridine
CldU	5-Chloro 2'-deoxyuridine
CMG	Cdc45-MCM2-7-GINS
CPT	Camptothecin
CRISPR	Clustered Regularly Interspaced Short Palindromic Repeats
CtIP	CtBP-interacting protein
DBD	DNA Binding Domain
DSB	Double strand break

dsDNA	Double-strand DNA
EdU	5-ethynyl-2’-deoxyuridine
EM	Electron microscopy
FANC/FA	Fanconi Anemia Complementation group/Fanconi Anemia
FBH1	F-box DNA Helicase 1
FIGNL1	Fidgetin like 1
GFP	Green Fluorescent Protein
gH2AX	Phosphoserine 139 H2AX
HARP	HepA related protein
HhH	Helix hairpin Helix
HIRAN	HIP116, Rad5p, N-terminal
HLTF	Helicase like Transcription Factor
HR	Homologous recombination
HRP	Horse Radish Peroxidase
HU	Hydroxyurea
IdU	5-Iodo-2’-deoxyuridine
IP-MS	Immunoprecipitation-Mass spectrometry
iPOND	Isolation of Proteins on Nascent DNA
MCM	Mini Chromosome Maintenance
OB	Oligonucleotide/Oligosaccharide binding protein
OH	Hydroxyl
PALB2	Partner and Localizer of BRCA2
PARI	PARP-1 Binding Protein
PARP	Poly (ADP-Ribose) Polymerase
PARPi	PARP inhibitor

PCNA	Proliferating Cell Nuclear Antigen
PCR	Polymerase Chain Reaction
PEI	Polyethyleneimine
PIP	PCNA Interacting Protein
PLA	Proximity Ligation Assay
POLK	Polymerase Kappa
POT1	Protection of Telomeres Protein 1
PRIMPOL	Primase and DNA directed Polymerase
RADX	RPA-like RAD51 antagonist on the X chromosome
RBD	RPA binding domain
RECQ1	RecQ-like 1
RIF1	Replication Timing Regulatory Factor 1
RING	Really Interesting New Gene
RPA	Replication Protein A
RSR	Replication stress response
SCE	Sister Chromatid Exchange
SETD1A	SET Domain Containing 1A
SIOD	SChimke Immuno-Osseous Dysplasia
SMARCAL1	SWI/SNF related, matrix associated regulator of chromatin subfamily A-like 1
SPR	Surface Plasmon REsonance
SRD	Substrate Recognition Domain
ssDNA	Single-strand DNA
SWI/SNF2	Switch/Sucrose Non Fermentable
TLS	Translesion synthesis
TS	Template Switching

Ub	Ubiquitin
UV	Ultra violet
WB	Western blot
WRN	Werner syndrome ATP-dependent helicase
WRNIP	WRN Interacting Protein
WT	Wild Type
XRCC3	X-ray Repair Cross Complementing Protein 3
ZRANB3	Zinc-Finger RANBP2-type containing 3

CHAPTER I

INTRODUCTION

DNA replication is a fundamental process for proliferation and cell survival in most dividing cells. In humans, over 6 billion base pairs of DNA must be copied completely and accurately during each cell division cycle. The fidelity of DNA replication is constantly challenged by stress from endogenous and exogenous sources, including unusual secondary structures, environmental genotoxins, collisions with transcription, and limiting nucleotide pools (Zeman and Cimprich, 2014). Thus, DNA repair is often coordinated with replication to ensure faithful and timely duplication of the genome. Copying errors and defects in DNA repair underlie diseases like cancer and neurodevelopmental disorders.

To combat the constant batter of genomic insults, organisms have evolved complex, overlapping pathways of protein networks to recognize, repair, and resolve the damage. One such mechanism is the replication stress response (RSR) which includes activation of the apical kinase, Ataxia-Telangiectasia and Rad3 related (ATR). ATR regulates cell cycle progression, origin firing, replication fork stability, and fork restart by phosphorylating numerous substrates (Saldivar et al., 2017). In addition to global RSR proteins, the replisome is equipped with specialized proteins that promote bypass, tolerance, or repair of various types of replication blocks.

This chapter discusses the replication associated repair mechanisms with a specific focus on fork reversal, the functions of single strand DNA (ssDNA) binding proteins in replication and repair, and the clinical relevance of fork reversal for tumorigenesis and chemotherapy.

DNA replication and Replication stress response

Replication fork structure

In some mammalian cells, DNA replication initiates at defined sites called origins. Once initiated, the replication machinery synthesizes DNA from bidirectional replication forks (Figure 1.1A). The

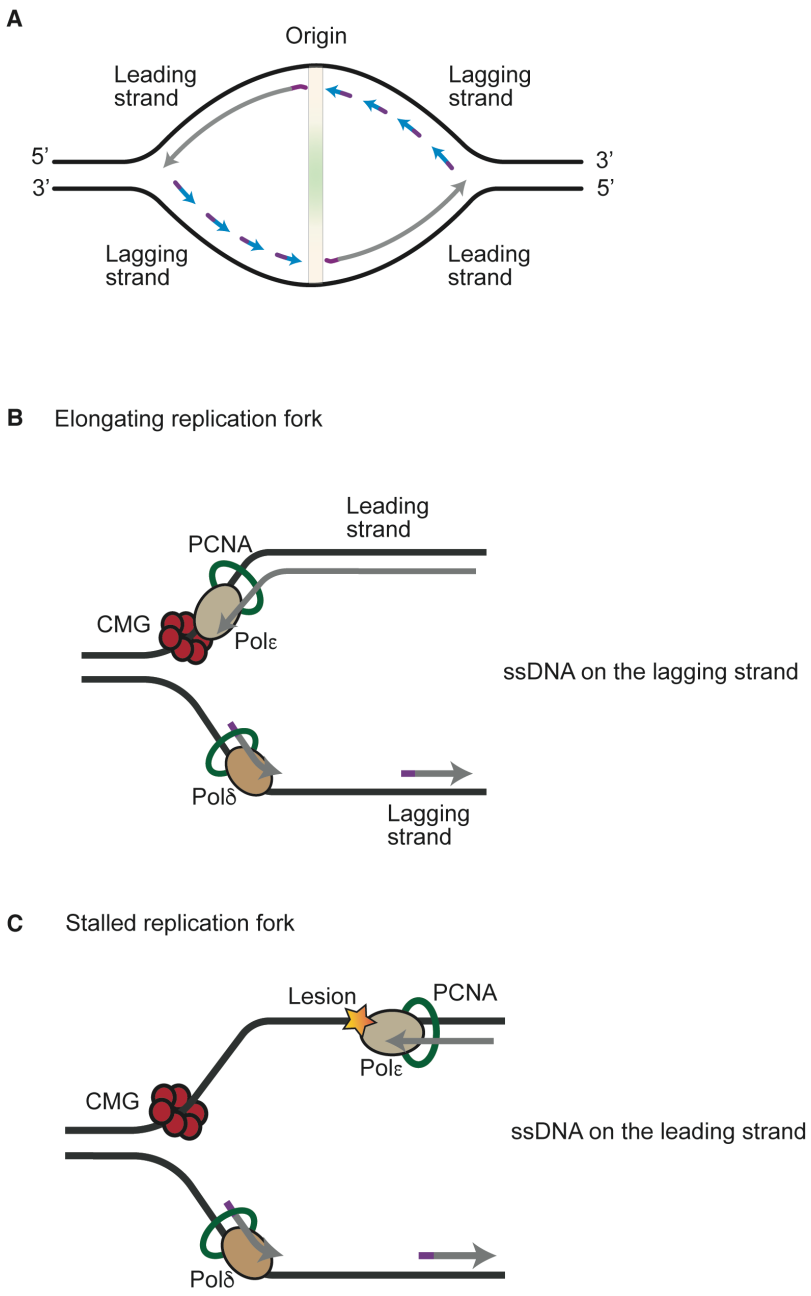

Figure 1.1. Simplified structure of a replication fork. (A) Schematic of replication origin. Each origin fires bidirectionally giving rise to two replication forks. (B and C) At elongating replication forks, small amounts of ssDNA are exposed at the lagging strand. However, upon stalling, functional uncoupling of helicase from the polymerase exposes large stretches of ssDNA on the leading strand. See text for details.

Cdc45-MCM2-7-GINS (CMG) helicase unwinds double strand DNA (dsDNA) duplex while the polymerases and Proliferating Cell Nuclear Antigen (PCNA) coordinate to synthesize the nascent daughter strands (Burgers and Kunkel, 2017). There is inherent asymmetry in the direction of synthesis due to the antiparallel nature of dsDNA template. The 'leading' strand is synthesized continuously by Polε while the 'lagging' strand is replicated discontinuously in the form of Okazaki fragments by Polδ. Additionally, Polα-primase initiates synthesis on both leading and lagging strands. During active replication, lagging strand synthesis lags behind the leading strand exposing stretches of ssDNA for short times (Figure 1.1B). Single molecule studies using purified proteins from *E.coli* also suggest that stochastic changes in DNA polymerase rates generate ssDNA at actively elongating replisomes (Graham et al., 2017). Whether the same mechanism occurs in eukaryotic cells is unknown.

Replication fork stalling and repair pathways

In most cases, replication stress only transiently pauses the replisome. Lesions on the lagging strand are more efficiently bypassed since a new Okazaki fragment can be synthesized downstream. However, leading strand lesions can be more persistent since repriming does not occur as frequently on the leading strand (Taylor and Yeeles, 2018). Instead, replication blocks on the leading strand 'stall' the replisome and functionally uncouple the CMG helicase from the polymerase (Figure 1.1C). This uncoupling leads to exposed ssDNA which is rapidly coated by the highly abundant ssDNA binding protein, Replication Protein A (RPA). RPA coated ssDNA promotes ATR-dependent signaling and serves as a platform to recruit several other repair proteins. This replication checkpoint stabilizes stalled forks and promotes their restart.

The nature of the lesion and genetic locus of the replication barrier can, in part, decide the pathway choice for repair. A few repair mechanisms are briefly described: i) Mutagenic repair is carried out by the error prone Translesion polymerases (TLS). At least five TLS polymerases have been implicated in bypass of lesions at a stalled fork in eukaryotes (Prakash et al., 2005; Waters et al., 2009). Alternatively, a specialized polymerase, PRIMPOL, can reinitiate synthesis downstream of a lesion on the leading strand leaving behind gaps that can be repaired by post-replicative gap filling mechanisms (Garcia-Gomez et al., 2013; Mouron et al., 2013). ii) Recombination-mediated repair pathways like Template Switching (TS) copy information from an

undamaged sister chromatid to use as template for synthesis. Usually regulated by PCNA polyubiquitylation, TS can be error-free. However, during Break Induced Replication (BIR), repair can be highly mutagenic and result in genomic rearrangements (Sakofsky and Malkova, 2017) (Figure 1.2). iii) Another mechanism for resolving fork stalling lesions is the remodeling of three-way replication forks into four-way junctions. This process, called fork reversal, occurs by regression of the replication fork causing reannealing and extrusion of the nascent strands resembling a 'chicken foot' structure (Figure 1.3).

Replication fork remodeling

Introduction to fork remodeling

Fork reversal was initially hypothesized to be a replication-coupled repair mechanism in mammalian cells and directly observed in bacteria but no evidence existed for a physiological role in eukaryotes (Atkinson and McGlynn, 2009; Higgins et al., 1976) Using electron microscopy (EM), reversed forks were observed in checkpoint-deficient *S.cerevisiae*, but were considered a pathological consequence of fork destabilization (Neelsen and Lopes, 2015; Sogo et al., 2002). More recent studies indicate that fork reversal may be frequent in vertebrates. In fact, EM analyses of replication forks purified from human cells revealed that ~30% of the detected forks are reversed in cells treated with sub-lethal doses of various genotoxic agents including cancer drugs that induce nucleotide depletion, oxidative base damage, UV photoproducts, or DNA crosslinks (Zellweger et al., 2015). Additionally, fork reversal has also been observed by 2-dimensional gels, studied biochemically using both protein extracts and purified proteins, visualized by imaging techniques, and characterized genetically in viruses, prokaryotic and eukaryotic cells (Kolinjivadi et al., 2017a; Kreuzer, 2013; Manosas et al., 2012; Neelsen and Lopes, 2015; Xia et al., 2019). Finally, identification and biochemical characterization of SWI/SNF2 family DNA translocases like SWI/SNF related, matrix associated regulator of chromatin subfamily A-like 1 (SMARCAL1), Zinc-Finger RANBP2-type containing 3 (ZRANB3),

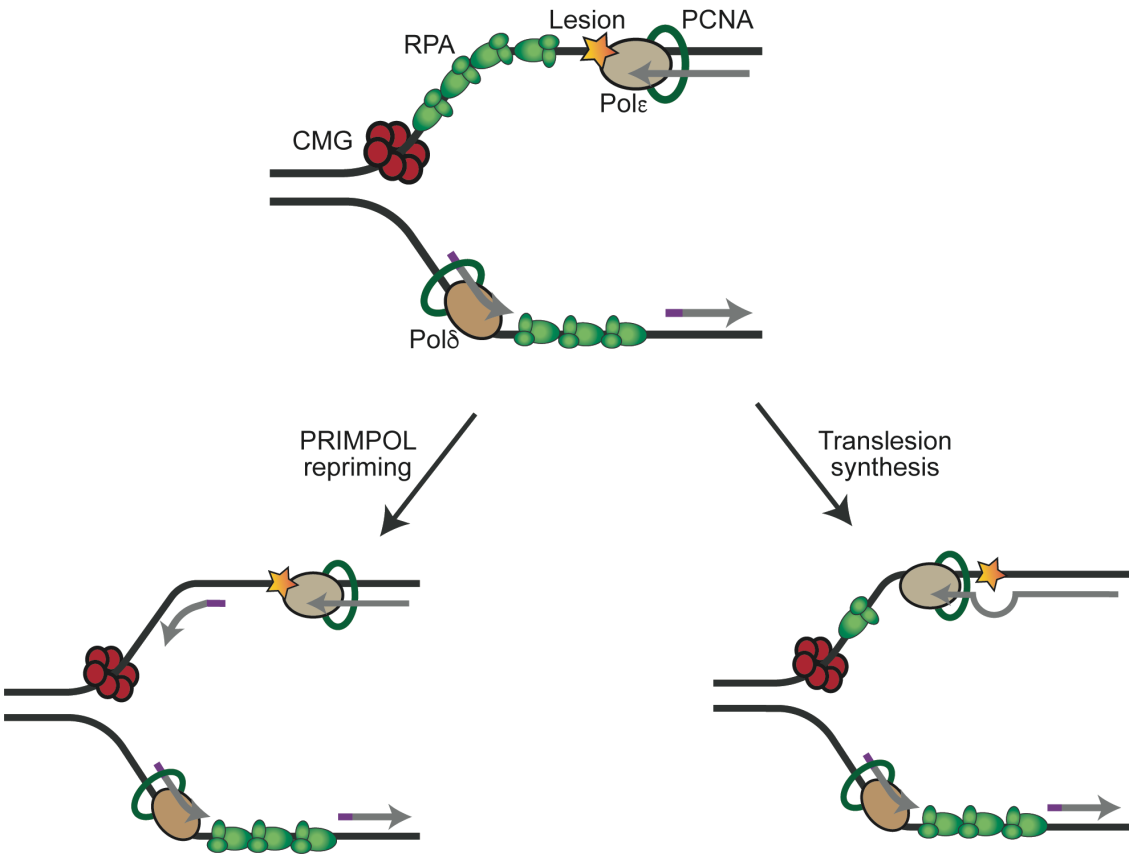

Figure 1.2. Overview of pathways to repair or bypass lesions at a stalled fork. Uncoupled, stalled forks can be restarted by Primpol-dependent repriming downstream of the lesion followed by post-replicative gap filling. Alternatively, low fidelity translesion polymerases are engaged to promote error-prone synthesis across the lesion.

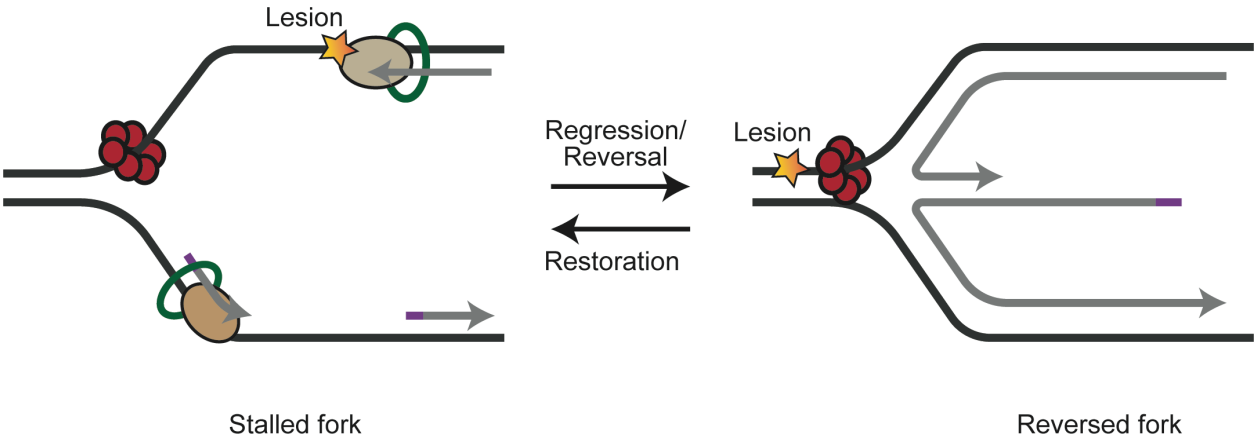

Figure 1.3. Fork reversal is a mechanism of damage tolerance. Fork reversal reanneals and extrudes the nascent DNA to convert a three-way junction to a four-way junction. It also places the lesion in the context of dsDNA, allowing repair processes to function. Conversion of four-way junction back into a three-way junction is known as fork restoration.

and Helicase like Transcription Factor (HLTF) as fork remodeling enzymes has led fork reversal to be accepted as a frequent, global stress response pathway for maintaining genome stability (Bansbach et al., 2009; Betous et al., 2012; Ciccia et al., 2012; Couch et al., 2013; Kile et al., 2015).

Fork reversal could be beneficial for several reasons: First, fork reversal may be a way to place the DNA lesion in the context of dsDNA to enable excision repair mechanisms to operate. Second, fork reversal could stably pause the stalled fork until a converging fork from a different origin completes replication. Third, TS mechanisms may use the regressed nascent DNA as the template to bypass the lesion. Finally, fork reversal could be an intermediate in a recombination pathway of fork restart (Cortez, 2019; Quinet et al., 2017).

While fork reversal stabilizes the stalled fork and promotes repair of the lesion, aberrant accumulation of these four-way junction structures can have deleterious consequences. For example, reversed forks have been implicated as the cause of double strand breaks (DSBs) associated with transcription-replication conflicts and UV-induced DNA damage (Courcelle et al., 2003; McGlynn and Lloyd, 2000). Additionally, in mammalian cells, dysregulation of the fork remodeler, SMARCAL1, either by overexpression or by ATR inhibition causes increased genome instability and breaks (Bansbach et al., 2009; Ciccia et al., 2012; Couch et al., 2013). The deleterious effects at a reversed fork can be traced to a few possibilities. First, the regressed arm of the reversed fork structure resembles a one-ended DSB that can be processed by a variety of nucleases such as MRE11, DNA2, or EXO1 (Lemacon et al., 2017; Schlacher et al., 2011). Second, accumulation of reversed forks can be recognized by structure specific endonucleases including MUS81 and the nuclease scaffold SLX4 to convert the fork to a DSB (Rondinelli et al., 2017). While regulated resection or cleavage by nucleases allows for repair by recombination, excessive nuclease activity at stalled forks can be detrimental to genome stability thus highlighting the need to tightly regulate fork reversal.

Excessive nucleolytic resection of reversed forks is termed ‘nascent strand degradation’ or ‘fork degradation’ and is considered a source of chromosomal abnormalities (Higgs et al., 2015; Schlacher et al., 2011). Moreover, fork degradation has emerged as a major determinant of chemotherapeutic sensitivity and cell survival (Ray Chaudhuri et al., 2016). To prevent fork degradation, several Homologous Recombination (HR) proteins like BRCA2 and RAD51 are

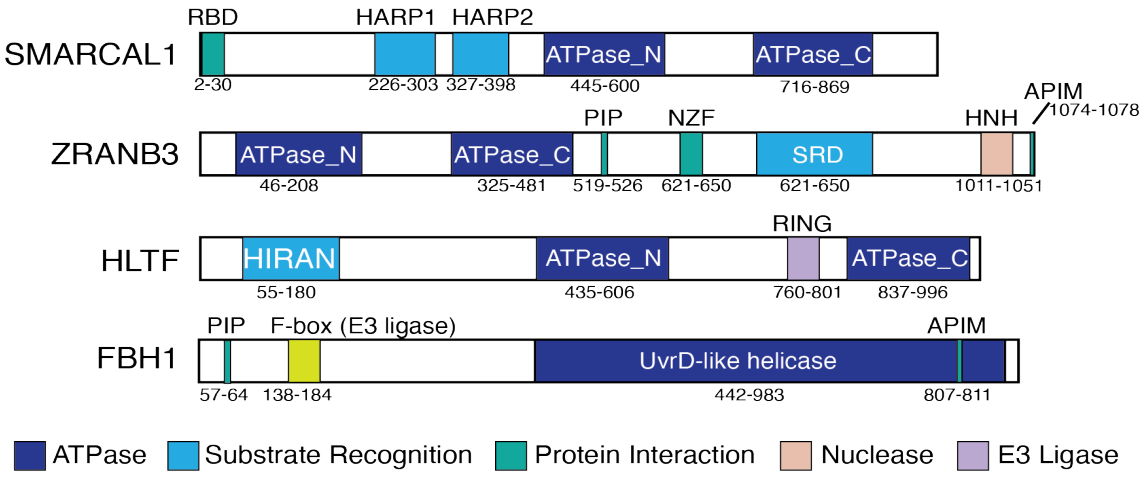

Figure 1.4. Domain structure of fork reversal enzymes. See text for details. RBD- RPA binding domain, HARP- HepA-related protein, HIRAN- HIP116, Rad5p, N-terminal. Figure adapted from Drs. Lisa Poole and David Cortez

implicated in the stabilization of the stalled fork in a process called ‘fork protection’ (described in detail below).

Fork remodelers

At least three ATP-dependent motor proteins and one helicase can catalyze fork remodeling *in vitro:* SMARCAL1, ZRANB3, HLTF, and F-Box containing Helicase1 (FBH1). In cells, silencing any one of the fork reversal enzymes reduces the number of reversed forks observed by EM (Betous et al., 2012; Blastyak et al., 2010; Ciccia et al., 2012; Fugger et al., 2015a; Kile et al., 2015; Kolinjivadi et al., 2017b; Vujanovic et al., 2017). This suggests that these motor proteins may work similarly. Multiple lines of evidence (as discussed below) indicate that a linear pathway for fork reversal may not be adequate to explain their functions *in vivo*. In any case, these translocases all regulate the stability of stalled replication forks through several mechanisms including fork remodeling.

SMARCAL1

SMARCAL1 contains two HARP domains that binds to fork junctions and shares similarity with the T4 bacteriophage UvsW fork reversal protein (Mason et al., 2014). Additionally, an ATPase domain helps translocate on the DNA backbone to remodel the fork substrate (Figure 1.4). Both DNA binding and ATPase activity of SMARCAL1 is required for ssDNA annealing activity on plasmid substrates (Yusufzai and Kadonaga, 2008). *In vitro*, RPA directly binds with and dictates SMARCAL1 substrate specificity to reverse forks with a leading strand gap similar to gp32 for UvsW in bacteriophage and SSB for RecG in *E.coli* (Betous et al., 2013a; Buss et al., 2008; Manosas et al., 2013; Mason et al., 2014). Importantly, this regulation by ssDNA binding proteins is not shared by other translocases.

In response to replication stress, SMARCAL1 co-localizes to replication forks with RPA and other markers of stressed forks (Bansbach et al., 2009; Yuan et al., 2009). Overexpression or depletion of SMARCAL1 in cells results in activation of the ATR-mediated stress response specifically in cycling cells. In addition, loss of SMARCAL1 sensitizes cells to replication stress and causes fork collapse (Bansbach et al., 2009). Inherited bi-allelic loss of *SMARCAL1* manifests as Schimke Immuno-Osseous Dysplasia (SIOD) in humans with diverse phenotypes including renal dysfunction, immune deficiencies, microcephaly, growth defects, and predisposition to cancer

(Boerkoel et al., 2002). Finally, unlike other translocases, SMARCAL1 has also been implicated in regulating telomere replication and Alternative lengthening of Telomeres (ALT) activity at telomeres (Cox et al., 2016; Poole et al., 2015).

ZRANB3

The domain structure of ZRANB3 is similar to SMARCAL1; it has an ATPase domain and a putative DNA interaction domain called the Substrate Recognition Domain (SRD). In addition, ZRANB3 has two PCNA interaction motifs [PCNA Interacting Protein (PIP) box and AlkB homolog 2 PCNA-interaction motif (APIM)] and an HNH endonuclease domain at the C-terminus (Figure 1.4). Like SMARCAL1, ZRANB3 is capable of annealing RPA-coated ssDNA in plasmid based assays (Yusufzai and Kadonaga, 2010). *In vitro*, ZRANB3 shows moderate preference to remodel forks with a lagging strand stall. Addition of RPA does not change the regression activity of ZRANB3 on the lagging strand gap, but inhibits ZRANB3 on the leading strand (Betous et al., 2013a). This highlights the differences in substrate preference between translocases (discussed below).

In cells, ZRANB3 is recruited to replication forks through a direct interaction with polyubiquitylated PCNA in response to replication stress (Ciccia et al., 2012). ZRANB3-deficient cells display higher rates of replication fork stalling, fork restart defects and increases in sister chromatid exchanges (SCEs), a marker of hyper-recombination (Ciccia et al., 2012). ZRANB3 deficiency also causes hyper-sensitivity to diverse DNA damaging agents (Ciccia et al., 2012; Weston et al., 2012; Yuan et al., 2012). Despite these striking phenotypes, ZRANB3 deficiency has not been directly associated with any human diseases; however, reports of *ZRANB3* mutations in endometrial cancers suggest it may function as a tumor suppressor (Lawrence et al., 2014). Finally, the endonuclease domain of ZRANB3 generates a nick two nucleotides into the DNA duplex on the leading strand template (Weston et al., 2012). However, the nuclease domain has not been well studied and has not been shown to have any physiological function at replication forks.

HLTF

HLTF is a replication fork remodeler with an ATPase domain similar to other translocases. In addition, HLTF consists of a HIRAN domain which recognizes DNA substrates and a RING domain that can ubiquitylate substrates (Figure 1.4).

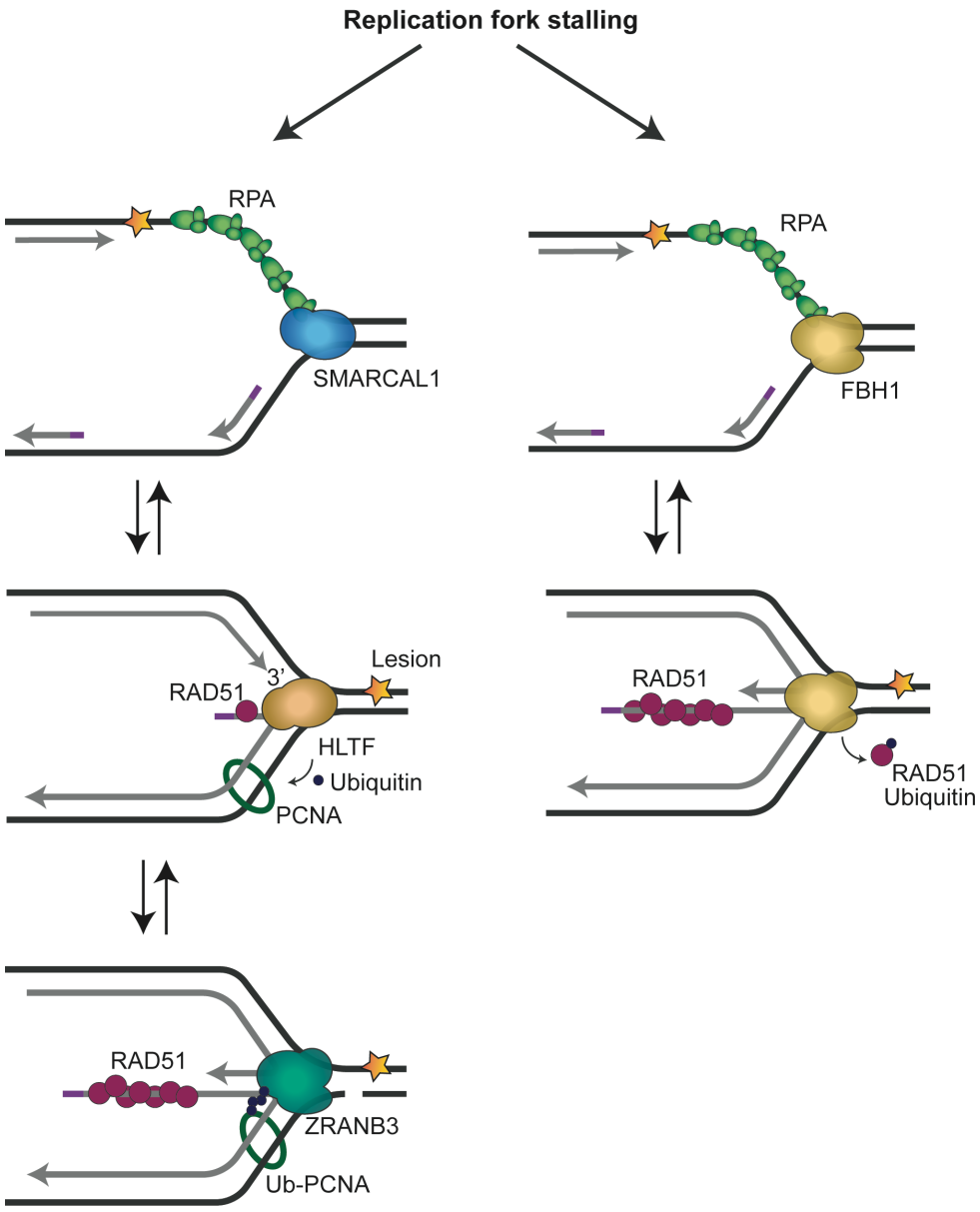

Figure 1.5. Model for replication fork remodeling pathways. See text for details. SMARCAL1, HLTF, and ZRANB3 utilize different substrate specificities to drive reversal presumably by "handing off" a substrate to the next enzyme. However, FBH1 uses its helicase activity to promote reversal. Both pathways depend on RAD51. Inactivation of the fork reversal enzymes routes the stalled fork intermediates into different recovery pathways.

In vitro, HLTF's HIRAN domain specifically recognizes and captures a 3'OH end of ssDNA to remodel fork substrates (Chavez et al., 2018; Kile et al., 2015). While HLTF does not show a preference for leading or lagging strand gapped substrates, it is modestly inhibited by RPA bound to gap on the lagging strand (Chavez et al., 2018). Moreover, HLTF is able to polyubiquitylate PCNA through its RING domain similar to Rad5 in yeast (Lin et al., 2011; Masuda et al., 2012; Unk et al., 2010).

Strikingly, HLTF-deficient cells fail to slow DNA replication fork progression and employ alternative modes of DNA synthesis, like PRIMPOL-mediated repriming, under conditions of replication stress induced by nucleotide depletion (Bai et al., 2020). These observations suggest that HLTF promotes fork reversal while disfavoring potentially mutagenic pathways like TLS and repriming. Additionally, loss of HLTF improves cancer cell viability when challenged with chemotherapeutic agents. Indeed, *HLTF* is frequently epigenetically silenced in colorectal cancers (Dhont et al., 2016; Moinova et al., 2002). More studies are needed to identify the mechanisms by which alternative replication stress tolerance and repair pathways are employed upon HLTF loss.

FBH1

FBH1, like HLTF, is a dual fork reversal motor protein and an E3 ubiquitin ligase. It belongs to an evolutionarily conserved family of UvrD helicases (Kim et al., 2002). FBH1 has a helicase domain at the C-terminus, two putative PCNA interaction domains, and an F-box domain that is part of an SCF^{FBH1} complex (Chu et al., 2015; Kim et al., 2002)(Figure 1.4). It is unknown if FBH1 has a leading or lagging strand substrate preference, however, FBH1 directly binds to ssDNA (Fugger et al., 2009). Additionally, RPA is known to stimulate the helicase activity of yeast FBH1 (Park et al., 1997). *In vitro*, RAD51 is ubiquitylated by the F-box domain of FBH1 to regulate HR in yeast (Chu et al., 2015; Lorenz et al., 2009). It is unclear if FBH1 primarily functions as a HR regulator in mammalian cells.

In response to replication stress, FBH1 co-localizes with RPA and other replication stress response proteins (Fugger et al., 2009). Like SMARCAL1 and ZRANB3, loss of FBH1 causes replication fork stalling, increased sensitivity to replication stress, increased SCEs, and reduced checkpoint signaling (Fugger et al., 2009; Fugger et al., 2015a; Simandlova et al., 2013). Recent studies indicate that the helicase activity of FBH1 is critical for fork remodeling, restart, and

signaling (Fugger et al., 2015a; Liu et al., 2020). Mutations in *FBH1* are frequently observed in melanoma cells, which strikingly exhibit increased survival in response to replication stress (Jeong et al., 2013).

Cooperativity or competition between remodelers?

As discussed above, SMARCAL1, ZRANB3, HLTF, and FBH1 all remodel fork substrates *in vitro.* Additionally, inactivation of any one of the enzymes reduces the number of reversed forks observed by EM. These observations predict that these enzymes operate in a linear pathway. However, their differences in substrate specificity and different phenotypic outcomes upon their inactivation suggest that a simple linear pathway may not explain all of their functions. For example, i) SMARCAL1, but not ZRANB3, HLTF or FBH1, is implicated in preventing ALT-like phenotypes (Cox et al., 2016). ii) HLTF-deficient cells exhibit resistance to replication stress, but loss of SMARCAL1, ZRANB3, or FBH1 causes increased sensitivity (Bai et al., 2020; Bansbach et al., 2009; Ciccia et al., 2012; Simandlova et al., 2013). iii) While SMARCAL1 is regulated by RPA *in vitro*, ZRANB3 or HLTF are largely insensitive to RPA for fork remodeling (Betous et al., 2013a; Chavez et al., 2018). iv) Perhaps, most strikingly, cells depleted of both ZRANB3 and SMARCAL1 display additive sensitivity to CPT (camptothecin) (Ciccia et al., 2012). However, these experiments were performed by RNAi depletion, so the phenotype could be due to a combination of hypomorphic conditions. v) FBH1 remodeling yields nuclease substrates that are protected by fork protection factors distinct from SMARCAL1, ZRANB3, and HLTF implying that there may be more than one fork reversal pathway (Liu et al., 2020).

Much work is needed to arrive at a unifying model for replication fork reversal, however, based on published and preliminary data, a working model can be hypothesized. It is likely that there are two pathways for reversal that depend on SMARCAL1/ZRANB3/HLTF or FBH1 enzymes. Different substrate specificities and regulatory mechanisms presumably govern which pathway and which enzyme in the pathway acts at any individual stalled fork. Within the SMARCAL1, ZRANB3, HLTF pathway, the enzymes may work sequentially with one enzyme “handing off” a substrate to the next. Initially, RPA may recruit SMARCAL1 to remodel the fork which may then be captured by HLTF to reverse the substrate and polyubiquitylate PCNA. This modification could then recruit ZRANB3 to ‘complete’ the reversal. This resembles a metabolic pathway in which

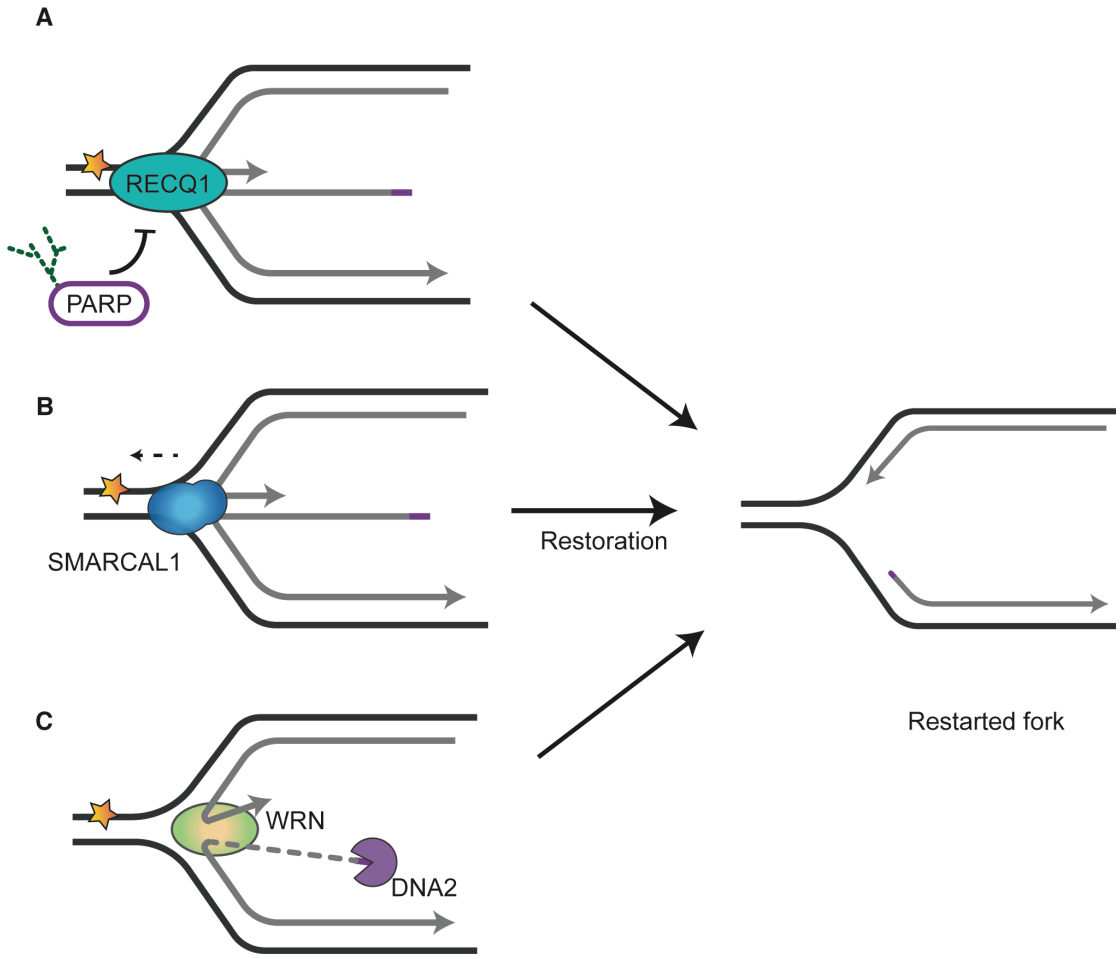

Figure 1.6. Pathways for stalled fork restart. (A) Reversed forks can be restarted by RECQ1-dependent branch migration which is inhibited by parylation of PARP (poly ADP-ribose polymerase 1). (B) Alternatively, fork restoration can restart stalled and can be catalyzed by SMARCAL1 as described in Figure 1.5. (C) Fork restart can also be performed by WRN-mediated unwinding followed by limited DNA2 degradation.

intermediate products can be utilized by other enzymes. Finally, some of the phenotypic outcomes that differ when individual fork remodeling proteins are inactivated may be caused by the use of alternative replication stress tolerance and repair mechanisms shunting intermediate products towards different outcomes (Figure 1.5)

Fork restoration

Multiple pathways can help restart replication after reversal. One such pathway is fork restoration. Restoration refers to the process of resetting a reversed fork to a three-way junction. In addition to some translocases, specialized factors are engaged at the fork to promote restoration. A major contribution to reversed-fork restart is provided by RECQ1, which is inhibited by poly(ADP-ribose) polymerase 1 (PARP1)-mediated parylation during replication stress. RECQ1 uses its ATPase activity to reverse branch migration and restore the classical three-way junctions upon release from replication stress and PARP inhibition (Berti et al., 2013; Zellweger et al., 2015) (Figure 1.6A). Another important pathway that promotes the restart of reversed forks involves controlled processing of the regressed arm by Werner syndrome ATP-dependent helicase (WRN) and DNA2 nuclease, which assists in dissolution of the reversed fork to promote HR-mediated restoration of the three-way junction (Thangavel et al., 2015) (Figure 1.6C). Moreover, SMARCAL1, ZRANB3, and HLTF also promote fork restoration although there are differences in their substrate preference. For example, SMARCAL1 restores both leading and lagging gapped forks equally. In contrast, HLTF and ZRANB3 preferentially restore forks containing a gap on the lagging strand (Chavez et al., 2018) (Figure 1.6B). It is unknown whether FBH1 is capable of promoting fork restoration *in vitro*.

ssDNA binding proteins

ssDNA binding proteins are typically characterized by the presence of one or multiple Oligonucleotide/Oligosaccharide-binding (OB) fold(s). In prokaryotes and eukaryotes, these proteins are required for many essential DNA transactions including replication, transcription, and recombination. Additionally, they represent the first line of response to replication stress. Therefore, ssDNA binding proteins are critical for genome maintenance and viability. In this section, I will highlight the functions of RPA, RAD51, and RADX at replication forks.

Replication Protein A (RPA) functions at replication forks

Exposed ssDNA during active replication or after stress induced stalling is rapidly bound by the ssDNA binding protein, RPA. RPA is a heterotrimer composed of three subunits- RPA70, RPA32, and RPA14. RPA binding to DNA has several functions. First, RPA-coated DNA serves as a platform to recruit several RSR proteins including the master kinase ATR, the essential recombinase RAD51, and fork remodeler SMARCAL1. Second, RPA regulates the activity of multiple RSR proteins like SMARCAL1 or PRIMPOL by directing their activity to the right context. Third, RPA protects the replication fork from SLX4-dependent nucleases to prevent DSB formation (Couch et al., 2013; Toledo et al., 2013). Finally, RPA melts secondary DNA structures to promote RAD51-mediated strand exchange (Bhat and Cortez, 2018; Sarbajna and West, 2014) (Figure 1.7).

At stalled forks, direct interaction with the 32C domain of RPA aids in the recruitment and regulation of SMARCAL1 activity (Bansbach et al., 2009; Ciccia et al., 2009). Specifically, RPA bound to leading strand gap stimulates SMARCAL1 activity but inhibits it when bound to lagging strand gap (Betous et al., 2013a). The polar binding of RPA on ssDNA facilitates this difference (Bhat et al., 2015). In contrast, ZRANB3 is inhibited by RPA on the leading strand and HLTF is modestly inhibited by RPA on the lagging strand template (Betous et al., 2013a; Chavez et al., 2018). Similar differences are observed between the translocases in their fork restoration activities. For example, SMARCAL1 preferentially restores forks with a lagging strand gap bound by RPA (Betous et al., 2013a). However, fork restoration by ZRANB3 and HLTF are inhibited by RPA on the lagging strand (Chavez et al., 2018).

In summary, RPA performs several critical functions in safeguarding replication fork integrity. Distinct substrate recognition due to multiple DNA binding modes, protein-interaction domains, and post-translational modifications all likely contribute to RPA function.

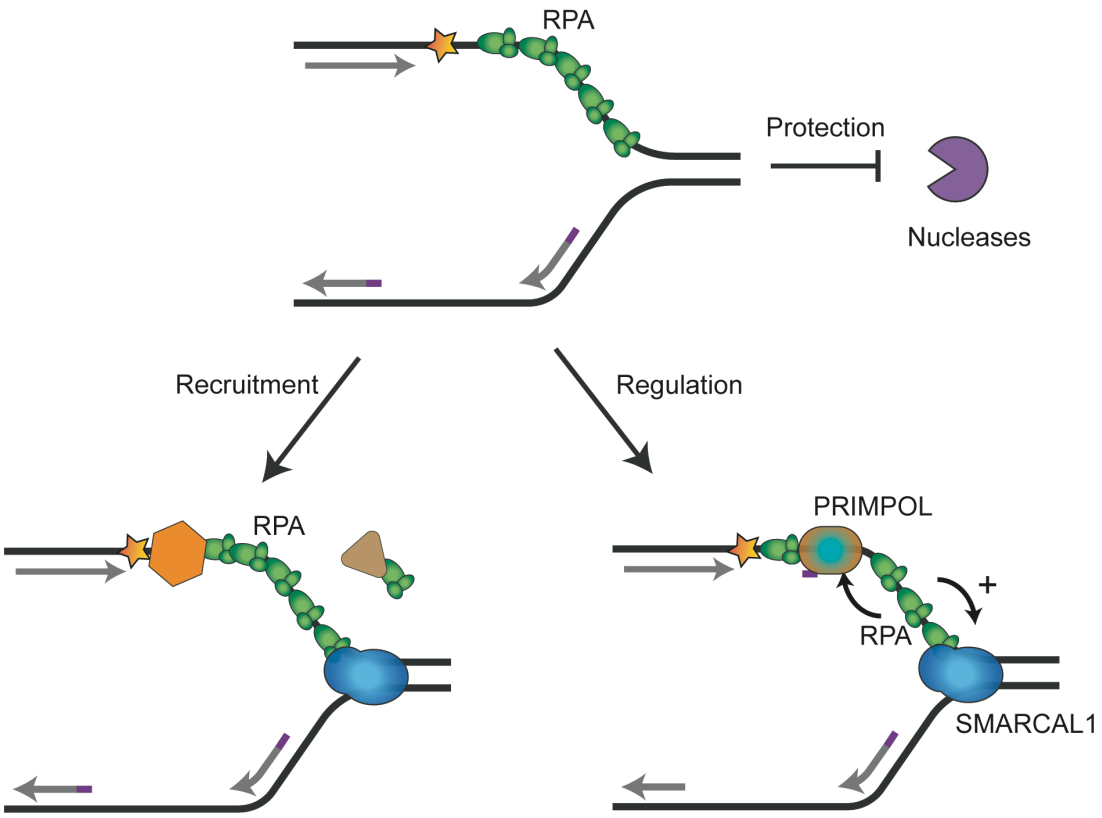

Figure 1.7. Functions of RPA at stalled forks. As the first responder to replication stress, RPA has multiple functions at a stalled fork. RPA-coated ssDNA prevents nuclease activity, recruits multiple repair proteins, and directs the activity of many proteins to the right context. All of these activities prevent genome instability.

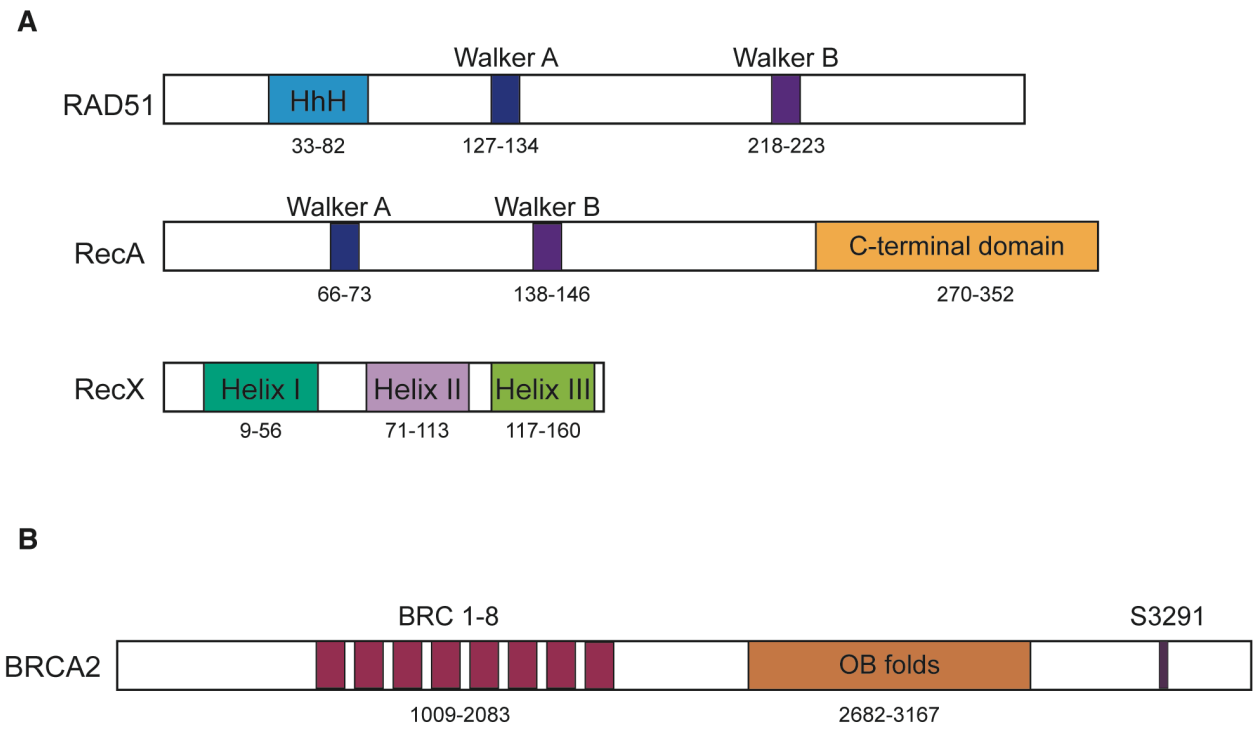

Figure 1.8. Domain structures of ssDNA binding proteins. HhH-Helix hairpin helix, OB-Oligonucleotide/oligopeptide binding. See text for details

Structure and functions of RAD51

RAD51 is an essential recombinase with well described functions in DSB repair by HR. In addition, RAD51 also has important functions at the replication fork. Regulation of RAD51 recruitment, stabilization and disassembly by protein-protein interactions and post-translational modifications are critical to modulate its functions at the fork. In this sub-section, I will summarize the physical and biochemical properties of RAD51, the need for mediators like BRCA2, and the functions of RAD51 on fork reversal and fork protection.

Domain structure of RAD51

RAD51 is a highly conserved ATPase that shares sequence and structural similarity to the *E.coli* ssDNA binding protein, RecA (Lusetti and Cox, 2002). Human RAD51 contains a core ATPase domain with Walker A and Walker B motifs important for binding and hydrolyzing ATP (Short et al., 2016; Xu et al., 2017a). Other domains include an N-terminal domain that mediates protomer-protomer interaction, a HhH (Helix hairpin Helix) domain that binds DNA, and a flexible interdomain linker (Figure 1.8A). Recent structural studies indicate that DNA binding may not require the HhH domain but instead require two disordered loops (Short et al., 2016). Moreover, six to eight nucleotides of ssDNA binding by a RAD51 monomer is required for maximal ATP hydrolysis (Tombline and Fishel, 2002). Importantly, the structure of RAD51 filament on DNA is important for its functions in DSB repair and at replication forks.

Physical and biochemical properties of the RAD51 filament

RAD51 has a lower affinity for both ssDNA and dsDNA (K_d~10^{-6} M) compared to RPA which has a high affinity for ssDNA (K_d~10^{-9} -10^{-11} M) and low affinity for dsDNA (K_d ~10^{-6} M). In addition, RAD51 has a 50-100-fold weaker ATPase activity compared to RecA (Tombline and Fishel, 2002). These observations imply that modulation of ssDNA binding and ATPase activity by regulatory proteins may have an important function in regulating RAD51 activity. Additionally, vertebrate RAD51 is essential for cell proliferation unlike its homologs in lower organisms like *E.coli*.

RAD51 exists in multiple oligomeric states dependent on its relative concentration in cells (Candelli et al., 2014; Davies and Pellegrini, 2007; Nomme et al., 2008; Yoshioka et al., 2003).

Structural evidence indicates that in the absence of nucleic acids, RAD51 forms ATP-bound heptamers in solution (Brouwer et al., 2018; Shin et al., 2003). These 'inactive' heptameric rings are loaded on to ssDNA with the help of mediators. Once loaded, RAD51 polymerization on DNA consists of two phases: a rate-limiting nucleation phase and a rapid growth phase (Hilario et al., 2009; Mine et al., 2007). Nucleation involves multimeric RAD51 species of varying sizes binding to 3-nucleotides at multiple, discontinuous sites along ssDNA (Qi et al., 2015; Ristic et al., 2005; Subramanyam et al., 2016). Single-molecule, real time experiments show that these multimers bind in a single kinetic step to ssDNA (Spirek et al., 2018). A minimum of 3-4 protomers of RAD51 on DNA is required for its filament growth. The nucleofilament is then elongated bidirectionally by the addition of RAD51 monomers or dimers (Qiu et al., 2013). Although RAD51 has a similar affinity to ssDNA and dsDNA, it preferentially polymerizes on ssDNA. Recent single-molecule studies indicate that this property is due to the molecular flexibility of DNA (Paoletti et al., 2020). In addition, a number of proteins such as RAD51 paralogs, Hop2-Mnd1, and BRCA2 are also known to increase RAD51 nucleofilament stability on ssDNA (Chi et al., 2007; Matsuzaki et al., 2019; Shivji et al., 2006).

RAD51 filament disassembly is important at late stages of HR-mediated repair to promote annealing and restoration of the double-stranded structure of DNA (Vasianovich et al., 2017). In bacteria, RecA turnover is mainly due to ATP hydrolysis since ADP-bound RecA has decreased affinity for ssDNA (Bell et al., 2012) (Figure 1.8A). In contrast, mammalian RAD51 filaments are disassembled by anti-recombinases such as PARI, FBH1, BLM, RECQL5, RAD54, and FIGNL1 (Bugreev et al., 2007; Hu et al., 2007; Matsuzaki et al., 2019; Moldovan et al., 2012; Pazin and Kadonaga, 1997; Simandlova et al., 2013). Additionally, ATP hydrolysis and post-translational modifications also regulate the nucleofilament stability. Although this process is still not fully understood, single molecule studies point to a model where filament dissociation occurs in multiple consecutive steps involving various species of RAD51 (Spirek et al., 2018).

Of particular interest to my thesis work is the disassembly of RecA filaments by RecX. Previous studies showed that in *E.coli*, RecX "caps" the 3' end of a growing RecA filament to prevent further growth while promoting passive disassembly from the 5' end (Drees et al., 2004). Further evidence from Surface Plasmon Resonance (SPR) experiments indicate that RecX binds at multiple points along the RecA filament to gain access to ssDNA and increase the number of 'ends' to promote active filament disassembly by promoting its ATPase activity

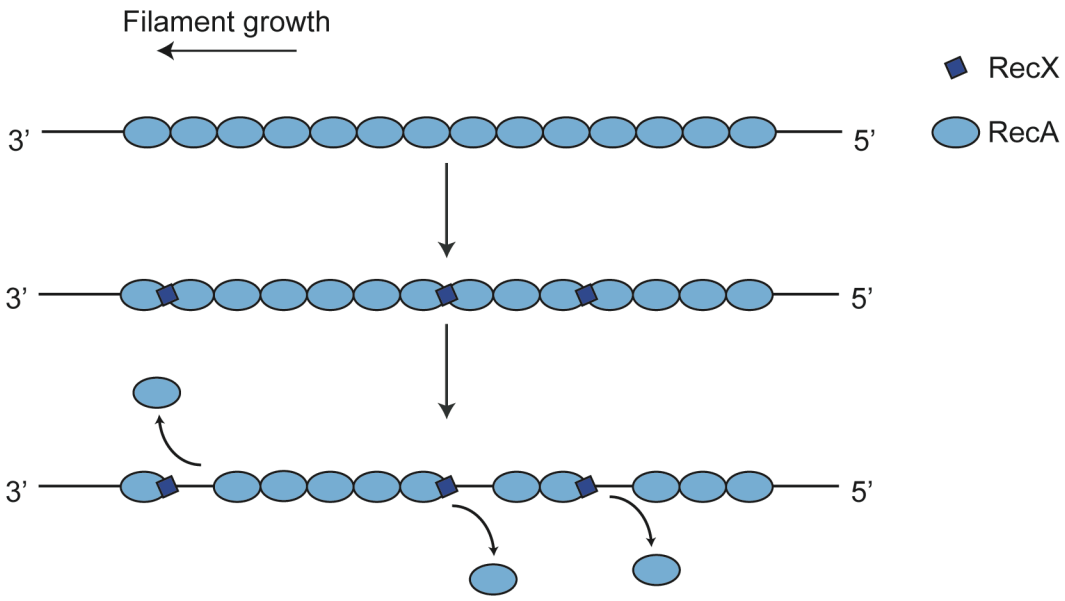

Figure 1.9. Model for RecX mediated disassembly of RecA. RecX caps the 3’ end of a growing filament to promote active disassembly of RecA.

	RAD51 mutant	DNA binding?	ATPase	Strand exchange	Fork reversal	Fork protection	References
RAD51 mutations	T131P	Yes	Yes	No	Yes	No	(Wang et al., 2015)
	K133R	Yes	No	Yes- *in vitro*	N.D.	Yes	(Morrison et al., 1999; Stark et al., 2002)
	K133A	Yes	No	No – *in vitro*	N.D.	No	(Chi et al., 2006; Forget et al., 2007)
	II3A	Yes; reduced	N.D.	No- *in vitro*	Yes	Yes- MRE11 No-DNA2	(Cloud et al., 2012; Mason et al., 2019)
	I278T	Yes; increased	Yes- In yeast (I345T)	N.D.	N.D.	N.D.	(Davies and Pellegrini, 2007; Fortin and Symington, 2002; Xue et al., 2021)

Table 1.1. Summary of RAD51 mutations. List of RAD51 mutants and their properties with appropriate references. N.D. - not determined. *In vitro* means that the function has been studied biochemically with purified proteins.

(Ragone et al., 2008). A similar, active filament dissociation model has also been proposed using *N.gonorrhoeae* RecX, further suggesting that RecA ATPase activity is important for its turnover (Gruenig et al., 2010). Paradoxically, RecX mediated inhibition of RecA nucleofilament stimulates its recombination functions (Cardenas et al., 2012; Gruenig et al., 2010) (Figures 1.8A and 1.9). Thus, modulation of RecA functions by mediator proteins like RecX are essential for its functions *in vivo*.

In summary, multiple layers of regulation control RAD51 filament assembly and disassembly to modulate its properties. While much remains to be understood, recent evidence from single molecule studies and insights from RecA and *S. cerevisiae* RAD51 have improved our understanding of mammalian RAD51 filament regulation.

RAD51 mutations

While homozygous loss of *RAD51* is embryonic lethal, mutations in *RAD51* are associated with genomic instability, Fanconi Anemia (FA), and predisposition to several cancers including breast and ovarian cancer (Bonilla et al., 2020; Grundy et al., 2020; Lim and Hasty, 1996). To date, over 90 mutations on *RAD51* have been identified but only a handful have been functionally characterized. A list of *RAD51* mutations and their phenotypes is shown in Table 1.1.

It is important to note that overexpression of RAD51 or gain-of-function mutations in *RAD51* also exhibit deleterious phenotypes such as increased recombination, resistance to chemotherapeutic drugs, dysregulation of cell cycle, and apoptosis (Klein, 2008). Consequently, many tumors frequently overexpress RAD51, likely contributing to drug resistance (Raderschall et al., 2002). Therefore, maintaining appropriate levels of RAD51 expression and activity is critical for HR, tumorigenesis, and chemotherapeutic response.

RAD51 regulation

RAD51 is regulated by multiple mechanisms such as transcription, post-translational modifications, and mediators that affect its abundance, recruitment, access to DNA, and filament stability. Unlike RPA, RAD51 requires mediators to load and stabilize on DNA (Bochkarev and Bochkareva, 2004). In mammalian cells, the most well-characterized positive regulators of RAD51 loading and filament stability include BRCA2 and RAD51 paralogs among many others.

BRCA2

BRCA2 is a major hereditary breast cancer susceptibility gene. Mutations in *BRCA2* are typically associated with predisposition to breast, ovarian, prostate, and pancreatic cancers in addition to several developmental defects (Ozcelik et al., 1997; Waddell et al., 2010). One of the major functions of BRCA2 is in HR. Genetic and biochemical evidence indicate that BRCA2 promotes HR by displacing RPA and loading RAD51 on ssDNA to initiate strand exchange (Kowalczykowski, 2015).

Mammalian BRCA2 is a relatively large protein (3418 amino acids) with multiple domains for RAD51 binding and regulation. The BRC 1-8 repeats, conserved across vertebrates in sequence and spacing, represent the 'core' of the protein (Bignell et al., 1997). The BRC repeats are all characterized by a FxTA motif which interact with RAD51 (Lo et al., 2003) (Figure 1.8B). Full-length BRCA2 or a peptide containing all BRC repeats promote RAD51-mediated strand exchange by stabilizing RAD51 on ssDNA while preventing RAD51 nucleation on dsDNA (Carreira et al., 2009; Jensen et al., 2010; Thorslund et al., 2010). The function of individual BRC repeats is unclear although biochemical evidence points to two classes of repeats: First, BRC 1-4 bind to RAD51 monomers or protomers with high affinity and reduce its ATPase activity thus promoting its nucleation on ssDNA over dsDNA. Second, BRC 5-8 binds to RAD51-ssDNA filament with high affinity thereby promoting stabilization (Carreira and Kowalczykowski, 2011). DNA-damage sensitivity in BRCA-mutant cells is rescued by expression of a BRC3-4-RPA fusion protein implying that RAD51 loading is necessary and sufficient for BRCA2 DSB repair (Saeki et al., 2006). Intriguingly, at high concentrations, individual BRC repeats inhibit RAD51 filament formation *in vitro* (Davies et al., 2001). Additionally, recent studies indicate that *C. elegans* BRC-2 functions primarily as a nucleation factor while RAD51 paralogs stabilize the nucleofilament (Belan et al., 2021). Taken together, the molecular basis for differential affinity and functionality of the BRC repeats remains to be understood.

In addition, BRCA2 has a RAD51-binding region at the C-terminus that is distinct in sequence and structure from the BRC repeats (Sharan et al., 1997). S3291 residue at the BRCA2 C-terminus is phosphorylated by Cyclin-dependent kinase 2 (CDK2) at the G2/M phase (Esashi et al., 2005). Upon phosphorylation, RAD51 binding to this region is abrogated. The C-terminus only interacts with RAD51 filaments and not monomers suggesting that it regulates filament stability (Davies and Pellegrini, 2007; Esashi et al., 2007). Interestingly, mutations in S3291 disrupt

RAD51 binding but do not confer DNA-damage sensitivity or compromise HR (Ayoub et al., 2009; Schlacher et al., 2011).

Finally, BRCA2 also binds directly to ssDNA through a DNA-binding domain (DBD) that contains a helical domain, multiple OB-folds, and a tower domain with a 3-helix bundle (3HB) that spans the C-terminus (Chen et al., 1998). Mutations in the 3HB domain compromise HR while deleting the entire DBD domain has little to no effect on HR if the interaction with another protein, PALB2, is intact (Siaud et al., 2011). These observations point to the remarkable plasticity of BRCA2 in modulating HR.

RAD51 paralogs

RAD51 paralogs are mediators of RAD51 nucleation and stability with functions in DSB repair, meiosis, and DNA replication although their precise function in cells is unknown. In vertebrates, there are seven paralogs, divided into three complexes: i) BCDX2 complex which consists of RAD51B, RAD51C, RAD51D, and XRCC2, ii) CX3 complex that consists of RAD51C and XRCC3, and iii) Shu complex which consists of SWS1 and SWSAP1. Mutations in any of the RAD51 paralogs leads to a wide range of phenotypes including growth defects, DNA damage sensitivity, reduced RAD51 foci, and compromised HR differing in severity depending on the paralog (Garcin et al., 2019).

RAD51 paralogs share 20-30% sequence identity with RAD51 and one another since all proteins share Walker A and B domains for ATP hydrolysis. Biochemical studies indicate that paralog complexes directly interact with RAD51 *in vitro*. In addition, all paralog complexes bind to a diverse range of DNA substrates including ssDNA, gapped circular DNA, 3' and 5' overhangs, and nicked duplex substrates (Masson et al., 2001). How the paralogs mechanistically aid in RAD51 filament assembly is still unknown. It has been hypothesized that the paralogs either promote elongation after initial BRCA2-mediated nucleation or cap off RAD51 filament to prevent disassembly. Indeed, recent single molecule studies suggest that yeast Rad55-Rad57 paralogs exhibit a chaperone like activity to antagonize Rad51 disassembly while stimulating its assembly on RPA coated ssDNA (Roy et al., 2021). Similarly, *C. elegans* BRC-2 nucleates RAD-51 on RPA-coated DNA, while RFS-1/RIP-1 paralog complex prevents dissociation and promotes filament growth

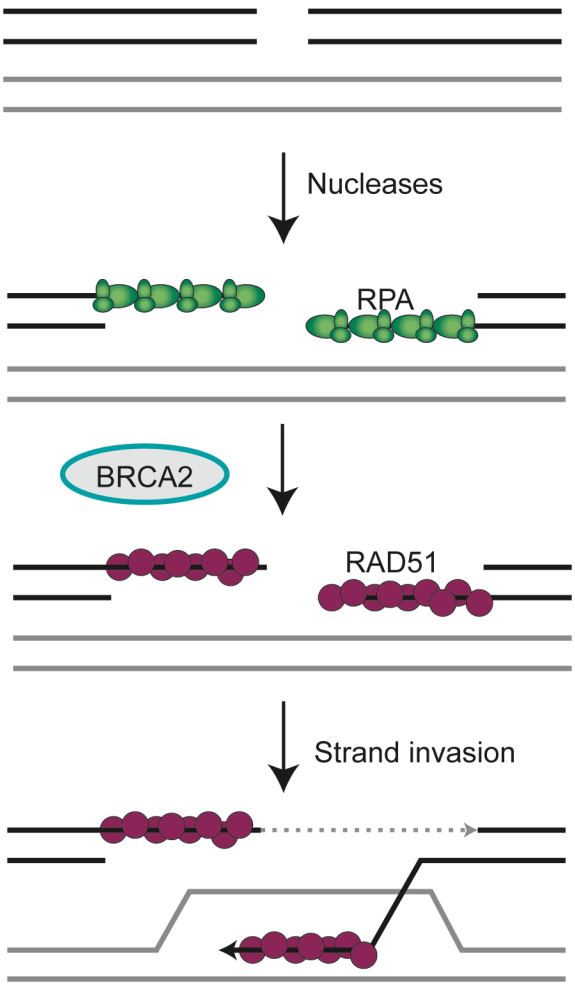

Figure 1.10. Simplified schematic of double strand break repair by RAD51. Upon induction of a double strand break, nucleases cleave the end of the DNA to expose overhangs. RAD51 loaded and stabilized to the exposed ssDNA with the help of BRCA2 promotes strand invasion and homology search.

(Belan et al., 2021). Therefore, vertebrate RAD51 filament assembly could have similar mechanisms of regulation by paralog complexes.

RAD51 functions at double-strand breaks

One of the most well-studied functions of RAD51 is at DSBs. Since this function of RAD51 has been extensively reviewed elsewhere, I will briefly introduce the functions of BRCA2 in DSB repair in this section.

Upon DSB induction, the ends are resected by nucleases like MRE11-RAD50-NBS1 (MRN) to expose ssDNA. RPA-coated ssDNA is subsequently replaced by RAD51 with the help of BRCA2, which helps load and stabilize RAD51 while promoting RPA eviction. RAD51 bound to ssDNA performs homology search and strand invasion. Strand invasion forms a D-loop structure. Eventually, RAD51 filaments are dissociated by anti-recombinases such as BLM to allow polymerases to replicate through the homologous template (Jasin and Rothstein, 2013; Wright et al., 2018). Importantly, loss of BRCA2 fails to displace RPA and load RAD51 resulting in HR defects (Kowalczykowski, 2015; Symington, 2014) (Figure 1.10). Additionally, RAD51 cannot form 'foci', regarded as sites of repair, in the absence of BRCA2 in response to DNA damage (Sharan et al., 1997). Consistent with its critical function in HR, BRCA2-deficient cells are sensitive to DNA-damaging agents that induce lesions typically repaired by HR like irradiation (IR), cross-linking agents, and PARP inhibitors (Bryant et al., 2005; Farmer et al., 2005; Kraakman-van der Zwet et al., 2002). Thus, BRCA2 is absolutely essential for RAD51-mediated DSB repair.

Fork reversal and fork protection functions of RAD51

Another recently discovered function for BRCA2 distinct from DSBs is replication fork protection (Hashimoto et al., 2010; Schlacher et al., 2011). Cells deficient in BRCA2 exhibit 'nascent strand degradation' or 'fork degradation', which refers to excessive resection of the regressed arm by nucleases such as MRE11 and DNA2 in response to fork stalling agents including hydroxyurea (HU) or camptothecin (CPT) (Schlacher et al., 2011). Stabilization of RAD51 filaments, mediated by BRCA2, is required to protect the regressed arm from nucleases. Indeed, mutations in the BRCA2 C-terminus which compromise RAD51 loading but not HR, is deficient for fork protection. This defect is rescued by overexpression of a RAD51 mutant that forms hyperstable filaments

(K133R) (Schlacher et al., 2011). Additionally, patients with a dominant mutation in *RAD51*, T131P, also exhibit fork degradation. T131P mutants display constitutive ATPase activity and are incapable of forming stable filaments even in the presence of BRCA2 (Wang et al., 2015). *In vitro*, ssDNA bound to RAD51 prevents MRE11-dependent degradation while RPA-ssDNA does not confer protection (Kolinjivadi et al., 2017b). Taken together, stable RAD51 filaments on the regressed arm of a reversed fork structure may allow for transient stabilization of the stalled fork.

In addition to BRCA2, many other fork protection factors have been recently identified including FA proteins, BOD1L, WRNIP, 53BP1, and RAD51 paralogs among many that are still being discovered. For example, BOD1L was described to protect forks through its interaction with the histone methyltransferase SETD1A which enhances FANCD2 dependent histone chaperone activity to mediate RAD51 recruitment (Higgs et al., 2018). Similarly, WRNIP protects forks from degradation by promoting RAD51 stability on stalled forks (Leuzzi et al., 2016). However, the mechanisms by which other fork protection proteins promote RAD51 functions and protect from fork degradation is still unknown. Another layer of complexity is the nuclease mediating the degradation. For instance, while degradation observed upon loss of BRCA1/2 or FA can be rescued by depleting MRE11/EXO1 or DNA2, some factors like BOD1L and 53BP1 are restored by DNA2 inhibition alone (Lemacon et al., 2017; Liu et al., 2020) (Figure 1.11A). Thus, defects in RAD51 loading or stabilization can cause MRE11/EXO1 or DNA2 dependent fork degradation, although the factors governing the choice of nuclease is unclear.

A few other fork protection pathways have also been described as RAD51-independent in different genetic contexts. For example, ABRO1, a paralog of ABRAXAS which is a BRCA1-interacting protein, was recently proposed to protect stalled forks from DNA2-nuclease independently of RAD51 (Xu et al., 2017b). Additionally, inhibition of PCNA-ubiquitylation stimulates MRE11-dependent nascent strand degradation that is thought to be RAD51 independent (Thakar et al., 2020). Moreover, whether fork protection proteins including AND-1, POLK, and RIF1 require RAD51 stabilization is unknown (Abe et al., 2018; Mukherjee et al., 2019; Tonzi et al., 2018). Taken together, what governs different fork protection pathways and choice of nucleases remains to be investigated.

EM studies point to a model where fork reversal is the entry point for nucleases to degrade the newly synthesized DNA (Kolinjivadi et al., 2017b; Lemacon et al., 2017; Mijic et al., 2017; Taglialatela et al., 2017). Indeed, blocking fork reversal by depletion of any of the translocases or

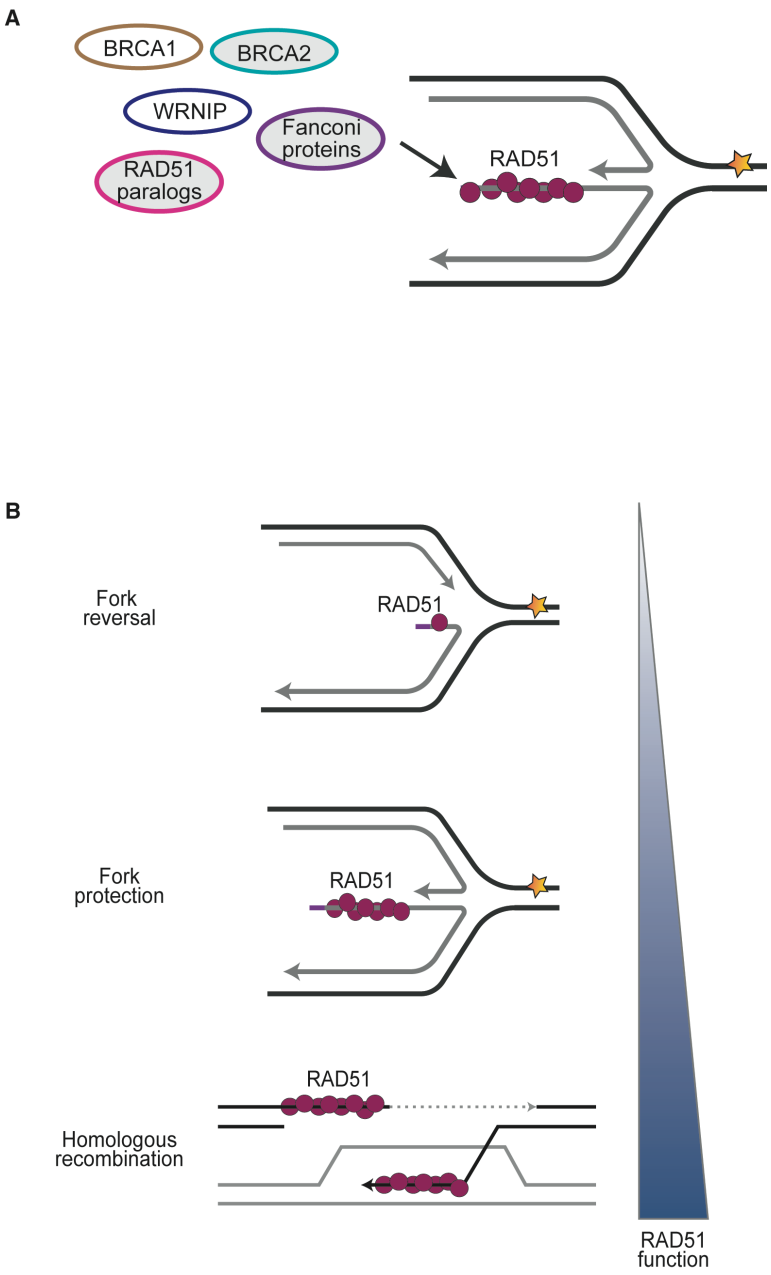

Figure 1.11. Illustration of differential requirements for RAD51. (A) Multiple fork protection proteins are implicated in the protection of reversed forks from nuclease degradation. (B) Increasing amounts of RAD51 protein/function may be required for fork reversal, fork protection, and homologous recombination.

helicases in BRCA-deficient cells prevents fork degradation. While fork reversal may be a prerequisite for degradation in most cases, whether reversal is mandatory for degradation is unclear (Berti et al., 2020a). Specifically, recent studies show that postreplicative ssDNA gaps behind the fork generated by PRIMPOL, may be a substrate for fork degradation by nucleases like MRE11 (Quinet et al., 2020).

Depletion of RAD51 also prevents fork degradation in BRCA-deficient cells, suggesting that RAD51 may be required for reversal. In support of this hypothesis, analyses of replication intermediates by EM reveal that fork reversal is not observed in RAD51-depleted BRCA-deficient cells (Mijic et al., 2017; Thangavel et al., 2015; Zellweger et al., 2015). Additionally, RAD51-mediated reversal was recently shown to be a global response to genotoxic stress (Zellweger et al., 2015). This function of RAD51 in promoting reversal was initially thought to be independent of BRCA2 since reversed forks accumulate in *BRCA2* mutant cells (Kolinjivadi et al., 2017b; Mijic et al., 2017). However, a recent study has shown that BRCA2 may be required to promote RAD51-mediated reversal in specific genetic contexts (Liu et al., 2020). How BRCA2 mechanistically promotes RAD51-dependent reversal and whether this is distinct from fork protection is unclear.

Mechanistically, how RAD51 catalyzes fork reversal is less well understood. For example, a recent report showed that the strand exchange activity of RAD51 may not be required for its fork reversal or fork protection function (Mason et al., 2019). Moreover, whether RAD51 catalyzes reversal or if it captures an already reversed fork to allow detection by EM is unknown. Regardless, modulating RAD51 levels by titrating in a potent siRNA showed that more RAD51 function is required for protection than reversal (Bhat et al., 2018). Indeed, cells expressing a partial loss of function mutant RAD51 (T131P) or cells treated with a RAD51 inhibitor (B02) exhibit fork degradation (Kolinjivadi et al., 2017b; Taglialatela et al., 2017; Wang et al., 2015) (Figure 1.11B).

RAD51 paralogs have also been recently shown to promote reversal in addition to protecting forks (Berti et al., 2020b). Specifically, the authors showed that BCDX2 complex is required to promote reversal in BRCA-deficient cells presumably by assisting RAD51 or by their intrinsic strand exchange or annealing activities. In contrast, the CX3 complex is dispensable for reversal but required for fork restart. Importantly, BCDX2 inactivation but not *XRCC3* inactivation rescues genome instability observed in BRCA-deficient cells similar to translocase inactivation implying

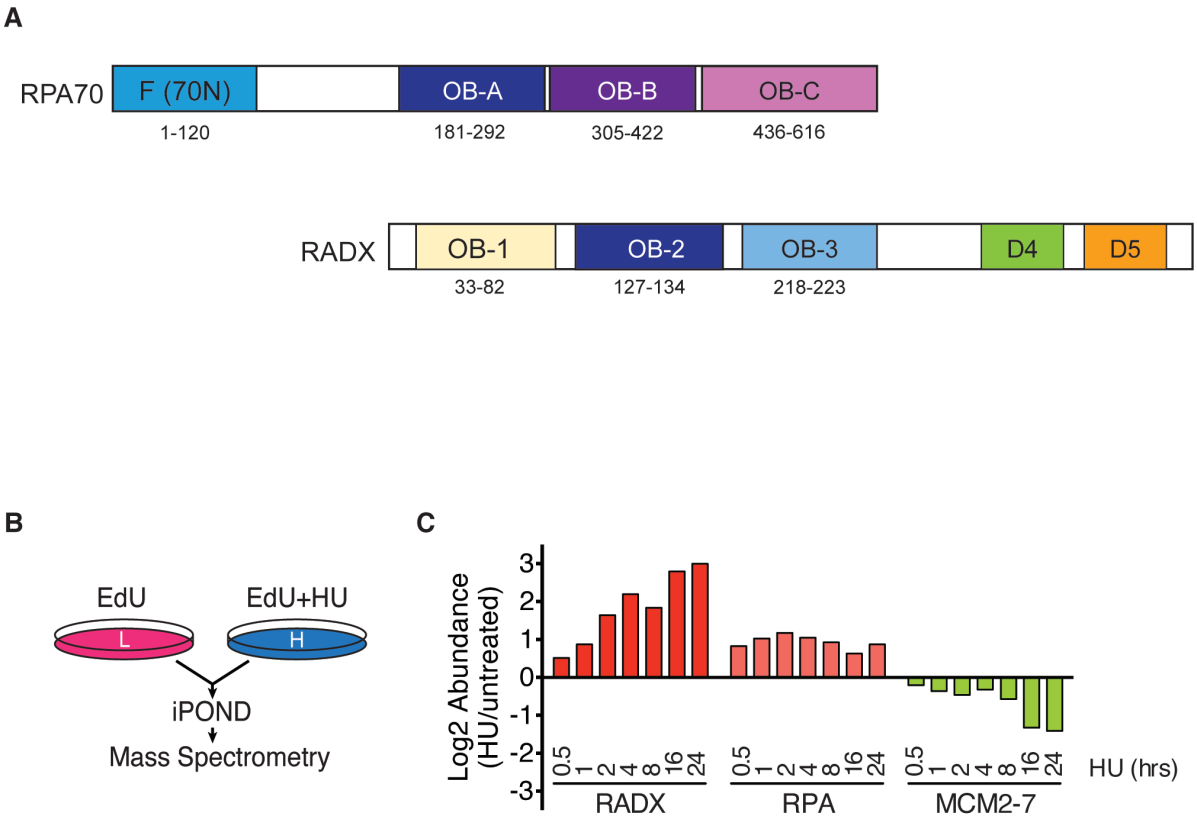

Figure 1.12. Domain structure and recruitment of RADX. (A) Domain structure of RADX and RPA. (B) Schematic of iPOND-SILAC used to identify proteins enriched at replication forks in HU-treated cells. (C) RADX recruitment is enriched at replication forks with increasing time in HU. Log_2 abundance ratios are depicted on the y-axis. Data adapted from Dungrawala et al., 2017.

that fork reversal needs to be tightly regulated to genome maintenance (Berti et al., 2020b; Taglialatela et al., 2017).

In summary, RAD51 has several functions in cells: i) DSB repair, ii) Fork protection, and iii) Fork reversal. It is likely that decreasing amounts of RAD51 function is required for these three processes (Figure 1.11B). Regulation of RAD51 function may occur through its many mediators in cells (described in previous sections) or through the amount of ssDNA. While the mechanisms of RAD51 function in reversal and protection are not well understood, it is clear that managing replication intermediates through tight regulation of RAD51 is essential. Failure to do so can generate mutations, drive genetic instability, and even promote diseases like cancers.

RADX (RPA-related RAD51 antagonist on the X chromosome)

The Cortez lab recently identified RADX (CXorf57) in a large-scale, proteomics screen called iPOND (isolation of proteins on nascent DNA) (Dungrawala et al., 2017). The functions of RADX at replication forks are important for maintaining fork stability and determining response to chemotherapy as discussed below. Further analysis identified that these functions are tied to RAD51 regulation at the replication fork (Adolph et al., 2021; Bhat et al., 2018; Dungrawala et al., 2017; Krishnamoorthy et al., 2021; Schubert et al., 2017).

Domain structure of RADX

Structural modeling and analysis of primary amino acid sequence predicts that RADX has five structured domains. At the N-terminus, RADX contains three OB-folds (OB1, OB2, and OB3) similar to RPA70N protein recruitment domain, the RPA70A high-affinity ssDNA binding domain, and the telomeric ssDNA binding domain of POT1, respectively. Domain 4 (D4) and Domain 5 (D5) at the C-terminus resemble the oligomerization domains of bacterial transcription factors DasR and NtrR, respectively (Remy Le Meur, unpublished) (Figure 1.12A). In contrast, Alphafold software predicts a fourth OB fold on RADX consisting of OB3 and D4 thus resembling RPA70.

Biochemical characterization of RADX

Structural modeling hypothesizes that RADX, like RPA, should preferentially bind to ssDNA.

Indeed, Pull-down and Electrophoretic mobility shift assays (EMSA) show that RADX has approximately 75-fold higher affinity for ssDNA than dsDNA. In addition, mutations in the OB-fold domain (OB2m) show decreased affinity to ssDNA. However, RADX OB2m protein shows residual ssDNA binding suggesting that RADX, like RPA, likely has multiple DNA binding domains (Dungrawala et al., 2017; Schubert et al., 2017). Using proximity ligation assay (PLA), Schubert *et al.*, also showed that RADX localizes to replication forks while RADX OB2m shows reduced localization indicative of a defect in ssDNA binding (Schubert et al., 2017).

Recent study shows that RADX directly interacts with ATP-bound RAD51 through a site on OB3 domain. Mutations in the RAD51-interaction residue (QVPK) abolishes its interaction with RAD51 although other functions such as ssDNA binding and recruitment to replication forks are still retained (Adolph et al., 2021). Finally, recent studies indicate that RADX D4 and RADX D5 may be important for oligomerization of RADX (Taha Mohamed, unpublished).

Functions of RADX

iPOND analyses showed that RADX is recruited to stalled forks and modestly enriched at elongating forks (Dungrawala et al., 2017) (Figure 1.12B). This recruitment is dependent on RADX binding to ssDNA since OB2m recruitment is reduced significantly in the presence of replication stress (Schubert et al., 2017).

To understand the function(s) of RADX at elongating and stalled replication forks, iPOND analysis was repeated with HU in RADX∆ cells. Interestingly, RAD51 was found to be the most enriched at stalled forks in RADX∆ cells as compared to parental cells. In contrast, other DNA damage response proteins like BRCA2, RPA, and MRN complex were neither enriched nor depleted at forks in RADX∆ cells as compared to control cells (Dungrawala et al., 2017). Importantly, this enrichment of RAD51 is not due to an increase in the amount of ssDNA. Quantitative immunofluorescence imaging shows an increase in the number and intensity of chromatin-bound RAD51 foci in the absence of RADX both in the absence of added exogenous stress, and in the presence of added stress like HU. Conversely, overexpression of RADX decreases RAD51 foci and this decrease in RAD51 is not apparent in cells overexpressing RADX OB2m. This implies that ssDNA binding of RADX is important for regulating RAD51 accumulation at unstressed and stalled forks (Dungrawala et al., 2017).
Biochemically, RADX antagonizes RAD51 by competing for the same ssDNA ligand. When RADX

is pre-bound to DNA and increasing amounts of RAD51 is added, RADX blocks RAD51 binding to DNA (Dungrawala et al., 2017). Similarly, using single molecule DNA curtain assays, Adolph et al., found that pre-bound RADX acts as a barrier for RAD51 nucleofilament assembly (Adolph et al., 2021). In contrast, pre-formed RAD51 filaments are disassembled by RADX as observed by negative-stain EM and *in vitro* competition assays. RADX can outcompete RAD51 for ssDNA binding even when RAD51 is at 10,000-fold molar excess. This is dependent on the ability of RADX to bind DNA and RAD51, since either a RADX mutant that abrogates most of its DNA binding activity (OBm) or its ability to interact with RAD51 (QVPK) cannot compete with or destabilize RAD51 from ssDNA (Adolph et al., 2021; Dungrawala et al., 2017).

Another mechanism by which RADX antagonizes RAD51 could be active displacement of RAD51 filaments by stimulating its ATP hydrolysis similar to RecA disassembly by RecX (discussed previously). Using a combination of *in vitro* ATPase assays and negative-stain EM, Adolph et al., found that RADX stimulates the ATPase activity of RAD51 and prevents the formation of RAD51-ssDNA nucleofilaments (Adolph et al., 2021). In addition, RADX inhibits RAD51-mediated strand exchange and D-loop formation *in vitro*. More importantly, RADX interactions with RAD51 and ssDNA are required to destabilize the RAD51 nucleofilament since neither RADX QVPK or RADX OB2m can destabilize the RAD51 filament. Thus, RADX directly binds to and regulates RAD51 nucleofilament dynamics (Adolph et al., 2021).

Finally, using single-molecule imaging, it was recently proposed that RADX condenses ssDNA. Intriguingly, RADX condenses RPA-coated ssDNA even when RPA is present 100-fold excess over RADX. The authors propose that the mechanism of action is through multimeric complexes of RADX which capture and bridge ssDNA *in trans*. Therefore, this is one possible mechanism by which RADX prevents loading of RAD51 and other ssDNA binding proteins – by compacting ssDNA (Zhang et al., 2020).

RADX maintains genome stability through regulation of RAD51

Silencing RADX in the absence of added exogenous stress decreases fork elongation rate, increases fork asymmetry and increases fork breakage dependent on MUS81. This is due to aberrant fork reversal likely due to the increase in RAD51 function (Figure 1.13). RADX-deficient

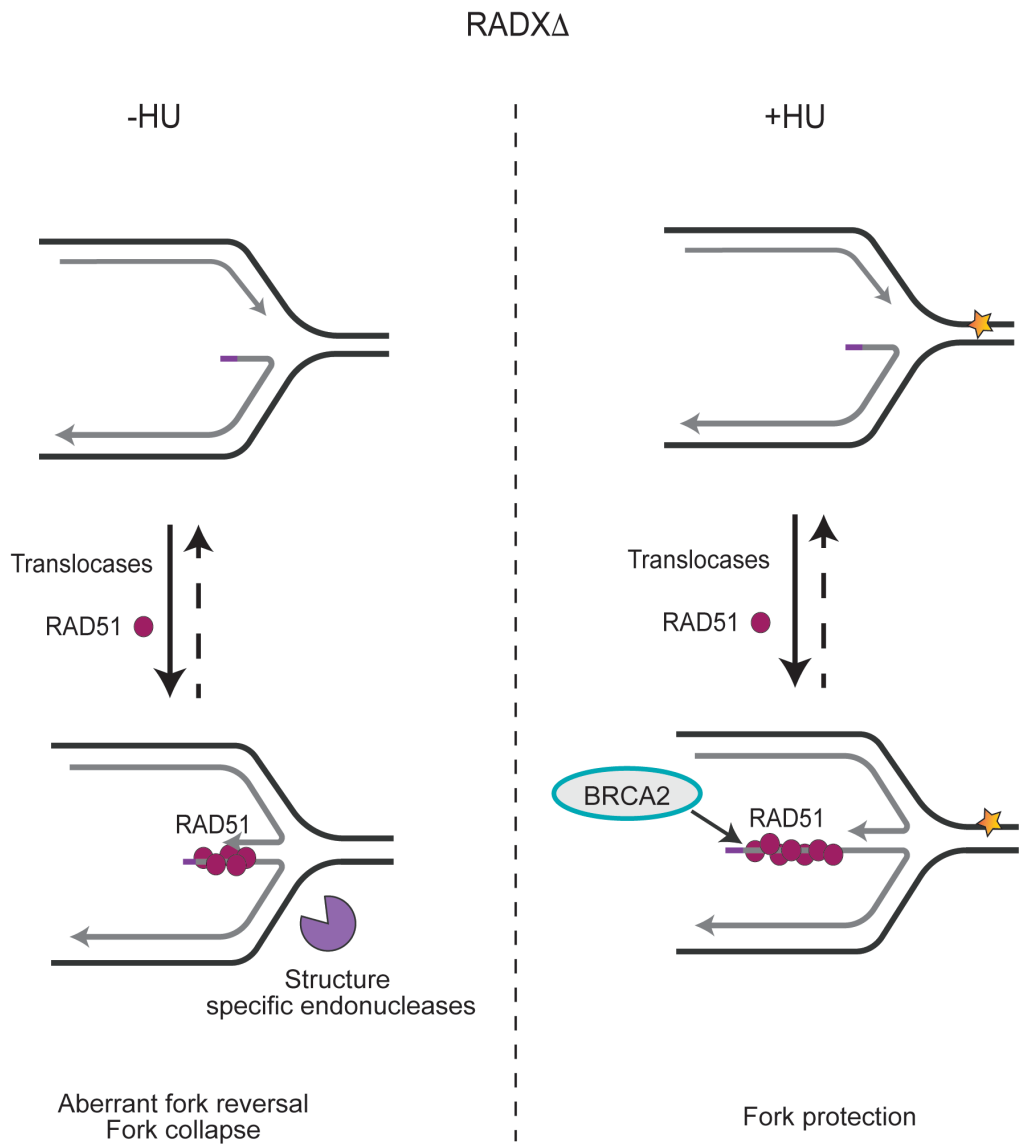

Figure 1.13. Functions of RADX in the absence and presence of added replication stress. See text for details. In the absence of added stress, loss of RADX promotes aberrant reversal and fork collapse. However, upon persistent stalling, silencing RADX rescues nascent strand degradation in cells deficient for fork protection factors.

cells accumulate excessive RAD51 at replication forks; The opposite is also true – overexpression of RADX reduces the amount of RAD51 at forks (Dungrawala et al., 2017); The replication problems in RADX-deficient cells including both the slow forks and DSBs can be rescued by knocking down RAD51; The replication problems in RADX-deficient cells can also be rescued by knocking down the fork reversal enzymes SMARCAL1 or ZRANB3 but not the RAD51 regulator BRCA2 (Dungrawala et al., 2017). These data suggest that aberrant fork reversal causes the problems in RADX-deficient cells since SMARCAL1, ZRANB3, and RAD51 are required for fork reversal but BRCA2 is not, at least in some genetic contexts (Lemacon et al., 2017; Mijic et al., 2017; Taglialatela et al., 2017; Vujanovic et al., 2017). Strikingly, while wild-type RADX can complement the replication fork defects; neither RADX OBm nor RADX QVPK mutants can complement RADX-deficient phenotypes (Adolph et al., 2021; Dungrawala et al., 2017). This suggests that the interaction between RADX-ssDNA and RADX-RAD51 are important for maintaining replication fork stability in the absence of added exogenous stress.

Importantly, RADX also regulates fork protection in cells experiencing persistent replication stress. Silencing RADX restores fork protection in cells deficient for BRCA1, BRCA2, FANCA, FANCD2, or BOD1L that have been treated with HU (Bhat et al., 2018) (Figure 1.13). Inactivating RADX prevents either MRE11- or DNA2-dependent fork degradation. Furthermore, RADX overexpression causes fork degradation that is dependent on these nucleases and fork reversal enzymes (Bhat et al., 2018). Thus, Bhat et al., hypothesized that RADX inactivation improves the ability of RAD51 to protect forks even when fork protection factors like BRCA2 are not present to stabilize the RAD51 filament. My work has revised this hypothesis to propose a new model in Chapter IV (also discussed in Chapter V).

Pathological consequences and therapeutic implications

Errors during DNA replication generate mutations that drive a majority of diseases like cancer. Consequently, many cancer treatments use chemotherapeutic agents that target the replication machinery. Thus, examining the mechanisms that regulate genome fidelity is critical for understanding the etiology of cancers and to also identify novel therapies.

As outlined above, defects in fork processing enzymes cause a variety of genetic conditions and

predispose to diseases like cancer. For example, loss of BRCA2 and RAD51 are embryonic lethal. In addition, both *BRCA2* and *RAD51* are mutated in a variety of cancers and FA-like diseases. Similarly, mutations in translocases such as SMARCAL1, ZRANB3, and HLTF cause predisposition to cancers. Thus, understanding the mechanism by which ssDNA binding proteins and translocases maintain replication fork stability is important to determine cellular responses to cancer treatment and rationally design more effective interventions.

BRCA2 mutant cells exhibit genome instability and defects in DSB repair. Thus, by exploiting synthetic lethal interactions, BRCA2 mutant cancers are often targeted for therapy with PARP inhibitors, such as Olaparib and Rucaparib (Helleday et al., 2005; Lord and Ashworth, 2017; O'Connor, 2015). PARP inhibitors (PARPi) typically work by trapping the enzyme PARP on ssDNA and negatively affecting single strand break repair. This, in turn, causes a greater dependence on DSB repair factors, such as BRCA2. Thus, PARP inhibitors are synthetic lethal with BRCA2 deficiency.

However, when BRCA2 cancers are targeted for therapy, many gain resistance. One mechanism by which these cells evade chemotherapy and acquire resistance is through restoration of replication fork protection independent of HR (Ding et al., 2016; Ray Chaudhuri et al., 2016) although some studies did not observe chemoresistance upon restoration of fork protection (Feng and Jasin, 2017). RAD51 acts at the crux of regulating both DNA replication and repair. Importantly, as outlined above, RAD51 is required for maintaining the equilibrium between replication fork reversal and fork protection. This balance of RAD51 function may be an important determinant of response to cancer therapy.

The biochemical mechanism underlying this form of resistance is unclear. Recent studies suggest that postreplicative gaps underlie the BRCA-like phenotype and this may be key to determine the sensitivity to chemotherapeutic agents. In agreement, restoration of gap suppression without restoring fork protection was sufficient to confer PARPi resistance in BRCA- and FA- deficient cells (Cong et al., 2021). In conclusion, while fork protection may confer chemoresistance in certain backgrounds, it is possible that other mechanisms which allow cells to evade catastrophic DSB-induction, such as postreplicative ssDNA gap accumulation, may determine PARPi sensitivity.

Thesis summary

Replication-coupled DNA repair is important to maintain genome stability and cell survival. ssDNA binding proteins are essential components of DNA replication, recombination, and repair processes. Unsurprisingly, ssDNA binding proteins are tightly regulated to prevent erroneous repair and cancer progression. Specifically, their transactions at reversed forks are becoming increasingly relevant to genome integrity, cell survival, and chemotherapy response. The mechanisms by which these ssDNA binding proteins specifically direct enzymes to the right substrates and how they regulate replication fork remodeling and fork protection is less well understood. My thesis project examines the regulation of RAD51 in fork reversal and fork protection. In Chapter III, I outline the functions of a newly characterized RPA-like ssDNA binding protein, RADX, and further characterize its mechanisms in fork protection. In Chapter IV, I identified the differential regulation of fork reversal by RADX in the presence and absence of exogenous stress. Importantly, I identified that RADX antagonizes RAD51 at unstressed and stalled replication forks to favor different phenotypic outcomes depending on the amount of ssDNA. Overall, my thesis project has changed the way we think about fork reversal and provides a mechanistic explanation for the requirement of a ‘metastable’ RAD51 filament to promote fork reversal.

CHAPTER II

MATERIALS AND METHODS

Immunofluorescence

40,000 U2OS cells plated on each well of a 96-well plate or $3X10^5$ U2OS cells plated on coverslip the day before were treated with 10mM EdU followed by treatment with or without HU. Cells were then washed 3X with PBS and then pre-extracted with cold 0.5% Triton X-100 in PBS (PBS-T) (20 mM HEPES pH 8, 50 mM NaCl, 3 mM MgCl2, 300 mM sucrose and 0.5% Triton-X) for 4 minutes on ice prior to fixing with 3% paraformaldehyde/sucrose for 10 minutes at room temperature. Cells were then blocked with 100ml (coverslips) or 80ml (96-well plate) of 10% goat serum in PBS-T and stained with primary and secondary antibodies diluted in blocking solution. A list of primary and secondary antibodies for immunofluorescence is listed in Table 2.1. Cells were then rinsed with 3X with PBS before mounting coverslips on Prolong Gold. Images were taken on Nikon Eclipse at 40X and analyzed using CellProfiler. For 96-well plates, 80ml of 1:3000 DAPI in PBS was added per well and incubated for 10 minutes at RT and washed 3X with PBS before imaging. Images were acquired in an unbiased manner using ImageXpress Micro (Molecular Devices). Automated intensity analyses were performed using the MetaXpress software.

For immunofluorescence with EdU, EdU was detected using click chemistry with Alexa Fluor-conjugated azide or biotin azide. The click reaction (1ml) buffer is made by adding the following components in order - 875ml PBS or 870ml PBS, 5ml fluor Azide – 488 or 594 or 10ml Biotin azide, 100ml 20mg/ml Na ascorbate and 20ml 100 mM copper sulfate.

Paraformaldehyde fix solution: 15g of paraformaldehyde was dissolved in 250mL water. The solution was incubated 20 minutes at 65 degrees in a water bath and then 3 drops of 10N NaOH were added. The solution was left in the water bath for an additional 5 minutes to allow the powder to completely dissolve. Then 50mL of 10X PBS and 10g of sucrose was added and the solution was brought to a final volume of 500mL with distilled water. The solution was sterile filtered,

aliquoted into single use tubes, and stored at -20 degrees.

Protein purification from bacteria

GST-RuvC was purified from Arctic Express *Escherichia coli* (Agilent technologies) as previously described with a few modifications (Thada and Cortez, 2019). Briefly, 5ml cultures were grown in Luria Bertani (LB) medium with the appropriate antibiotic overnight. Next day, cells were seeded 1:40 into 200ml LB without antibiotics until O.D ~0.6. Bacteria are then induced with 1mM IPTG for 3h at 30°C or 0.1mM for 16h at 18°C. Bacteria are resuspended in NET buffer (25 mm Tris (pH 8), 50 mM NaCl, 0.1 mM EDTA, 5% glycerol, 1mM DTT, 5 µg/ml aprotinin, and 5 µg/ml leupeptin) and sonicated. Triton X-100 was then added to a final concentration of 1%, and lysates were incubated on ice for 30 min. Following centrifugation, cleared lysates were incubated with GSH-Sepharose beads (GE Healthcare) for 2.5 h at room temperature followed by 4°C overnight. Beads were then washed three times with NET buffer and 1% Triton X-100. Bound proteins were eluted using elution buffer (75 mM Tris (pH 8), 15 mM Glutathione, and 5 µg/ml leupeptin). The eluate was then concentrated using speed vac and dialyzed into 20 mm HEPES-KOH (pH 7.5), 50 mm NaCl, and 1 mm DTT twice, once for 2 h, and then again overnight.

Protein purification from baculovirus infected Sf9 cells

His-MBP-RADX and His-MBP-RADX QVPK was purified from baculovirus infected *Sf9* cells as previously described (Adolph et al., 2021). Briefly, cells were lysed in buffer containing 20 mM Tris (pH 7.5), 150 mM NaCl, 10 mM NaF, 10 mM sodium phosphate monobasic, 10 mM sodium pyrophosphate, 1% Triton X-100, 10% glycerol, 1 mM DTT, and a cOmplete protease inhibitor cocktail tablet (Roche). After high-speed centrifugation, the cleared lysates were incubated with Talon metal affinity resin for 2 hours at 4°C. The beads were washed once in buffer containing 1% Triton X-100, 500 mM NaCl in PBS and then washed in buffer containing 50 mM Tris (pH 8.0), 300 mM NaCl and increasing amounts of imidazole (5-20 mM). The bound proteins were eluted in 50 mM Tris (pH 8.0), 300 mM NaCl, 10% glycerol, and 1 mM DTT and 200 mM imidazole. The fractions containing protein were then subjected to size exclusion chromatography on a Superdex 200 10/300 Increase GL (GE Healthcare) in elution buffer with added protease inhibitors.

Antibody	Species	Dilution	Company	Catalog number	Notes
RAD51	Mouse	1:250	Abcam	ab213	Overnight incubation at 4°C
BrdU (IdU)	Mouse	1:5	BD	347580	
BrdU (CldU)	Rat	1:25	Abcam	ab6326	
γH2AX (JBW301)	Mouse	1:9000	Millipore	05-636	
HA	Rat	1:500	Roche	11867423001	
53BP1	Rabbit	1:1000	Abcam	ab175933	No pre-extraction required
Alexa Flour 488 or 594 azide		1:250	Invitrogen	A10266 or A10270	
RPA	Mouse	1:200	Abcam	Ab2175	
Biotin	Rabbit	1:200	Cell signaling	5597	
RuvC	Mouse	1:250	Santacruz	5G9/3	

Table 2.1. Summary of antibodies for immunofluorescence

FLAG-SMARCAL1 and FLAG-ZRANB3 were purified from baculovirus-infected insect cells using the same methodology as previously described (Betous et al., 2013b). Briefly, cells were lysed in 20 ml buffer containing 20 mM Tris (pH 7.5), 150 mM NaCl, 0.1 mM EDTA, 1 mM DTT, 0.2 mM PMSF, 1 mg/mL leupeptin, 1 mg/mL aprotinin, and 0.1% Triton X-100. After high-speed centrifugation, the cleared lysates were incubated with 250 µl Flag-M2 beads (Sigma) for 4h at 4°C. The beads were washed three times in LiCl buffer (lysis buffer containing 0.3 M LiCl) and twice in KCl buffer (20 mM HEPES at pH 7.6, 20% glycerol, 0.1 M KCl, 1.5 mM MgCl2, 0.2 mM EDTA, 1 mM DTT, 0.2 mM PMSF, 0.01% IGEPAL CA-630). The bound proteins were eluted in 2 ml KCl buffer containing 0.25 mg/mL FLAG peptide on ice, concentrated using Amicon Ultra-4 50K MWCO (Millipore) flash-frozen, and stored at −80°C. Generally, one can expect concentrations of SMARCAL1 and ZRANB3 around 1-5 µM and ~300-500 nM for RADX.

Protein purification from 293T

GFP-FLAG-RADX and GFP-FLAG-RADX QVPK was purified from 293T cells in the presence or absence of 3 mM hydroxyurea for 5 hours. Cells were lysed in buffer containing 20 mM Tris (pH 8.0), 150 mM NaCl, 0.5% NP40, 1mM EDTA and a cOmplete protease inhibitor cocktail tablet (Roche). Clarified lysates were incubated with FLAG M2 Magnetic Beads (Sigma) for 2 hours at 4°C. The beads were washed twice in lysis buffer, twice in lysis buffer containing 0.3mM LiCl, twice in ATP buffer containing 50mM Tris (pH 8.0), 200mM NaCl, 5mM MgCl2, 5mM ATP and twice in elution buffer containing 50 mM Tris (pH 8.0), 150 mM NaCl, 10% glycerol, 5mM MgCl2 and 1 mM DTT. The bound proteins were eluted in elution buffer with 0.25 mg/mL Flag peptide for 90 minutes at 4°C. The eluate was depleted of RPA contamination. ProteinG magnetic beads were incubated with RPA antibody at 4°C for 90 minutes followed by incubation with eluate for 1 hour at 4°C. The eluate was concentrated with Amicon Ultra-4 50K MWCO (Millipore) flash-frozen, and stored at −80°C.

Electron microscopy

For EM analysis of replication intermediates, I collaborated with Jessica Jackson from Dr. Vindigni lab at Washington University, St. Louis. I purified genomic DNA while Jessica completed the rest of the processing and imaged the grids. The protocol is as described below

5-10 x10^6 U2OS cells transfected with the indicated siRNAs were collected immediately after treatment with 3 mM hydroxyurea for 5 hours. Untreated cells were also included. DNA was cross-linked by incubating with 10 µg/mL 4,5′,8-trimethylpsoralen followed by a 3-minute exposure to 366 nm UV light on a precooled metal block, for a total of three rounds. Cells were lysed and genomic DNA was isolated from the nuclei by proteinase K digestion and chloroform-isoamyl alcohol extraction. Genomic DNA was purified by isopropanol precipitation and digested with PvuII HF with the appropriate buffer for 4 hours at 37°C. Replication intermediates were enriched on a benzoylated naphthoylated DEAE-cellulose (Sigma-Aldrich) column. Samples were prepared for visualization by EM by spreading the purified, concentrated DNA on a carbon-coated grid in the presence of benzyl-dimethyl-alkylammonium chloride, followed by platinum rotary shadowing. Images were obtained on a JEOL JEM-1400 electron microscope using a bottom mounted AMT XR401 camera. Analysis was performed using ImageJ software (National Institute of Health). EM analysis allows distinguishing duplex DNA—which is expected to appear as a 10 nm thick fiber after the platinum/carbon coating step necessary for EM visualization—from ssDNA, which has a reduced thickness of 5-7 nm. Criteria used for the assignment of a three-way junction, indicative of a replication fork, include the joining of three DNA fibers into a single junction, with two symmetrical daughter strands and single parental strand. Reversed replication forks consist of four DNA fibers joined at a single junction, consisting of two symmetrical daughter strands, one parental strand and the addition of a typically shorter fourth strand, representative of the reversed arm. The length of the two daughter strands corresponding to the newly replicated duplex should be equal (b = c), whereas the length of the parental arm and the regressed arm can vary (a ≠ b = c ≠ d). Conversely, canonical Holliday junction structures were characterized by arms of equal length (a = b, c = d). Particular attention is paid to the junction of the reversed replication fork in order to observe the presence of a bubble structure, indicating that the junction is opened up and that it is simply not the result of the occasional crossover of two DNA molecules. These four-way junctions of reversed replication forks may also be collapsed and other indicators such as daughter strand symmetry, presence of single-stranded DNA at the junction or the entire structure itself, all are considered during analysis (Neelsen et al., 2014). The frequency of reversed forks in a sample is computed using the Prism software.

Radioactive labeling of substrates

5µl of 10µM oligonucleotide was labeled in a 20µl reaction with 3µl Hot ATP and 2µl 10X PNK buffer for 2 hours at 37°C. Following the reaction, the enzyme can be inactivated by heating the reaction to 65°C for twenty minutes. The labeled substrate was then separated from unincorporated 32γP-ATP using a P30 Tris chromatography column (BioRad). To use the P30 columns, mix the resin well before opening and snapping the bottom. Spin at 850 rcf (on SOFT mode) in an Eppendorf tabletop centrifuge for 2 minutes. Rinse the column with 500ul TE (0.1mM EDTA, 20mM Tris-HCl pH 7.5) 2X. Spin at 900 rcf for 2 minutes after each wash. Add up to 50µL of sample. Spin another 2 minutes at 850 rcf. The flow-through contains the labelled substrate. The concentration of the eluate can be estimated by the volume of the elution. I typically recover in the range of 500nM-1.25µM.

Preparation of fork regression substrates

I have used the same substrates that Drs. Remy Betous and Kamakoti Bhat used. The oligos are listed in the table below (Table 2.2.). Oligos were ordered from IDT and were PAGE purified.

Preparation of fork junction (3 oligo; leading strand gap)

5′ ^{32}P-labeled nascent lag82 (135 nM final) was annealed with unlabeled parental lag122 (160 nM final) in 1X saline-sodium citrate (SSC) buffer in 20ul reaction. The reaction is heated for 3 minutes at 95°C and gradually cooled down to room temperature overnight. I do this in the heat block and cover with a layer of aluminum foil over which I place a stack of paper towels and put on the lid to cool gradually overnight.

The following day, unlabeled parental lead122 (175 nM final) was added to the annealed lag reaction from the previous day and annealed in 25mM Tris acetate pH 7.5, 5mM Magnesium acetate, 0.1mg/ml BSA, 2 mM DTT at 75°C for 3 minutes and then cooled down to room temperature for 3-4 hours. This is also done on the heat block using the same method detailed

	Substrate structures	Label	Sequence
Fork reversal	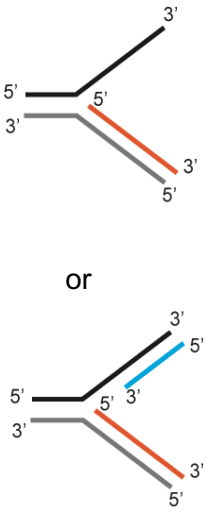	Lead 122	CGTGACTTGATGTTAACCCTAACCCTAAGATATCG CGTTATCAGAGTGTGAGGATACATGTAGGCAATTG CCACGTGTCTATCAGCTGAAGTTGTTCGCGACGT GCGATCGTCGCTGCGACG
		Lag122	CGTCGCAGCGACGATCGCACGTCGCGAACAACTT CAGCTGATAGACACGTGGCAATTGCCTACATGTAT CCTCACACTCTGAATACGCGATATCTTAGGGTTAG GGTTAACATCAAGTCACG
		Lag82	TCAGAGTGTGAGGATACATGTAGGCAATTGCCAC GTGTCTATCAGCTGAAGTTGTTCGCGACGTGCGAT CGTCGCTGCGACG
		Lead52	CGTCGCAGCGACGATCGCACGTCGCGAACAACTT CAGCTGATAGACACGTGG

Table 2.2. List of oligonucleotides used for making fork regression substrates. The underlined letters indicate mismatches to prevent spontaneous branch migration.

above. Following the annealing, the substrate was gel purified using an 8% 1X TBE gel run at 80V for 60 minutes at room temperature. The wet gel was wrapped in saran wrap, taped to a cassette and a whatmann paper dotted with diluted 32γP-ATP as ladder was taped beside the gel. The gel was exposed to a screen for 30 minutes. The band is excised and transferred to a 3500 MWCO snake skin membrane in 2ml 0.25X TBE and electro-eluted for overnight at 60V in an EtBr-free box. The eluted buffer was concentrated using speed vac 0.1mTorr for 4h and stored at -20°C until further use. The concentration of the substrate was determined using the products (see below) as standards.

Preparation of fork junction (4 oligo; leading strand gap)

5′ ^{32}P-labeled nascent lead52 (135 nM final) was annealed with unlabeled parental lead122 (160 nM final) in 1X SSC buffer in 20ul reaction. Separately, unlabeled lag82 (160nM final) was annealed with lag122 (160nM final) in 1X SSC buffer. The reaction is heated for 3 minutes at 95°C and gradually cooled down to room temperature overnight.

The following day, the leading and lagging substrates from the previous day were combined in a 50ul reaction and annealed in 25mM Tris acetate pH 7.5, 5mM Magnesium acetate, 0.1mg/ml BSA, 2 mM DTT at 75°C for 3 minutes and then cooled down to room temperature for 3-4 hours. The annealed substrate was purified using the same protocol as described above.

Creating the products for the reaction (to run as size controls)

The product for the 3-way junction substrate is labeled lag82. For the 4-way junction, anneal unlabeled lag82 (160nM final) and labeled lead52 (135 nM final) in 1X annealing buffer. The reaction was heated for 3 minutes at 75°C and then cooled to room temperature. The concentration of products is ~150nM.

Fork regression assays

The reactions were performed essentially as described previously (Betous et al., 2013a). Briefly,

1 nM (molecules) DNA substrate was used for fork reversal assays. The assays were carried out in reaction buffer containing 25 mM Tris- HCl pH 7.5, 5 mM MgCl2, 2 mM DTT, 10mM NaCl, 0.1 mg/ml BSA, and 2.5 mM ATP. Master-mixes were prepared on ice and when indicated, RAD51 was added to the master-mix for 5 minutes. Next, reactions were supplemented with other recombinant proteins such as 10nM RPA and increasing concentrations of RADX and incubated for 10 minutes at room temperature. Then, 2nM SMARCAL1 was added to the reaction and incubated for an additional 20 minutes at 37°C before the reactions were terminated by addition of 4 µL stop buffer (1mg/ml Proteinase K, 0.2% SDS [w/v], 30% glycerol, 25mg/ml Ficoll) and incubation for 20 minutes at 37°C. Samples were loaded onto 10% polyacrylamide (19:1 acrylamide:bisacrylamide) gels and separated for 60 minutes at 80 V at room temperature. The gels were dried, imaged, and quantified using a phosphorimager.

Telomere PNA FISH

Telomeric Peptide Nucleic Acid Fluorescence *In situ* Hybridization (PNA FISH) was essentially carried out as described previously (Celli and de Lange, 2005). Briefly, cells were treated with 0.1 µg/ml colcemid for 2 hours before collecting. Harvested cells were incubated for 20min at 37°C with 75mM KCl to allow the cells to swell, fixed with cold 3:1 methanol:glacial acetic acid, and dropped onto glass slides. Cells were then rehydrated in PBS, fixed with 4% formaldehyde, treated with 1mg/ml pepsin at 37°C, dehydrated sequentially in 70%, 95%, and 100% ethanol, and air-dried. Slides were then hybridized with Cy3-TelC (Cy3-CCCTAACCCTAACCCTAA-3′) in hybridization mix (10 mM Tris-HCl pH 7.2, 70% deionized formamide, 0.5% blocking reagent [Roche 11096176001]), washed twice with hybridization wash buffer I (70% formamide, 10 mM Tris-HCl pH 7.2, 0.1% BSA), and washed three times in hybridization wash buffer II (100mM Tris-HCl pH 7.2, 150 mM NaCl, 0.08% Tween-20) with DAPI added to the second wash. Slides were dehydrated with an ethanol series, air-dried, and mounted with Prolong Gold. Images were obtained using a 40X oil objective (Nikon Eclipse Ti). For aphidicolin treatment, 0.2 µM aphidicolin was added to cells for 40h prior to harvesting.

DNA fiber analysis using spreading

DNA fiber analysis of DNA replication was carried out essentially as described previously (Couch

et al., 2013) with few modifications. Briefly, cells were labeled with 20 μM CldU for 20 minutes, washed twice with HBSS and labeled with 100 μM IdU for 20 minutes. Cells were washed twice again with HBSS and then treated with or without HU prior to collection. Cells were collected and resuspended at a concentration of $1x10^6$ cells/ml in cold PBS. The labelled cells were diluted 1:2 with unlabeled cells to keep the final volume above 50ul and 2μl of the diluted mix was spread in a thin line onto a glass slide. The slide was allowed to dry for 6 minutes, following which 10μl of spreading buffer (0.5% SDS, 200 mM Tris-HCl pH 7.4, 50 mM EDTA) was added to the sample for 6 minutes. The fibers were then stretched by tilting the slides at 15° angle and allowed to air-dry for 40 minutes before being fixed for two minutes with a 3:1 methanol: acetic acid mixture. The slides were dried for twenty minutes and stored at -20 degrees overnight. The next day, DNA was denatured in 2.5M HCl for 70 minutes, washed three times with PBS and blocked in 10% goat serum/PBS with 0.1% triton X-100 for 1 hour. The DNA was stained with 100 μl of antibodies recognizing IdU and CldU for 2 hours (rat monoclonal anti-BrdU (anti-CldU) and mouse anti-BrdU (anti-IdU) 1/100 diluted in blocking solution) and probed with 100 μl of secondary antibodies (goat anti-rat IgG Alexa Fluor 594 and Goat anti-mouse Alexa Fluor 488 1:350 in blocking solution) for 1 hour in the dark. The slides were them mounted using prolong Gold with no DAPI and allowed to dry overnight in the dark. Images were obtained using a 40X oil objective (Nikon Eclipse Ti) and fiber lengths analyzed using NI-elements software.

DNA fiber analysis using combing

After harvesting, 650,000 U2OS or 350,000 HCT116 cells were pelleted, resuspended in 45ul of cold PBS and mixed with 45ul of Buffer 2 (1.5% low melting agarose in PBS) held at 50°C. The mixture was then pipetted into molds and allowed to set at 4°C for 30 minutes. The plugs were immersed in ~250ul of Buffer 3 (450mM EDTA pH 8.0, 20mg/ml proteinase K, 0.01% Sarkosyl) per plug and incubated at 50°C overnight. The next day, the plugs were washed in 15ml of 1X TE buffer three times for at least an hour each. The plugs were then melted in Buffer 7 (100mM MES pH 5.7) at 68°C for 20 minutes and at 42°C for 10 minutes, then 1.5ul of b-agarase was added to each plug and held at 42°C overnight. Melted plugs were mixed with 1.2ml of Buffer 7 in a reservoir and combed onto coverslips using the Fibercomb Molecular Combing instrument from Genomic Vision. The coverslips were stained as described above with the following modifications. Coverslips were denatured in 0.5M NaOH, 1M NaCl for 8 minutes at room temperature, washed

with 3X PBS, and dehydrated sequentially with 70% ethanol, 90% ethanol, and 100% ethanol for 5 minutes each. The coverslips were blocked with 10% goat serum/PBS with 0.1% triton X-100 for 1 hour. The DNA was stained with at least 50ul of 1:25 rat monoclonal anti-BrdU (anti-CldU) and 1:5 mouse anti-BrdU (anti-IdU) diluted in blocking solution. The coverslips were probed with 50 µl of secondary antibodies (goat anti-rat IgG Alexa Fluor 594 and Goat anti-mouse Alexa Fluor 488 1:250 in blocking solution) for 1 hour in the dark. The slides were them mounted using prolong Gold with no DAPI and allowed to dry overnight in the dark. Images were obtained using a 40X oil objective (Nikon Eclipse Ti) and fiber lengths analyzed using NI-elements software.

Strand exchange assay

The strand exchange assay was performed as described and conditions adapted from (Bugreev and Mazin, 2004). Briefly, fX174 circular ssDNA (30 mM) was incubated with RAD51 (7.5 mM) for 10 minutes at 37°C in buffer containing 20 mM HEPES pH 7.5, 1 mM MgCl2, 1 mM CaCl2, 2 mM ATP, 1 mM DTT, and 100 mM (NH4)2SO4 added at the time of dsDNA addition. Then, RPA was added to the reaction at a final concentration of 2 mM and further incubated for 10 minutes. The reaction was initiated by the addition of 30 mM fX174 dsDNA, linearized by ApaL1, and the reaction proceeded for 180 minutes. The addition of RADX (150 nM) is indicated in the reaction scheme. Time points were taken at 0, 30, and 180 minutes by removal of 7 ul of reaction mixture into 3 mL of 0.5% SDS and 0.5 mg/mL proteinase K, and incubated for 20 minutes at 37°C. After addition of loading dye, the deproteinized samples were loaded onto a 1% agarose gel in 1X TAE buffer and electrophoresed at 20V for 16 hr. The products were visualized after one- hour ethidium bromide staining and quantified using ImageLab software (BioRad) Total percent strand exchange was calculated using the integrated intensities of the dsDNA and product bands, and the formula (JM/1.5)+NC/((JM/1.5)+NC)+ dsDNA (Liu et al., 2011).

Displacement loop assay

32P-labeled oligonucleotide D1 (3 mM) which is complementary to positions 1932–2022 of pBluescript SK DNA was incubated with RAD51 (1 mM) in buffer containing 25 mM TrisOAc pH 7.5, 20 mM KCl, 1 mM CaCl2, 1 mM ATP and 1 mM DTT for 5 min at 37°C. RADX was added to the reactions at the same time as the addition of supercoiled pBluescript SK (35 mM base pairs)

to initiate the reaction. Reactions were incubated at 37°C and at the indicated time point (0, 5, 15 min) an aliquot of the reaction was removed and added to SDS (0.5%) and Proteinase K (5 mg/ml) to deproteinize the reactions, followed by a 20 min incubation at 37°C. All reaction products were resolved on a 1% agarose gel, dried and visualized using a phosphorimager (Typhoon FLA 7000, GE Healthcare) and quantified using ImageLab (BioRad).

Neutral comet assay

Cells were seeded the day before the treatment at $1X10^5$ cells per well of a 6-well dish. On the day of the treatment, cells were treated and harvested by trypsinization. Cells were washed once with cold PBS then resuspended at $2x10^5$ per mL in cold PBS. During this time, low melting temperature agarose (Trevigen) was melted at 95 deg and held in a 42 or 37-degree water bath. To prepare slides, 10µl of cell suspension was mixed with 100 µL of agarose and spread into one well of a COMET slide (Trevigen). Slides were allowed to gel for 30 minutes at 4 degrees. Slides were then immersed in pre-chilled Lysis Buffer (Trevigen) for 1 hour at 4 degrees or overnight at 4 degrees. Slides were rinsed twice with pre- chilled TAE (40 mM Tris Base, 20 mM Acetic acid, 1 mM EDTA, pH 8.45), then washed for 30 minutes by immersing in TAE at 4 degrees. Slides were then electrophoresed for 45 minutes at 1 V/cm immersed to a depth of at least 0.5 cm in TAE [this translates to 21V and 850 ml buffer on our apparatus]. After electrophoresis, slides were immersed in DNA Precipitation Solution (1M NH4Ac, 87% EtOH) for 30 minutes at room temperature. Next, slides were immersed in 70% ethanol for 30 minutes at room temperature then dried for 15 minutes at 45 degrees and stored overnight at room temperature. Slides were stained with 250uL per well of 1X SYBR Green I (Trevigen) diluted in 1X TE for 30 minutes at room temperature. SYBR Green solution was decanted and slides allowed to dry at least 30 minutes before visualizing. At least 100 cells were scored for each condition.

Alamar blue viability assay

Cell Plating: 72 hours post siRNA transfection, U2OS cells were trypsinized and plated in 96-well plates at a density of 4,000 ($4x10^3$) cells per well in a volume of 100µL. For a full 96 well dish, 15mL of DMEM + 7.5% FBS with $6x10^5$ cells is required to give $4x10^3$ cells/100µL.

Preparing Drugs: Drug dilutions at 10X higher than the desired concentration were prepared and 200 µL was pipetted into one column of a 96 well plate. Using automatic pipettes, 10µL of drug

per well was pipetted into the 96 well plates with cells.

Drug ranges
HU: 0.1-10mM
CPT: 0.1-20nM

Day 3 or 4 after drug addition, media was replaced with diluted alamar blue (Invitrogen) according to manufacturer's instructions, incubated and read.

Clonogenic viability assay

For clonogenic survival assays, appropriate number of cells were plated and treated with Olaparib or hydroxyrurea for approximately two weeks. Colonies were stained by methylene blue staining (48% methanol, 2% methylene blue, 50% water) and scored. All clonogenic survival assays were completed in triplicate.

Western blotting

Cells were lysed with NP-40 lysis buffer (1% NP-40, 50mM Tris pH 7.4, 150mM NaCl, 0.1% SDS, 1mM DTT, and protease inhibitor tablets) for 30 minutes on ice and spun at 16500rcf for 20 minutes to remove insoluble fractions. The lysate was then quantified using DC assay (BioRad) according to manufacturer's instructions. 2x SDS loading buffer (50µg/mL SDS, 25% glycerol, 156mM Tris pH 6.8, 12.5mg/mL bromophenol blue) was added to sample and boiled for 5 minutes. Samples were separated by gel electrophoresis on polyacrylamide gels and protein was transferred to nitrocellulose or PVDF membrane at 4°C with constant current at 0.2mA for between 4-8 hours. Antibodies used for protein detection are detailed in Table 2.3. The membrane was blocked with 5% milk diluted in 1x TBST and antibodies were diluted in 1% milk in TBST. Blots processed by Chemiluminescence (HRP) were blocked and antibodies were diluted according to manufacturer's instructions. Note that for RADX, at least 90ug of protein is required for a visible band on the blot.

Cell culture

U2OS and HEK293T cells were cultured in DMEM with 7.5% fetal bovine serum (FBS). RPE-hTERT cells were cultured in DMEM F12, 7.5% FBS, and 7.5% sodium bicarbonate. CAPAN-1 and DLD-1 cells (gift from Dr. Douglas Bishop) were cultured in RPMI with 20% FBS, and 1mM sodium pyruvate. BJ-hTERT and T131P cells were cultured in DMEM with 15%FBS and MEM Non-Essential Amino Acids (NEAA). HCT116 cells were culture in McCoy's medium with 7.5% FBS. HeLa1.3 with long telomeres were a gift from Dr. Titia de Lange and were cultured in DMEM with 10% FBS.

Transfection reagents

siRNA transfections were performed using Dharmafect-1 (Dharmacon) in a 60mm dish format for U2OS, A549 and BT549 cells, Dharmafect4 (Dharmacon) for CAPAN-1 cells and RNAiMax (Thermo Fisher) for RPE-hTERT and 293T cells according to manufacturer's instructions. Forward transfection protocol using RNAimax (Thermo Fisher) was performed in 35mm dishes for the fibroblast cell lines (BJ and T131P). Plasmid transfections were performed using Polyethyleneimine (PEI) or FUGENE HD according to manufacturer's instructions. Transfections are carried out as listed in Table 2.4

Proximity ligation assay

To determine nascent chromatin localization, cells were plated in a 96-well plate and labeled with 10 mM EdU for 20 min. Cells were permeabilized using 0.5% Triton X-100 solution (20mM HEPES, 50mM NaCl, 3mM MgCl2, 300mM Sucrose and 0.5% Triton X-100) and fixed in 3% paraformaldehyde minutes on ice. Cells were then incubated in 10% goat serum followed by antibodies to FLAG (Sigma F3165) and anti-biotin to recognize EdU after conjugation to biotin azide (Cell Signaling 5597). Proximity ligation was completed according to the manufacturer's protocol (Sigma) and images were obtained and quantified using a Molecular Devices ImageXpress instrument.

	Antibody	Species	Dilution	Company	Catalog number	Notes
Western blot	RADX	Rabbit	1:1000	Novus Biologicals	NBP2-13887	Load at least 90μg; probe overnight at 4°C
	RAD51	Rabbit	1:1000	Abcam	Ab63801	
	BRCA2	Mouse	1:50	Calbiochem	OP95	Load 80μg
	GAPDH	Mouse	1:1000	Millipore	MAB374	
	RTEL1	Rabbit	1:500	Novus Biotechne	NBP2-22360	
	ABRO1	Rabbit	1:1000	Abcam	ab83860	
	BOD1L		1:500	N/A	Gift from Grant Stewart	Lyse in Urea buffer
	MUS81	Mouse	1:1000	Abcam	ab14387	
	SMARCAL1-909	Rabbit	1:1000	Open	Custom antibody	
	ZRANB3	Rabbit	1:500	Bethyl	A303-033A	Run longer to separate from non-specific band
	RPA32	Mouse	1:1000	Abcam	ab2175	
	RPA32 S4/S8	Rabbit	1:1000	Bethyl	A300-245A	
	HA	Rat	1:500	Roche	11867423001	
	KU80	Rabbit	1:1000	Abcam	ab33242	
	KU70	Mouse	1:1000	Abcam	ab3114	
	BRCA1	Mouse	1:100	Oncogene	OP92	Load 80μg
	HLTF	Rabbit	1:1000	Abcam	ab183042	
	RuvC	Mouse	1:1000	Santacruz	5G9/3	
	DNA2	Rabbit	1:1000	Abcam	ab96488	
	FANCA	Rabbit	1:500	Bethyl	A301-980A	
	FANCD2	Mouse	1:500	Santacruz	sc-20022	

Table 2.3. Summary of antibodies used for western blotting

	Cell line	Forward/ Reverse	Number of cells	Transfection protocol
siRNA transfection	U2OS	Reverse	$3X10^5$ cells in 60mm dish	6.4μl of Dharmafect + 40pmoles of siRNA; 500μl optimem each --Incubate 20 minutes at room temperature and add dropwise to cells
	HCT116	Reverse	$1X10^6$ cells in 35mm dish	5μl RNAimax + 20pmoles siRNA in 200μl of optimem each --Incubate 15 minutes at room temperature and add dropwise to cells
	RPE-hTERT	Reverse	$13X10^5$ cells in 60mm dish	5.9μl of RNAimax + 40pmoles siRNA in 500μl optimem each --Incubate 15 minutes at room temperature and add dropwise to cells
	HeLa1.3	Reverse	$1X10^6$ cells in 35mm dish	5μl RNAimax + 25pmoles of siRNA; 250μl of optimem each --Incubate 15 minutes at room temperature and add dropwise to cells
	293T	Reverse	$1X10^6$ cells in 35mm dish	5μl RNAimax + 20pmoles of siRNA; 200μl of optimem each --Incubate 15 minutes at room temperature and add dropwise to cells
	DLD-1	Reverse	$3X10^5$ cells in 60mm dish	6.4μl of Dharmafect + 40pmoles of siRNA; 500μl optimem each --Incubate 20 minutes at room temperature and add dropwise to cells
Plasmid transfection	U2OS	Forward	1.2×10^5 cells in 35mm dish	1μg DNA+4μl Fugene in 100μl Optimem --Incubate 5 minutes at room temperature and add dropwise to cells
	293T	Forward	$3X10^6$ cells in 100mm dish	4μg DNA in 100μl Optimem. Add 24μl PEI --Incubate 15 minutes at room temperature and add dropwise to cells

Table 2.4. Summary of transfection conditions used in this work

Generation of cell lines stably overexpressing cDNA

Virus production: 2-3x10^6 GP2-293 cells were plated in a 10cm dish. 24 hours later 1 μg of pVSV-G and 2μg of pLEGFP-CX (*neo*-RADX or *neo*-RADX QVPK or *neo*-RADX OBm) was transfected using 1 mg/ml PEI. The next day, cells were washed with PBS and 5-6ml of complete media was added. 48 hours later, media was collected in a 15ml tube and placed at 4 degrees. Another 5-6 ml of complete media was added to transfected cells. 24 hours later, media was collected and pooled. 10-12ml of collected media was spun at low speed to pellet any cell debris. The supernatant was transferred to a new 15ml tube, aliquoted and stored at -80 degrees for future use.

CRISPR-Cas9 editing

U2OS RADXΔ, SMARCAL1Δ, ZRANB3Δ, HLTFΔ, SMARCAL1/ZRANB3/HLTF triple knockout, and FBH1Δ cells were generated using CRISPR/Cas9 as described previously (Dungrawala et al., 2017; Liu et al., 2020). Briefly, cells were transfected with pSpCas9(BB)-2A-Puro 4 (Addgene plasmid no. 48139) containing guide RNAs listed in Table 2.5, selected with 2 μg/ml puromycin for two days prior to plating for individual clones. Homozygous editing of the locus was confirmed by genomic DNA PCR and sequencing. The cell lines were also validated for loss of expression by immunoblotting.

	gRNA target	gRNA sequence
CRISPR-Cas9	RADX	CACCGAATCAAAACTGCGATACTA and CACCGTTACCATTACATGTTAAAC
	SMARCAL1	GCCCAGATTGCATCAACGTCG
	ZRANB3	AGCTTTGCTCTTAGTCTGTC
	HLTF	CACCGGTTGGACTACGCTATTACAC
	FBH1	CAGGAAGCTTGGTCCTCTGA

Table 2.5. sgRNA sequences used for CRISPR-Cas9 editing

CHAPTER III

RADX MODULATES RAD51 ACTIVITY TO CONTROL REPLICATION FORK PROTECTION[1]

PREAMBLE

I began working on the RADX project in my first year in the lab. This chapter represents some of my initial work on this project that was published as an article in Cell Reports. While I am listed as the second author on the manuscript, I completed approximately half the experiments in the paper. I have indicated the contributions from Drs. Kamakoti Bhat and Huzefa Dungrawala where appropriate.

INTRODUCTION

ssDNA binding proteins regulate DNA replication, recombination and repair. In eukaryotes, the major ssDNA binding proteins at replication forks include RPA and RAD51. RAD51 is best known for its ability to form nucleoprotein filaments on resected double-strand breaks and catalyze strand invasion for HR (Kowalczykowski, 2015). RAD51 also has at least two functions at stalled replication forks. First, it cooperates with SNF2 family DNA translocases to promote fork reversal (Betous et al., 2012; Ciccia et al., 2012; Kile et al., 2015; Vujanovic et al., 2017; Zellweger et al., 2015). Second, in cooperation with BRCA2, RAD51 inhibits degradation of the nascent DNA after fork reversal of persistently stalled forks (Hashimoto et al., 2010; Lemacon et al., 2017; Mijic et al., 2017; Schlacher et al., 2011; Taglialatela et al., 2017). In addition to BRCA2-deficiency, loss of several other HR proteins cause nascent-strand degradation (Higgs et al., 2015; Schlacher et al., 2011; Schlacher et al., 2012). At least two nucleases, MRE11 and DNA2, are involved. How these pathways work together to maintain fork stability is still unclear. Small amounts of nuclease action could be beneficial to remove DNA lesions or end binding proteins, control the amount of

[1] This chapter was adapted from Bhat *et al*., 2018

ssDNA at a stalled fork, remodel the reversed fork and promote fork restart (Thangavel et al., 2015); however, unregulated degradation causes genome instability (Schlacher et al., 2011; Schlacher et al., 2012).

Fork reversal may be independent of BRCA2 in some genetic contexts, thus explaining how nascent strand degradation can proceed from reversed forks in BRCA2-deficient cells (Mijic et al., 2017). How RAD51 gains access to persistently stalled forks without BRCA2 to mediate an exchange with RPA is unknown. Nonetheless, the need for RAD51 to promote reversal explains why silencing RAD51 using RNA interference is reported to not cause degradation (Mijic et al., 2017; Thangavel et al., 2015; Zellweger et al., 2015). Paradoxically, some RAD51 mutations and inhibitors do yield fork degradation (Dungrawala et al., 2017; Kolinjivadi et al., 2017b; Leuzzi et al., 2016; Mijic et al., 2017; Su et al., 2014; Taglialatela et al., 2017; Zadorozhny et al., 2017), raising the possibility that either fork reversal is not always required for nucleases to degrade the nascent strands or these ways of inhibiting RAD51 only interfere with some of its activities. Finally, as described earlier, fork degradation may be an important determinant of the viability of BRCA2-deficient cells and their sensitivity to PARP inhibitors (Ding et al., 2016; Dungrawala et al., 2017; Ray Chaudhuri et al., 2016; Rondinelli et al., 2017).

We recently identified a new ssDNA binding protein called RADX (introduced in Chapter I) (Dungrawala et al., 2017). RADX negatively regulates RAD51 accumulation at replication forks and we proposed that this regulation prevents inappropriate RAD51-dependent fork reversal in the absence of added replication stress. Presumably, at persistently stalled forks, the negative regulation of RAD51 by RADX is overcome by the positive regulation conferred by BRCA2 to sustain fork protection. Consistent with this hypothesis, knocking out RADX restores fork protection to BRCA2-deficient cells.

In this study, we sought to further test the hypothesis that RADX acts as a RAD51 antagonist and use RADX as a tool to investigate how fork protection pathways operate. Our findings support the model that RADX is a RAD51 antagonist that ensures the right amount of RAD51 fork reversal and protection activities to maintain genome stability. We also find a requirement for higher cellular levels of RAD51 to protect persistently stalled forks than to promote fork reversal.

Results

RADX silencing suppresses MRE11 and DNA2-dependent fork degradation in cells with impaired RAD51 filament stability

Multiple HR proteins including BRCA1 protect the nascent DNA at replication forks from MRE11 digestion by promoting RAD51 filament stability. To test the hypothesis that silencing RADX would restore fork protection in cells with decreased RAD51 activity, we utilized siRNA to deplete BRCA1 in U2OS cells and induce nascent strand degradation (Schlacher et al., 2011). Silencing RADX is sufficient to restore fork protection to BRCA1- depleted cells (Figures 3.1Aand 3.1B). This is not an off-target effect of siRNA since deletion of RADX using CRISPR-CAS9 also prevents nascent strand degradation after BRCA1 silencing (Figure 3.1C). RADX-deficiency also restores fork protection to BRCA1-depleted RPE-hTERT cells (Figure 3.1D), indicating that this effect is not cell-type specific. We did not observe any defects in fork protection upon RADX depletion alone, either by siRNA or RADX deletion (Figure 3.1). These results differ from a previous report that suggested RADX deficiency causes nascent strand degradation (Schubert et al., 2017). The reason for this difference is explained in Chapter IV.

In addition to their function in interstrand crosslink repair, the FA pathway proteins FANCA and FANCD2 also prevent MRE11-dependent nascent strand degradation (Schlacher et al., 2012). The exact mechanism by which these proteins act is unknown, but since RAD51 overexpression rescues the fork degradation in FA cells, we predicted that RADX depletion should also suppress this phenotype. Indeed, silencing FANCA or FANCD2 in U2OS cells causes fork degradation and silencing RADX restores fork protection in these cells (Figures 3.1E and 3.1F). As expected, silencing RADX also restores fork protection to fibroblasts harboring a FA-patient derived mutation in FANCD1/BRCA2 (Figure 3.1G).

We next asked if silencing RADX restores fork protection in contexts of reduced RAD51 filament stability and DNA2 nuclease activity. Recently, BOD1L was shown to suppress fork degradation by promoting RAD51 filament stability, but the degradation in BOD1L-deficient cells is MRE11-independent. Instead, DNA2 degrades the nascent DNA in this setting (Higgs et al., 2015). To test if RADX also regulates fork protection in cases where the degradation is dependent on DNA2, we utilized siRNA against BOD1L and RADX. RADX silencing restored fork protection to the

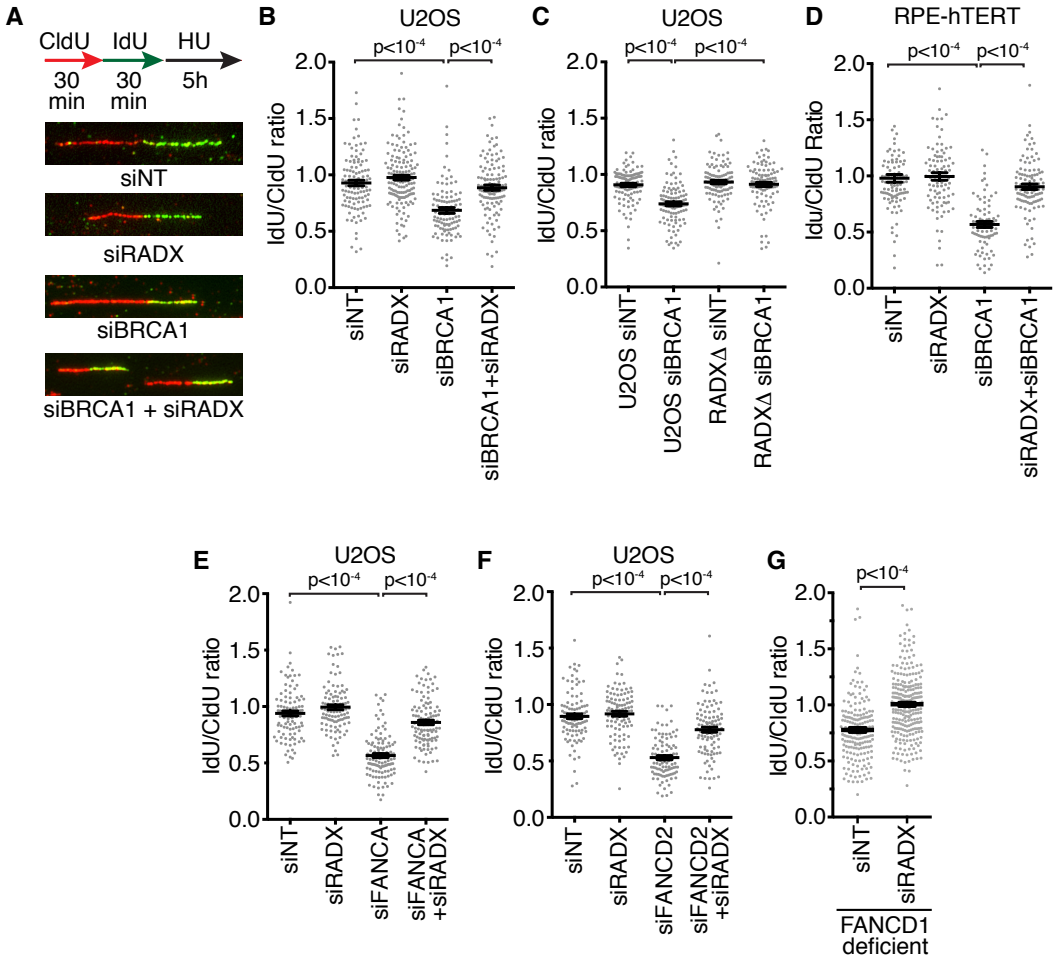

Figure 3.1. RADX silencing rescues the MRE11-dependent fork protection defects caused by loss of RAD51 stability (A) Graphical depiction of the fork protection assay with representative images. (A, B, C, E, F) U2OS or RADXΔ U2OS, (D) RPE-hTERT, (G) FANCD1/BRCA2-mutant fibroblasts, or (H) fibroblasts expressing the T131P RAD51 mutant were transfected with the indicated siRNAs then labeled sequentially with CldU and IdU before treatment with 3mM HU for 5 hours. The lengths of DNA fibers were measured and mean+/−SEM of the IdU/CldU ratio is depicted. P values were derived from Kruskal-Wallis ANOVA with a Dunn's post-test. Each experiment was repeated at least twice and a representative result is depicted. (siNT = non- targeting siRNA). Repeats of all figures were performed by Dr. Kami Bhat, Dr. Huzefa Dungrawala, and me.

BOD1L-deficient cells (Figure 3.4A). Thus, RADX deficiency restores fork protection irrespective of the nuclease mediating the degradation.

DNA2 also degrades nascent DNA in U2OS cells without any genetic perturbation when these cancer cells are treated with HU for long times (Thangavel et al., 2015). While RAD51 depletion rescues the fork degradation phenotype, RADX deletion does not restore fork protection in this circumstance (Figure 3.4B).

Restoration of fork protection to BRCA1-deficient U2OS cells does not cause resistance to PARP inhibitor or replication stress agents

Fork protection may be an important determinant of the chemosensitivity of BRCA-deficient cells to PARP inhibitors like Olaparib (Ding et al., 2016; Ray Chaudhuri et al., 2016). Consistent with this idea, RADX silencing not only confers fork protection to BRCA2-mutant cells, but also improves their viability and resistance to Olaparib even though it does not alter HR (Dungrawala et al., 2017). Therefore, Kami tested if the restoration of fork protection in BRCA1-deficient RADXΔ cells is accompanied by an increase in cell viability and Olaparib resistance. BRCA1 knockdown reduces U2OS cell viability, and RADX deletion conferred a small, but significant, increase in viability to BRCA1-depleted cells in the absence of any drug (Figure 3.2A), consistent with what was observed in BRCA2-deficient cells (Dungrawala et al., 2017). However, unlike in BRCA2-deficient cells, RADX loss did not confer Olaparib-resistance to BRCA1-depleted U2OS cells (Figure 3.2B). RADX loss also did not confer hydroxyurea or camptothecin resistance to BRCA1-depleted cells (Figures 3.3A, 3.3B, and 3.3C). In fact, the HU sensitivity caused by silencing RADX or BRCA1 by themselves is further increased in cells deficient for both proteins. Thus, despite restoring fork protection to BRCA1-deficient cells, RADX deficiency does not necessarily improve their sensitivity to replication stress inducing agents.

Overexpression of RADX causes nascent strand degradation that is rescued by inhibition of MRE11 or ZRANB3

While silencing RADX can restore fork protection to RAD51-compromised cells, RADX overexpression causes nascent strand degradation (Dungrawala et al., 2017). If the fork degradation is due to reduced RAD51 function, then it should be dependent genetically on the same factors that cause nascent strand degradation in BRCA2-deficient cells including the

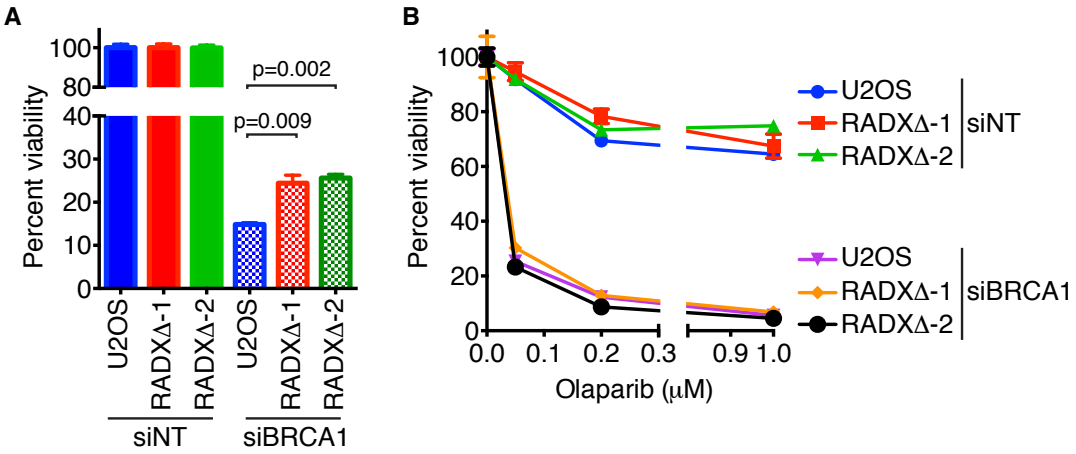

Figure 3.2. RADX loss partially restores viability in BRCA1-deficient cells but does not confer Olaparib resistance. (A and B) siRNA transfected parental or RADXΔ U2OS were plated for clonogenic survival assays in the absence (I) or presence (J) of drug. P values were calculated from a two-way ANOVA with Tukey's post-test. Mean+/−SEM from n=3 is depicted. Dr. Kami Bhat generated all the data in this figure.

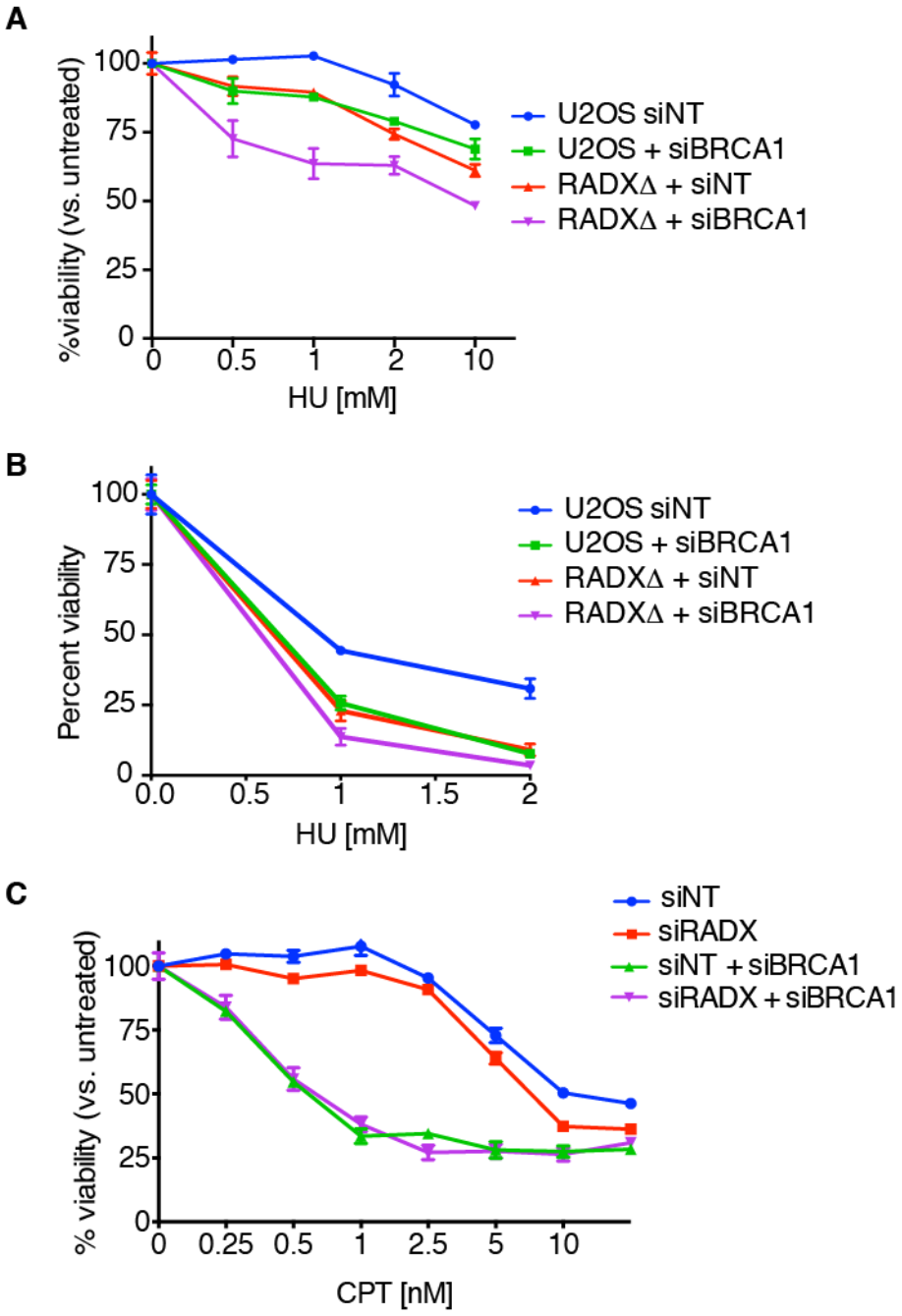

Figure 3.3. RADX deletion does not rescue the HU or CPT sensitivity in BRCA1-deficient cells. Parental or RADXΔ U2OS cells were transfected with the indicated siRNAs. Transfected cells were treated with the indicated concentrations of HU or CPT for 24h and examined for proliferation with alamar blue after two days (A and C) or clonogenic survival after 10-14 days (B). Mean+/-SEM from n=3 is depicted.

MRE11 nuclease and the fork reversal enzymes SMARCAL1 and ZRANB3 (Kolinjivadi et al., 2017b; Mijic et al., 2017; Taglialatela et al., 2017). As predicted, inhibiting MRE11 (Figure 3.4C), depleting SMARCAL1 or ZRANB3 rescues the fork degradation caused by RADX overexpression (Figures 3.4D and 3.4E). I also observed a partial rescue of the RADX overexpression-induced fork degradation by silencing DNA2 (Figure 3.4F). The ability of either DNA2 or MRE11 inhibition to rescue fork degradation in RADX overexpression cells is consistent with the idea that RAD51 destabilization can lead to either MRE11-dependent degradation as in BRCA2-deficient cells, or DNA2-dependent degradation, as in BOD1L-deficient cells.

Differential requirements of RAD51 in fork reversal and protection

RADX deficiency in unstressed cells causes replication fork breakage that can be rescued by silencing fork reversal proteins including RAD51, ZRANB3, and SMARCAL1 (Dungrawala et al., 2017). Thus, we hypothesized that RADX prevents fork reversal by antagonizing RAD51 at unstressed forks; a model that is consistent with the reduced amount of RAD51 at forks in RADX overexpressing cells (Dungrawala et al., 2017). However, if RAD51 is required for fork reversal, which is in turn required for fork degradation, we might have expected that RADX overexpression in HU-treated cells would inhibit RAD51-dependent fork reversal yielding stable nascent strands instead of the fork degradation that we observed. A possible explanation is that different RAD51 functions could be needed for fork reversal and fork protection and RADX only antagonizes the fork protection function. Alternatively, the same RAD51 function could be required for both reversal and protection, but more of it may be needed for fork protection than fork reversal. Consistent with the second hypothesis, knocking down RAD51 with multiple different siRNAs yields different phenotypic outcomes – fork stability or degradation (Figure 3.5A). Importantly, titrating the amount of a potent RAD51 siRNA into cells to yield partial RAD51 knockdown initially yields fork degradation at low concentrations and fork protection at higher concentrations (Figure 3.5B). The same result is observed with a second potent RAD51 siRNA (Figure 3.5C). These results indicate that the different siRNA results are not due to off-target effects but rather that the amount of RAD51 in the cell determines whether forks reverse and are then protected from nucleases. Consistent with this interpretation and our model that RADX negatively regulates RAD51, even a modest knockdown of RAD51 with an siRNA concentration that caused fork degradation in wild-type U2OS cells is sufficient to prevent degradation in U2OS cells overexpressing RADX (Figure 3.5D). This is presumably because the combination of partial

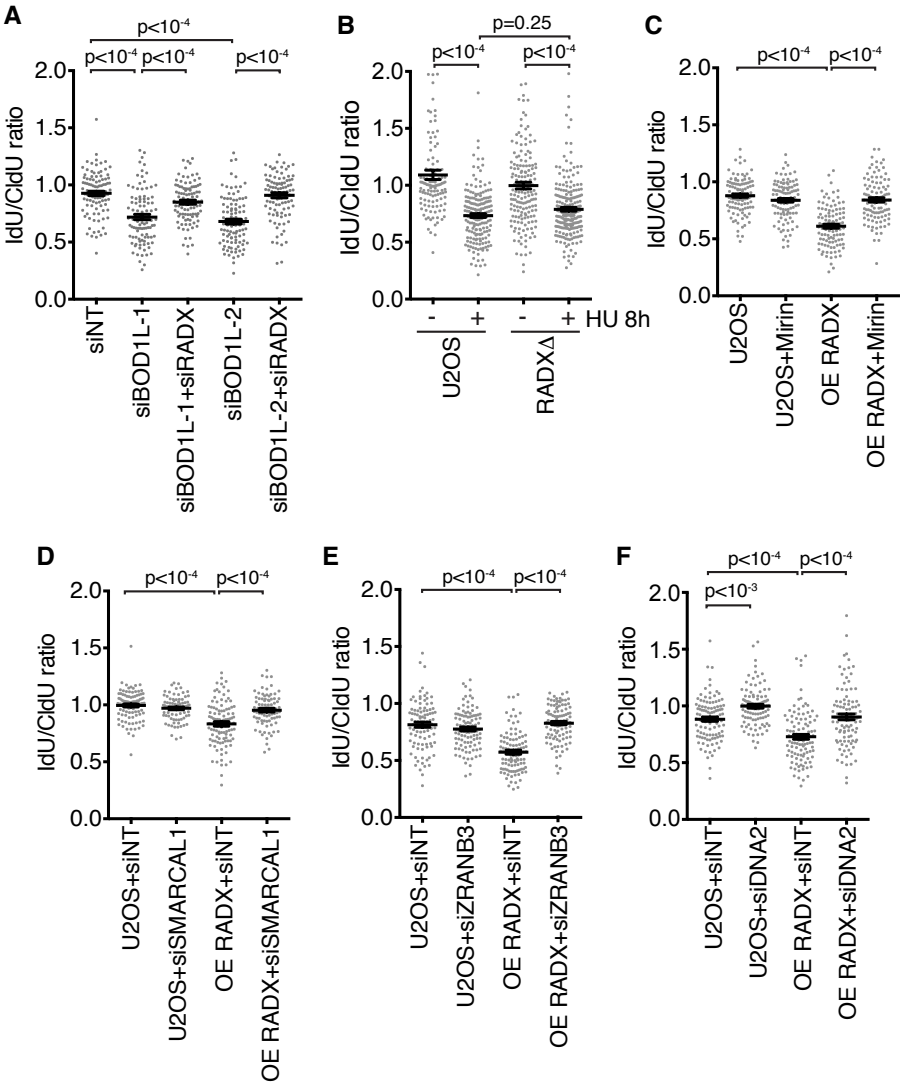

Figure 3.4. RADX silencing rescues DNA2 dependent fork degradation and RADX overexpression causes degradation of reversed forks (A–F) Fork protection assays were completed in U2OS cells or RADX overexpressing (OE RADX) U2OS cells transfected with the indicated siRNAs or treated with Mirin. All cells were treated with HU for 5 hours except for an 8-hour treatment in (B). P values were derived from Kruskal-Wallis ANOVA with a Dunn's post-test.

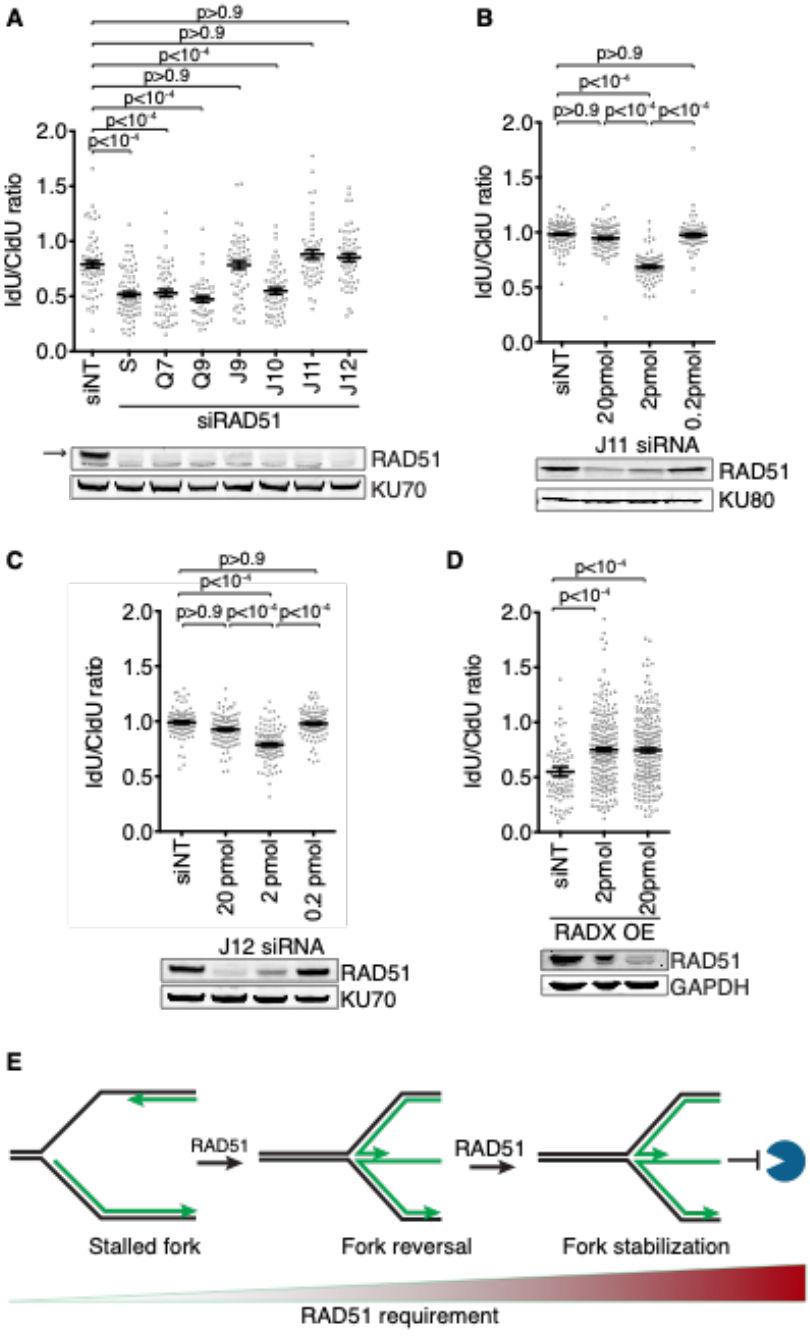

Figure 3.5. More RAD51 is required for fork protection than fork reversal (A) Fork protection assays in U2OS cells transfected with seven different RAD51 siRNAs. (B–D) U2OS or RADX overexpressing (OE RADX) cells were transfected with the "J11" siRNA (B and D) or "J12" siRNA (C) to RAD51 at the indicated amounts prior to performing the fork protection assay. P values were derived from Kruskal-Wallis ANOVA with a Dunn's post-test. Immunoblots from transfected cells corresponding to the same samples are shown below the graphs. (E) Model illustrating differential RAD51 requirements. Data in panels A and D were collected by Dr. Huzefa Dungrawala.

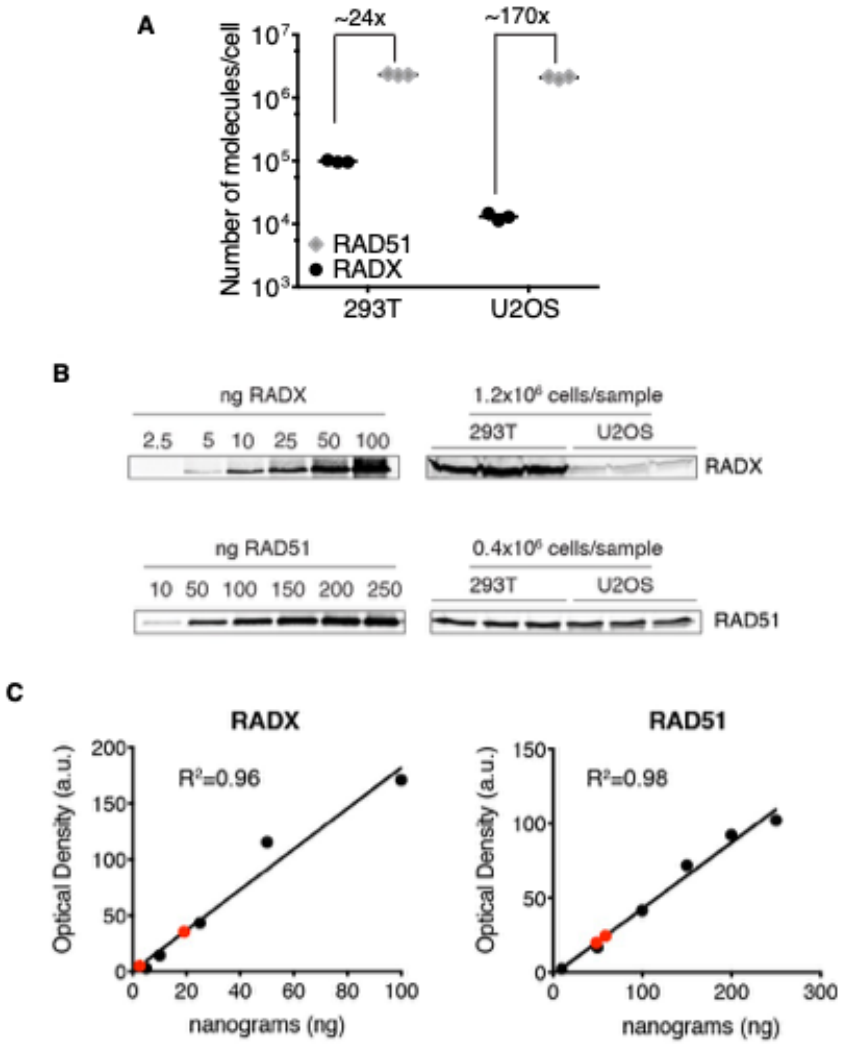

Figure 3.6. Quantitation of RAD51 and RADX molecules per cell. Purified recombinant RAD51 or RADX was used to generate a standard curve to compare to total cell lysates from HEK293T and U2OS cells. Immunoblots were quantitated using an Odyssey imaging system. All the data in this figure were generated by Dr. Huzefa Dungrawala.

RAD51 knockdown by siRNA and RAD51 inhibition by overexpressing RADX reduces RAD51 activity below the threshold required to promote fork reversal.

RADX is expressed at lower levels

RAD51 is abundantly expressed in both 293T and U2OS cells (~$2X10^6$ molecules/cell in both cell types) (Figure 3.6A). On the other hand, RADX is expressed at comparatively low levels (~$1X10^5$ molecules/cell in 293T and ~13000 molecules/cell in U2OS) (Figures 3.6A, 3.6B, and 3.6C). Despite being 24x or 170x less abundant than RAD51 in 293T or U2OS cells respectively, the strong affinity of RADX for ssDNA suggests there is sufficient RADX in cells to inhibit RAD51 from binding ssDNA. Thus, additional regulatory mechanisms controlled by BRCA2 or other RAD51 mediator proteins are essential to overcome the antagonistic activities of RADX.

Discussion

Our data indicates that loss of RADX mimics RAD51 overexpression and confers fork protection to cells lacking BRCA1/2, FANCA, FANCD2 or BOD1L—all situations where RAD51 filament stability is compromised. RADX loss prevents both DNA2- and MRE11- dependent fork degradation. Conversely, RADX overexpression mimics loss of BRCA1/2 and results in fork instability that is dependent on fork reversal. RADX can outcompete RAD51 for ssDNA even when present at concentrations that are 10,000-fold less than RAD51. Positive RAD51 regulators like BRCA2 are thus required to balance the antagonistic functions of RADX.

The deleterious effects of both decreasing and increasing RADX expression levels and its relative stoichiometry with RAD51 is reminiscent of the relationship between the bacterial RecX and RecA proteins (Cox, 2007). In contrast to RecX and RecA, we have not observed evidence for a trimeric complex between RADX, RAD51, and ssDNA. Thus far, our data is most consistent with a competition mechanism to explain how RADX antagonizes RAD51. However, we cannot rule out the possibility that a trimeric complex could be detectable using other experimental conditions. Furthermore, the ability of RADX to easily outcompete RAD51 for ssDNA binding biochemically may be modulated by other proteins or regulatory mechanisms in cells.

An alternative model for how RADX depletion causes fork protection would be for RADX to activate or recruit the fork degradation nucleases. We do not favor this model for the following reasons: First, there is no difference in the amount of MRE11 or DNA2 at replication forks in RADXΔ cells (Dungrawala et al., 2017). Second, there is no difference in the amount of ssDNA or RPA S4/S8 phosphorylation upon RADX depletion (Dungrawala et al., 2017). Third, RADX silencing does not cause sensitivity to ionizing radiation (Dungrawala et al., 2017). Fourth, RADX silencing prevents both MRE11- and DNA2- dependent nascent strand degradation. Fifth, RADX silencing does not prevent the DNA2- dependent fork degradation caused by long HU treatments in U2OS cells with functional BRCA-RAD51. Finally, RADX overexpression causes decreased RAD51 accumulation in HU- or IR-treated cells (Dungrawala et al., 2017), which would be the opposite of what would be expected if RADX promoted the activities of MRE11 and DNA2. Thus, we favor the model that RADX functions either directly or indirectly by regulating RAD51.

Since RADX overexpression results in fork degradation, it must be insufficient to prevent the fork reversal function of RAD51 in the presence of persistent replication stress. Consistent with this idea, RADX overexpression results in only a partial decrease in RAD51 foci formation in HU-treated cells (Dungrawala et al., 2017). Thus, similar to the loss of BRCA2, the partial decrease in RAD51 function by RADX overexpression is sufficient to cause defects in fork protection, but not in fork reversal unless combined with partial silencing of RAD51 expression.

Finally, we found that the amount of RAD51 function is critical to determining the fate of persistently stalled forks. Wild-type levels allow stalled forks to be reversed which can serve as a way to accomplish template switching, repair DNA damage or otherwise promote fork restart. Moderately reduced levels of RAD51 can still facilitate fork reversal but are unable to stabilize the reversed fork leading to excessive nuclease mediated resection and genome instability if forks are persistently stalled. Very low levels of RAD51 prevent any fork reversal yielding stable nascent strands but defects in fork restart and challenges in completion of DNA replication. RADX helps to balance RAD51 activities ensuring its fork reversal and protection activities operate appropriately to maintain genome stability.

Replication fork protection as a determinant of chemosensitivity

Whether replication fork protection is an important determinant of PARP inhibitor and replication stress cell sensitivity appears to be dependent on genetic background and experimental model (Ding et al., 2016; Dungrawala et al., 2017; Feng and Jasin, 2017; Ray Chaudhuri et al., 2016; Yazinski et al., 2017). For example, loss of some factors like EZH2 and MUS81 restore fork protection and chemoresistance only to BRCA2-mutant but not BRCA1-mutant cells (Lemacon et al., 2017; Rondinelli et al., 2017). Our results suggest RADX also differentiates between BRCA2 and BRCA1 since deleting RADX confers partial chemoresistance to BRCA2-deficient U2OS cells but not BRCA1-deficient U2OS cells despite rescuing fork protection in both settings. The specific HR gene mutation and its severity in disrupting function may determine whether restoring fork protection would be sufficient to generate drug resistance. Identifying drug-resistance mechanisms in patients will be critical to test this idea.

CHAPTER IV

RADX PREVENTS GENOME INSTABILITY BY CONFINING REPLICATION FORK REVERSAL TO STALLED FORKS[2]

Introduction

Replication fork reversal is a replication stress tolerance mechanism that promotes replication-coupled DNA repair or bypass of DNA damage (Berti et al., 2020a; Cortez, 2019). Multiple proteins regulate the formation and stabilization of reversed forks, as unregulated fork reversal can slow replication elongation, increase the frequency of double-strand breaks (DSBs), cause extensive degradation of nascent DNA, and result in genome instability.

The recombinase RAD51 is required to promote fork reversal (Zellweger et al., 2015) and protect the nascent DNA from degradation (Hashimoto et al., 2010; Schlacher et al., 2011). The RAD51 reversal function is thought to involve a metastable RAD51 filament (Berti et al., 2020a). In most cases, reversal does not require BRCA2, although it may be involved in circumstances in which RAD51 function is partly compromised (Liu et al., 2020). Instead, other RAD51 regulators including RAD51 paralogs assist fork reversal (Berti et al., 2020b), but exactly how RAD51 promotes reversal is unknown.

A reversed fork is the substrate for nascent strand degradation, as inactivating fork reversal enzymes such as SMARCAL1, ZRANB3, HLTF, or FBH1 block degradation (Higgs et al., 2015; Kolinjivadi et al., 2017b; Lemacon et al., 2017; Liu et al., 2020; Mijic et al., 2017; Taglialatela et al., 2017). Fork protection is thought to require RAD51 nucleoprotein filaments that are stabilized by BRCA2. These stable filaments protect the nascent DNA from nucleases including MRE11 and DNA2 (Hashimoto et al., 2010; Schlacher et al., 2011; Thangavel et al., 2015). Many proteins in addition to BRCA2 and RAD51 prevent nascent strand degradation, and they organize into at least two pathways depending on whether the translocases SMARCAL1, ZRANB3, and HLTF or

[2] This chapter was adapted from Krishnamoorthy *et al.,* 2021

FBH1 cooperate with RAD51 to remodel the fork (Liu et al., 2020). forks, whereas potently silencing RAD51 expression prevents fork reversal and inhibits nascent strand degradation (Bhat et al., 2018; Taglialatela et al., 2017).

Moreover, different levels of RAD51 function are required for fork reversal and fork protection (Bhat and Cortez, 2018; Bhat et al., 2018). Consistent with this hypothesis, reducing the concentration of RAD51 in cells or reducing its ability to bind DNA using a chemical inhibitor, B02, causes deprotection of reversed RADX is a single-strand DNA (ssDNA) binding protein important for replication fork stability (Dungrawala et al., 2017; Schubert et al., 2017). In the absence of added replication stress, RADX inactivation causes slow replication elongation and increased DSBs (Dungrawala et al., 2017; Schubert et al., 2017). RADX competes with RAD51 for ssDNA, directly interacts with RAD51, destabilizes the RAD51 nucleofilament, and inhibits RAD51-dependent processes *in vitro* (Adolph et al., 2021). Inactivating RAD51 rescues the slow replication elongation and elevated DSBs observed in RADX-deficient cells (Dungrawala et al., 2017) . These data suggest that RADX antagonizes RAD51 to maintain genome stability during DNA replication. In cells experiencing persistent replication stress caused by hydroxyurea (HU), RADX overexpression reduces the amount of RAD51 at forks and promotes fork degradation (Bhat et al., 2018). In addition, RADX inactivation restores fork protection in BRCA2-, BRCA1-, or FANCD2-deficient cells treated with HU (Bhat et al., 2018; Dungrawala et al., 2017). On the basis of the antagonistic relationship between RADX and RAD51 found in biochemical experiments and in unstressed cells, and the observations that RADX inactivation or overexpression increases or reduces RAD51 levels at forks, respectively, we proposed that the rescue of fork protection by RADX inactivation could be due to restoration of sufficient RAD51 activity to protect reversed forks in these cells (Bhat and Cortez, 2018; Bhat et al., 2018; Dungrawala et al., 2017). In other words, we hypothesized that removing a negative regulator of RAD51 like RADX may compensate for inactivating positive regulators such as BRCA2. However, this hypothesis does not explain why RADX accumulates at persistently stalled forks (Dungrawala et al., 2017; Schubert et al., 2017).

In this study, I find that consistent with our previous hypothesis, RADX inhibits aberrant fork reversal and prevents fork collapse in unstressed cells. However, I now find that RADX promotes the formation of reversed fork structures in cells experiencing persistent replication stress. Our results indicate that RADX has two apparently opposite functions to regulate fork reversal depending on the amount of replication stress. To explain these observations, I propose a unifying

model in which the RADX-dependent destabilization of the RAD51 nucleofilament can either inhibit or promote fork reversal depending on whether forks are actively elongating or stalled. These results are reminiscent of *N. gonorrhoeae* RecX, which stimulates functions of the recombinase RecA (the RAD51 ortholog) in cells even though it inhibits its biochemical activities (Gruenig et al., 2010).

Results

RADX inhibits inappropriate fork reversal in the absence of exogenous stress

RADX inactivation causes slow replication elongation and increased fork collapse in the absence of added replication stress (Dungrawala et al., 2017; Schubert et al., 2017). Inactivating the fork reversal enzymes SMARCAL1, ZRANB3, or HLTF using small interfering RNA (siRNA) or CRISPR-Cas9 gene editing rescues the slow fork elongation phenotype caused by RADX silencing in U2OS and hTERT-RPE-1 cells (Figures 4.1A and 4.2A-D). Additionally, inhibiting PARP with the small-molecule inhibitor olaparib, which was previously reported to prevent fork reversal by promoting fork restoration (Berti et al., 2013), also rescued the fork elongation defect in RADXΔ cells (Figure 4.1B). In contrast, silencing MUS81 or inhibiting MRE11 did not rescue fork speeds, indicating that the fork elongation defects in the absence of RADX are unlikely to be due to fork cleavage or nuclease degradation (Figures 4.2E and 4.2F). Finally, inactivating SMARCAL1, ZRANB3, or HLTF also reduces the frequency of DSBs observed in U2OS cells lacking RADX, suggesting that these breaks are a consequence of aberrant fork remodeling (Figure 4.1C; (Dungrawala et al., 2017)).

These data collectively suggest that RADX prevents inappropriate fork reversal at unchallenged forks that otherwise would impair replication elongation and increase the frequency of fork collapse. To further test this hypothesis, in collaboration with Dr. Vindigni, I analyzed replication intermediates using electron microscopy (EM). As predicted, silencing RADX either by siRNA transfection (siRADX) or by CRISPR-Cas9-mediated gene editing (RADXΔ) increased the frequency of reversed forks observed by EM in the absence of added replication stress (Figures 4.1D and 4.4). Thus, we conclude that RADX inhibits fork reversal in the absence of replication stress.

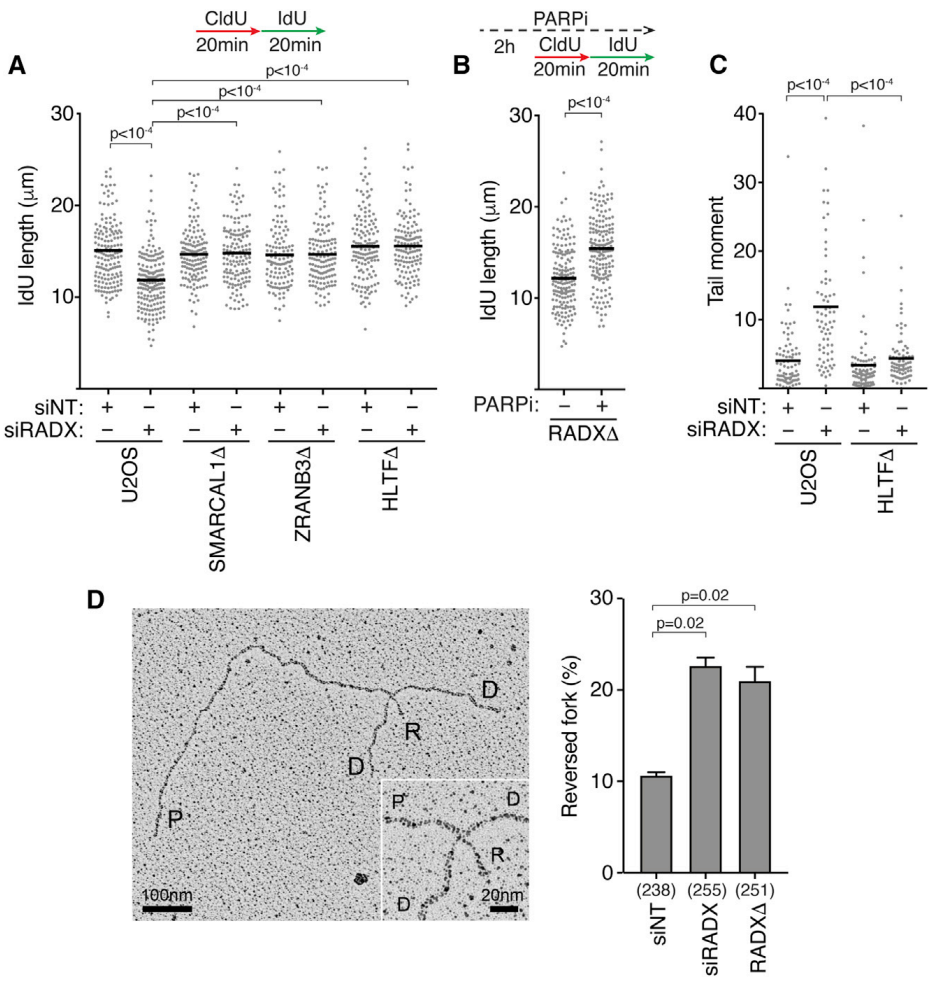

Figure 4.1. RADX inhibits inappropriate fork reversal in the absence of replication stress
(A) U2OS cells transfected with the indicated siRNAs (NT, non-targeting) were labeled with CldU followed by IdU, and DNA combing was used to measure elongation rates. A one-way ANOVA with Tukey's multiple-comparison test was used to calculate p values in all DNA fiber experiments. (B) Replication fork elongation was monitored using DNA combing in RADXΔ cells treated with 10 μM olaparib as indicated. (C) DSBs were measured by neutral comet assay in wild-type (WT) or HLTFΔ U2OS cells transfected with the indicated siRNAs. A Kruskal-Wallis test was used to calculate p values in all comet assays. All fiber and comet assays are representative experiments of at least n = 3 biological replicates. (D) Example of a reversed replication fork imaged by EM, and the mean ± SEM percentage of reversed forks from three experiments is shown (inset, magnified four-way junction at the reversed fork; P, parental strands; D, daughter strands; R, reversed strands). The number of replication intermediates analyzed for each condition is indicated in parentheses. A Welch's test was used to calculate p values. Panels D and E were generated in collaboration with Jessica Jackson and Dr. Alessandro Vindigni.

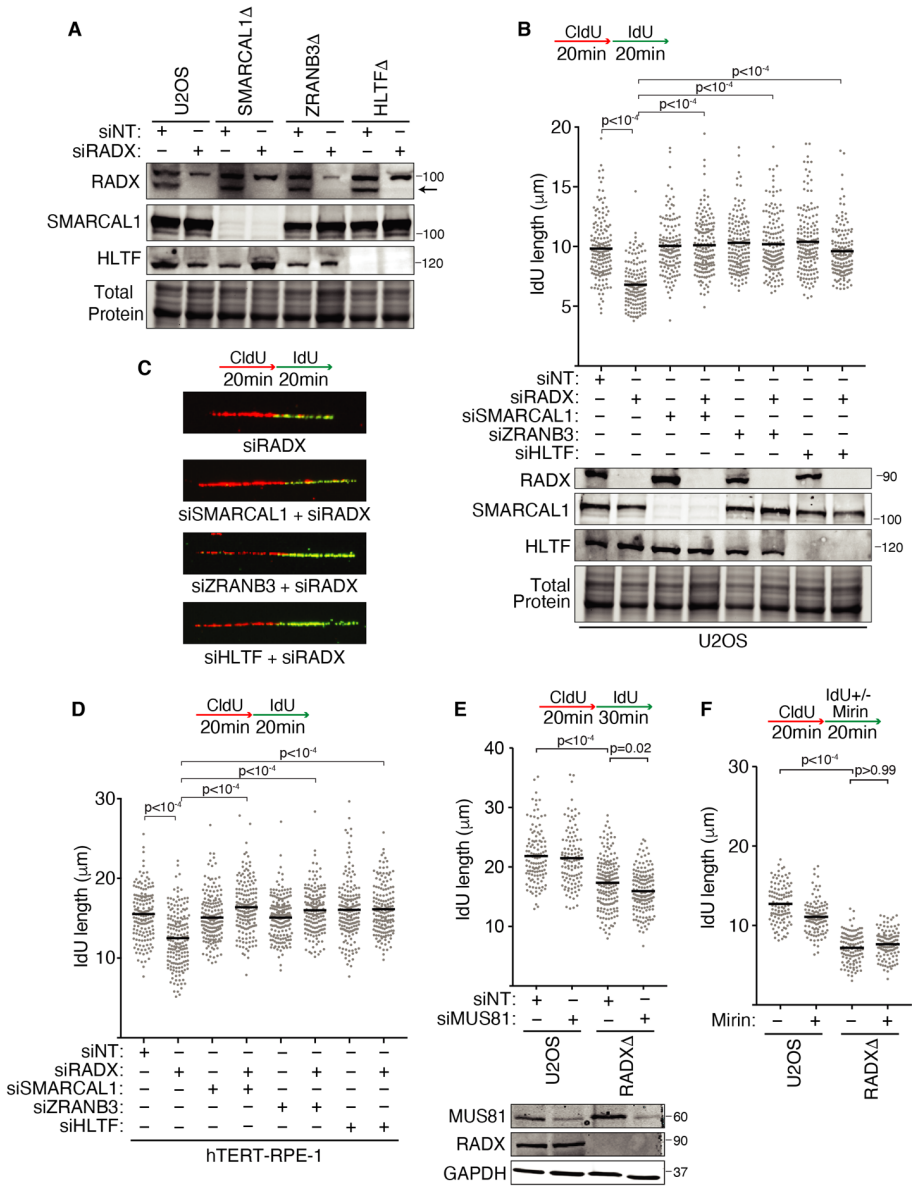

Figure 4.2. Aberrant fork reversal causes fork collapse in RADX-deficient cells.
(A) Immunoblots of U2OS and SMARCAL1D, ZRANB3D, and HLTFD cell lysates after transfection of the indicated siRNAs (siNT = non-targeting). (B) Replication elongation rate was measured by DNA fiber spreading after transfection of U2OS cells with siRNAs. Immunoblots of cell lysates are shown. (C) Representative DNA combing images of replication tracts stained with antibodies to CldU and IdU. (D) Replication elongation rate was measured by DNA combing after transfection of hTERT-RPE-1 cells with siRNAs. (E and F) Replication elongation rate was measured by DNA combing (E) or fiber spreading (F) in wild-type or RADXD U2OS cells transfected with the indicated siRNA or treated with 100μM Mirin. All experiments were completed at least twice. A one-way ANOVA with Tukey's multiple comparison test was used to calculate p values for all fiber experiments.

RADX inactivation blocks nascent strand degradation at persistently stalled replication forks without restoring RAD51 localization

We previously reported that inactivating RADX in U2OS cells blocks nascent strand degradation when BRCA2 or BRCA1 is also inactivated (Bhat et al., 2018; Dungrawala et al., 2017). I confirmed that this effect was not cell type specific, as RADX silencing by RNAi also prevents nascent strand degradation in BRCA2-depleted hTERT-RPE-1 cells and BRCA2Δ DLD1 cells (Figured 4.3A and 4.3B). I also found that despite causing elevated levels of DSBs when silenced by itself in HU-treated cells, RADX silencing reduces the fork breakage observed in BRCA2-deficient cells, which previously was reported to be dependent on fork reversal (Figures 4.3C) (Lemacon et al., 2017).

As RADX inactivation increases the amount of RAD51 localized to replication forks (Dungrawala et al., 2017), we previously hypothesized that inactivating RADX at persistently stalled forks prevents nuclease-mediated nascent strand degradation by improving the stability of RAD51 filaments on the reversed forks. This hypothesis predicts that RADX inactivation should restore RAD51 localization to stalled forks in BRCA2-deficient cells. To test this prediction, I performed quantitative immunofluorescence imaging of chromatin-bound RAD51 in S-phase cells. As shown previously, silencing BRCA2 reduces the intensity and number of RAD51 foci, while silencing RADX modestly increases the intensity and number of RAD51 foci in HU-treated cells (Figure 4.3D; (Dungrawala et al., 2017; Taglialatela et al., 2017)). However, contrary to our expectation, silencing RADX in the absence of BRCA2 did not appreciably restore the number or intensity of RAD51 foci. Silencing RADX also did not increase RAD51 localization to stalled forks in BRCA1-deficient cells (Figure 4.3D). Thus, the ability of RADX inactivation to prevent nascent strand degradation and fork cleavage when fork protection factors are inactivated may not result from restoration of RAD51 localization to reversed forks.

To further test this idea, I reasoned that if RADX inactivation restores fork protection to reversed forks by stabilizing RAD51 filaments, then loss of RADX should not rescue nascent strand degradation in cases in which fork protection is independent of RAD51 filament stability. For example, ABRO1 was reported to protect reversed forks independently of RAD51 (Xu et al., 2017b). Thus, if RADX inactivation restores RAD51 filament stability on reversed forks, it should not rescue the nascent strand degradation in ABRO1-deficient cells. In contrast to this prediction, RADX silencing does restore fork protection in ABRO1-depleted cells (Krishnamoorthy et al.,

2021). Furthermore, I confirmed that a reversed fork is the substrate for degradation in cells lacking ABRO1, as inactivating the fork reversal protein ZRANB3 or HLTF also prevents nascent strand degradation when ABRO1 is silenced (Krishnamoorthy et al., 2021). These observations are inconsistent with the idea that RADX inactivation restores fork protection by increasing the stability of RAD51 filaments on reversed forks.

Partial depletion of RADX causes nascent strand degradation

I did not observe nascent strand degradation in either our RADXΔ cells generated by CRISPR-Cas9 or after transfection with RADX siRNA. However, (Schubert et al., 2017) reported nascent strand degradation when they silenced RADX with siRNA. To further explore how RADX inactivation affects fork stability, I tried to reconcile these observations. RNAi may not fully inactivate RADX, so I considered the possibility that partial RADX loss might yield a different effect than complete loss of function, as we had previously found for RAD51 (Bhat et al., 2018). To test this hypothesis directly, I used different concentrations of RADX siRNA to obtain varying levels of silencing. A 5 nM concentration of RADX siRNA caused efficient knockdown with little RADX protein visible by immunoblotting, while 0.5 nM of the same siRNA yielded only partial knockdown (Figure 4.5A). Strikingly, the partial RADX knockdown cells treated with HU underwent extensive nascent strand degradation even though the cells with more efficient RADX knockdown did not (Figure 4.5A). The same result was obtained with a second siRNA to RADX (Figure 4.5A). Partial knockdown of RADX did not yield fork degradation in RADXΔ cells indicating that these are not off-target effects of the siRNAs (Figure 4.7A). Moreover, nascent strand degradation upon partial RADX inactivation was also observed in hTERT-RPE-1 cells, indicating that this effect is not cell type specific (Figure 4.7B)

The fork degradation caused by partial depletion of RADX siRNA is prevented by treatment with mirin, which inhibits MRE11 (Dupre et al., 2008), or C5, which inhibits DNA2 (Liu et al., 2016), or by inactivating SMARCAL1, ZRANB3, or HLTF (Figures 4.5B, 4.5C, and 4.7C). Thus, the resection substrate in these cells is likely a reversed fork that is degraded by MRE11 or DNA2. These results phenocopy the effects previously reported for RAD51 (Bhat et al., 2018). RAD51 partial knockdown by siRNA, inhibition with a small-molecule inhibitor, or mutation also yields nascent strand degradation that is dependent on fork reversal (Bhat et al., 2018; Taglialatela et al., 2017; Wang et al., 2015). Strikingly, either efficient or partial knockdown of RADX in cells treated with the RAD51 inhibitor B02 largely restores fork protection (Figure 4.5D). A

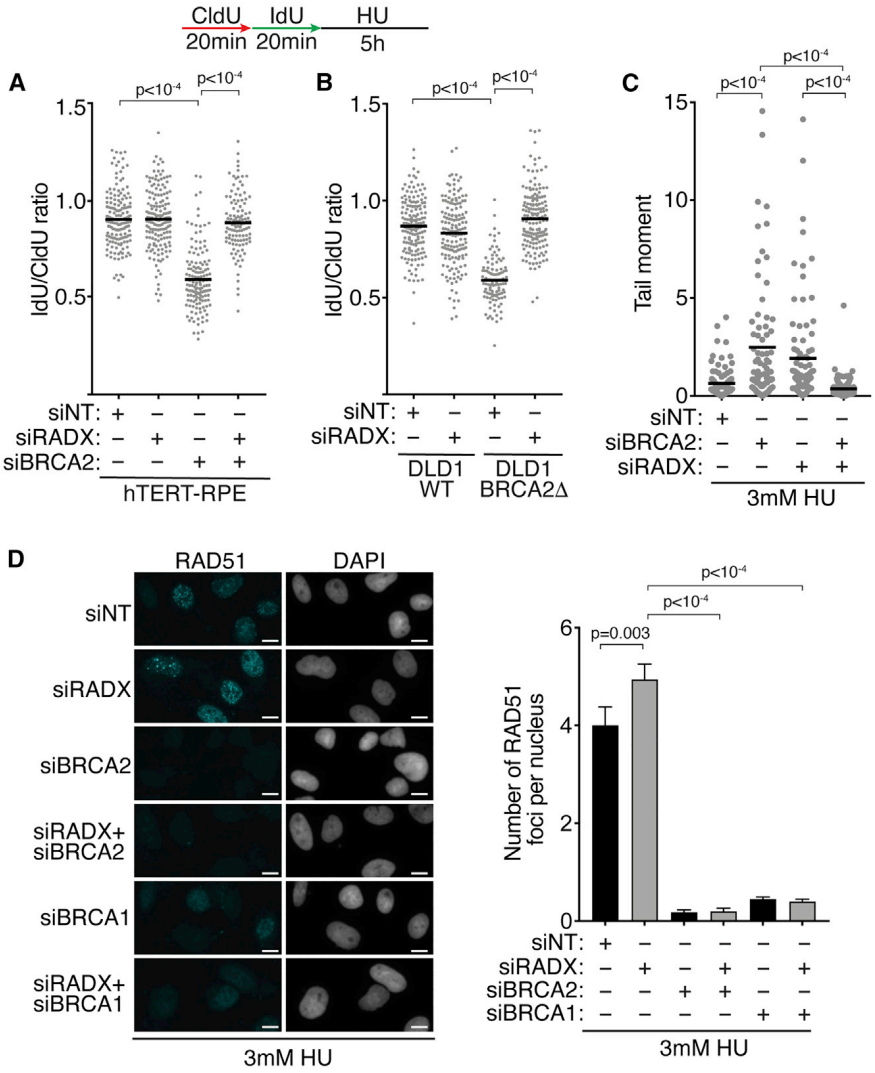

Figure 4.3. RADX silencing protects stalled forks from degradation in the absence of BRCA2 without restoring RAD51 localization

(A and B) Fork protection assays were completed in (A) hTERT-RPE-1 or (B) DLD1 cells with and without BRCA2 after transfection of the indicated siRNAs. (C) Neutral comet assay in siRNA-transfected U2OS cells treated with 3 mM HU for 5 h. (D) U2OS cells transfected with siRNA were labeled with 10 μM EdU for 20 min, treated with 3 mM HU for 5 h, and stained for RAD51 and EdU. Representative images of RAD51 staining and the number of chromatin-bound RAD51 foci per nucleus is shown (mean ± 95% confidence interval). Scale bar, 10 μm. A Mann-Whitney test was used to calculate p values.

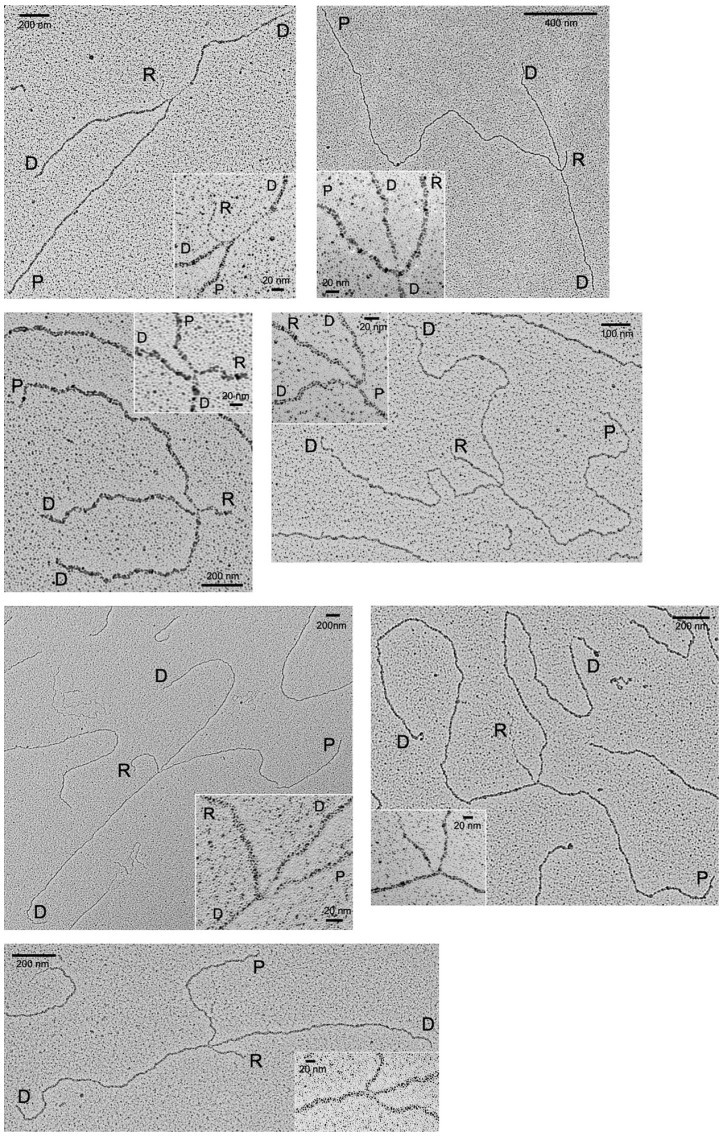

Figure 4.4. Representative Electron Microscopy images. Representative EM images are shown. Inset, magnified four-way junction at the reversed fork; P, parental strands; D, daughter strands; R, reversed strands. Images were generated by Jessica Jackson.

parsimonious explanation for these results is that in the presence of HU, RADX functions like RAD51 to help generate a reversed fork substrate for degradation, even though in the absence of added replication stress, it inhibits fork reversal.

RADX is required for fork-reversal-dependent telomere catastrophe in cells experiencing added replication stress

I next looked for additional contexts to test the hypothesis that RADX inhibits fork reversal in the absence of added replication stress but is needed to promote fork reversal in the presence of replication stress. One such context is at telomeres where telomerase binding to reversed forks in RTEL1-deficient cells causes telomere catastrophe (Figure 4.5A; (Margalef et al., 2018). If RADX is needed to promote fork reversal, then we might expect RADX inactivation to rescue the telomere catastrophe in RTEL1-deficient cells. Conversely, if RADX prevents fork reversal, then its inactivation would have no effect or increase telomeric dysfunction. As previously reported, inactivating RTEL1 in HeLa cells with long telomeres increased the frequency of telomere fragility and heterogeneity and co-depleting the fork reversal enzyme ZRANB3 rescues these phenotypes linking them to fork reversal (Figures 4.6B-4.6D; (Margalef et al., 2018). Inactivating RADX by itself did not cause a significant increase in telomere heterogeneity or fragility (Figures 4.6C and 4.6D). When RADX and RTEL1 were co-depleted, I observed a small but statistically insignificant decrease in fragility and no change in heterogeneity compared with RTEL1 inactivation by itself (Figures 4.6C and 4.6D). These data suggest that in the absence of added replication stress agents, loss of RADX has only minor effects on telomere stability and is not required for formation of reversed forks at telomere sequences in RTEL1-deficient cells. I next repeated the experiments in the presence of aphidicolin to increase replication stress levels and generate more persistently stalled forks. As expected, addition of aphidicolin increases telomere catastrophe in RTEL1-deficient cells (Figures 4.7D and 4.7E). In this condition, RADX inactivation by itself had no effect on telomere fragility or heterogeneity, but inactivating RADX in the aphidicolin-treated, RTEL1-deficient cells rescued the telomere fragility and heterogeneity, similar to inactivating ZRANB3 (Figures 4.6E and 4.6F). These results are consistent with the idea that in the presence of added replication stress, RADX is needed to generate the reversed forks that are a source of the telomere instability in RTEL1-deficient cells.

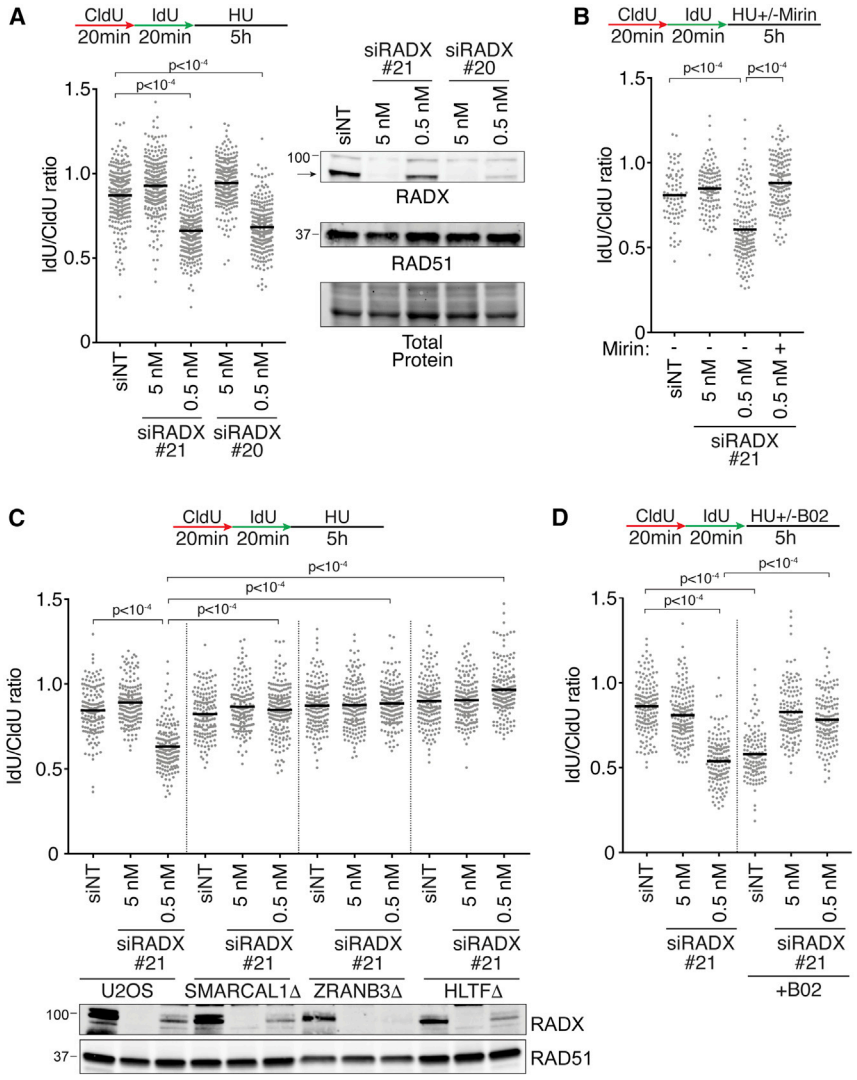

Figure 4.5. Partial depletion of RADX causes nascent strand degradation
(A–D) Fork protection assays were performed in WT, SMARCAL1Δ, HLTFΔ, or ZRANB3Δ U2OS cells transfected with the indicated amount of each siRNA. Cells were treated with (B) 100 μM mirin or (D) 25 μM B02 where indicated. A one-way ANOVA with Tukey's multiple-comparison test was used to calculate all p values. All experiments were completed at least twice.

RADX promotes fork reversal in the presence of persistent replication stress

The simplest explanation of the fork protection and telomere stability data is that RADX is needed to generate reversed forks in cells experiencing persistent replication stress. To directly test this hypothesis, I collaborated with Dr. Vindgni and used EM to observe the frequency of fork reversal in HU-treated cells. As reported previously, treatment with HU yields a high frequency of reversed forks (Figures 4.8A and 4.8B). Depletion of RADX by siRNA (siRADX) or inactivation by CRISPR-Cas9 (RADXΔ) consistently decreased the percentage of reversed forks although not to the levels of unstressed cells (Figure 4.8B).

RADX binds RAD51 and ssDNA to promote fork reversal in the presence of persistent replication stress

In unstressed cells, the ability of RADX to prevent fork instability is dependent on its direct interactions with RAD51 and ssDNA (Adolph et al., 2021; Dungrawala et al., 2017). To test whether the same mechanisms operate in stressed cells, I analyzed the activities of RADX separation of function mutants with diminished ssDNA binding activity (RADX OB2m; (Dungrawala et al., 2017) or an inability to interact with RAD51 (RADX QVPK; (Adolph et al., 2021). First, I examined if transient overexpression of these proteins caused nascent strand degradation in HU-treated cells, as previously observed for wild-type RADX (Dungrawala et al., 2017). In contrast to wild-type RADX, the RADX QVPK or RADX OB2m mutants do not cause nascent strand degradation when overexpressed in U2OS cells (Figures 4.9A and 4.10A). The RADX overexpression-induced nascent strand degradation is rescued by overexpressing RAD51, suggesting that it is due to a reduction in the stability of RAD51 filaments on reversed replication forks (Figure 4.10A).

I next examined fork protection in RADXΔ cells complemented with wild-type, QVPK, or OB2m RADX. As we previously reported, expression of the wild-type RADX protein decreases after a few passages to a level that no longer causes fork deprotection and permits nascent strand degradation when BRCA2 is silenced (Figure 4.9B; (Adolph et al., 2021)). In contrast, cells expressing only the RADX QVPK or RADX OB2m proteins have stable forks when BRCA2 is silenced, similar to RADXΔ cells, consistent with the idea that RADX binding to RAD51 and ssDNA is needed to enable fork reversal in cells experiencing persistent stress (Figures 4.9B and 4.10B).

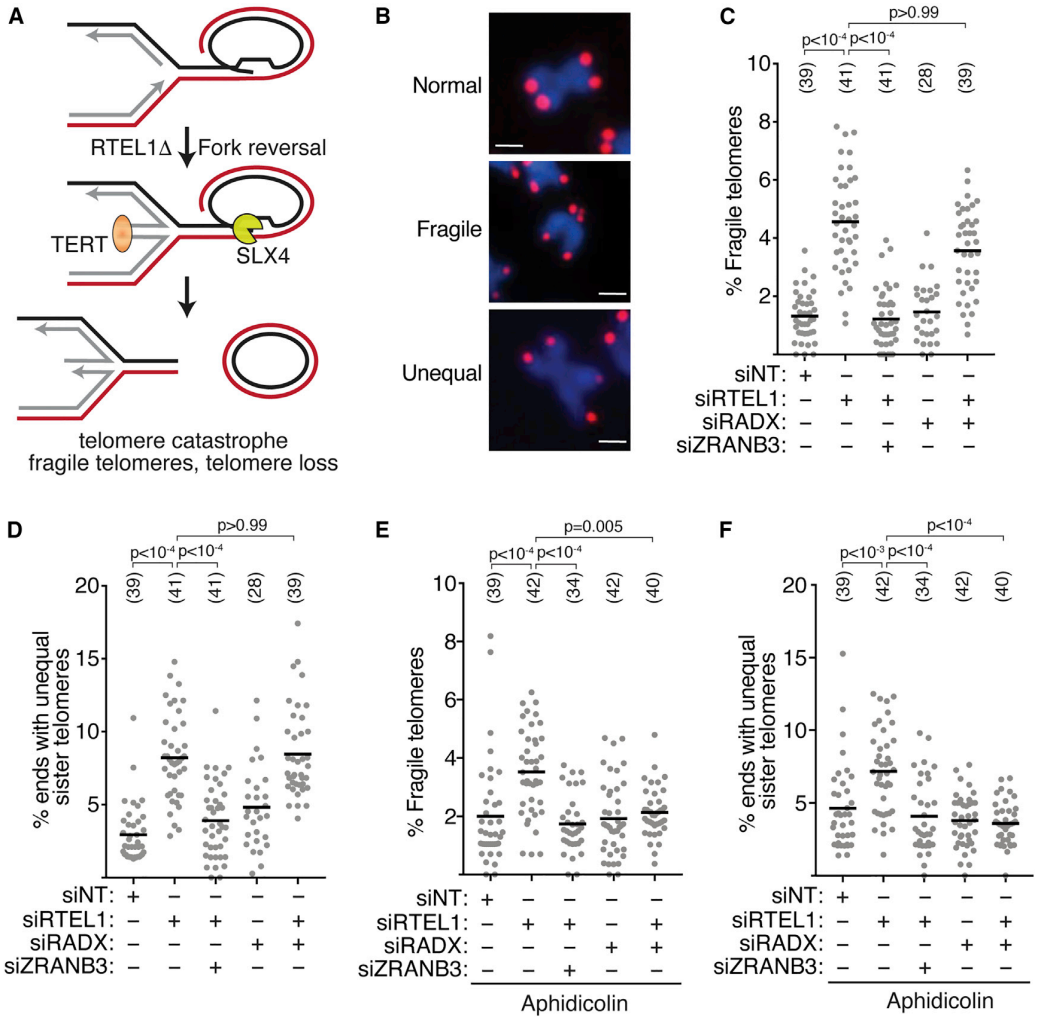

Figure 4.6. RADX inactivation rescues fork-reversal-dependent telomere instability only in cells treated with aphidicolin

(A) Schematic model indicating that fork reversal causes telomere catastrophe in RTEL1-deficient cells (Margalef et al., 2018). (B) Representative images of normal, fragile, and unequal telomeres. Scale bar, 1 μm. (C and D) Quantification of fragile telomeres (C) and telomere heterogeneity (D) in cells transfected with siRNAs. (E and F) Quantification of fragile telomeres (E) and telomere heterogeneity (F) in cells transfected with siRNAs and treated with 0.2 μM aphidicolin for 40 h. Each data point represents a metaphase spread. All experiments were completed at least three times. Parentheses indicate the number of total metaphases analyzed. p values were calculated using a Kruskal-Wallis test.

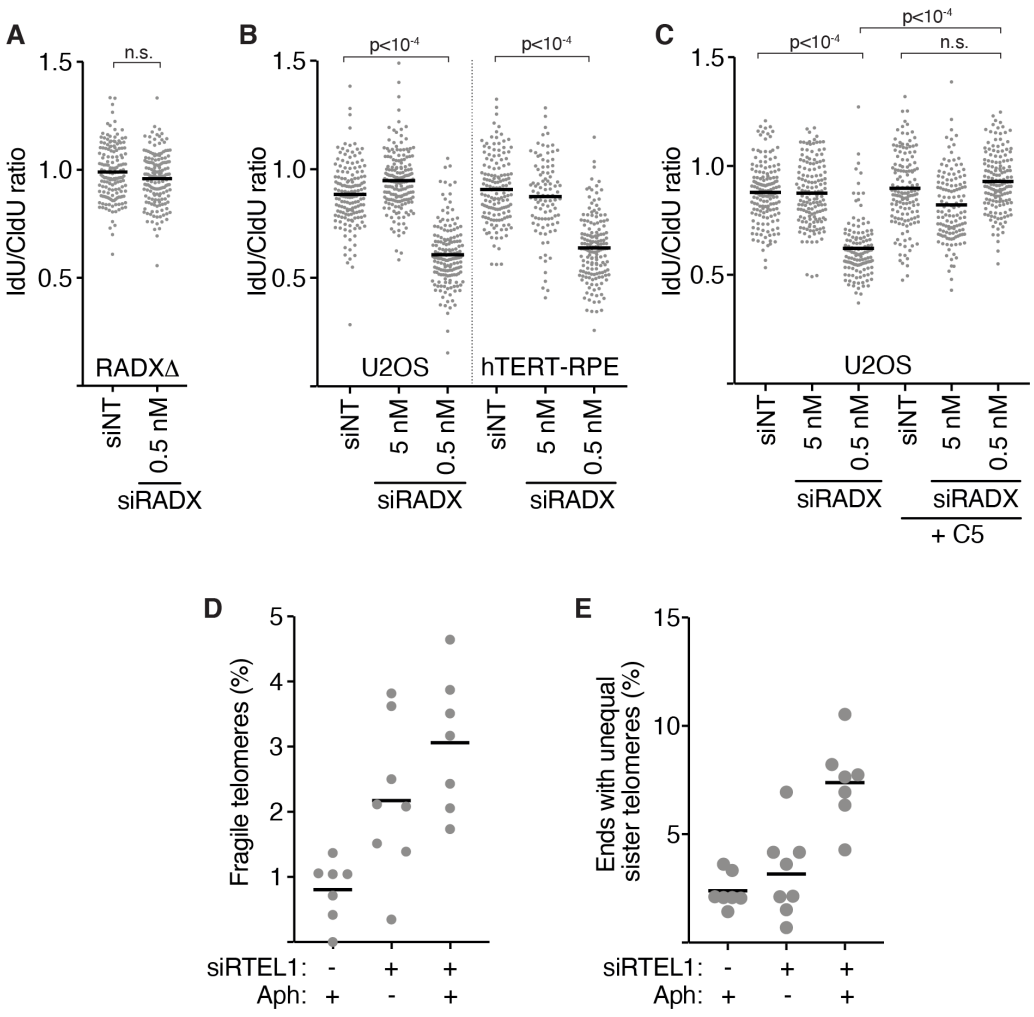

Figure 4.7. Partial silencing of RADX causes nascent strand degradation while addition of aphidicolin increases telomere catastrophe in RTEL1-deficient cells. (A-C) Fork protection assays were performed after transfection with 0.5 or 5nM of RADX siRNA #21 or 5nM non-targeting (NT) siRNA. Transfections with 0.5nM of RADX siRNA were supplemented with NT siRNA to reach a total of 5nM. Cells were treated with 20μM of the C5 DNA2 inhibitor where indicated. A one-way ANOVA with Tukey's multiple comparison test was used to calculate all p values. (D) Quantification of fragile telomeres and (E) telomere heterogeneity in cells transfected with the indicated siRNAs and treated with or without 0.2μM aphidicolin for 40h.

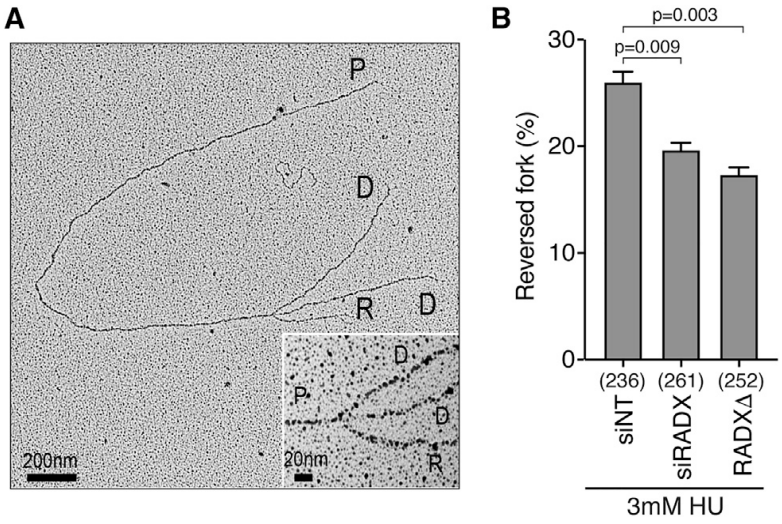

Figure 4.8. RADX inactivation suppresses fork reversal in cells experiencing persistent replication stress

(A) Example of a reversed fork observed by EM (inset, magnified four-way junction at the reversed fork; P, parental strands; D, daughter strands; R, reversed strands). (B) Quantitation of fork reversal measured by EM in the indicated U2OS cells treated with 3 mM HU for 5h (n = 3; mean ± SEM). The number of replication intermediates analyzed for each condition is indicated in parenthesis. p values were calculated using a Welch test. Data were generated in collaboration with Jessica Jackson and Dr. Alessandro Vindigni.

To explain the paradoxical observations for RADX function in unstressed and stressed cells, I reasoned that RADX could either “switch” from an antagonist of RAD51 in the absence of stress “metastable” RAD51 filament proposed to be needed to reverse forks (Berti et al., 2020a). To test to a positive regulator of RAD51 with persistent stress or that it may continue to antagonize RAD51 biochemically in the presence of stress but that this function may help generate the if RADX switched from an antagonist of RAD51 to a positive regulator of RAD51, Madison (a post-doc in the lab) purified GFP-FLAG-RADX from unstressed and HU-treated 293T cells (Figure 4.11). Both RADX proteins inhibited RAD51-mediated strand exchange and D-loop formation as efficiently as MBP-RADX purified from insect cells, whereas the RADX-QVPK protein did not (Figures 4.11B and 4.11C; (Adolph et al., 2021). Thus, RADX purified from untreated and HU-treated cells have similar biochemical activities. Furthermore, the ability of RAD51 overexpression to rescue the phenotypic effect of RADX overexpression in HU-treated cells (Figure 4.10A) also suggests that it remains a RAD51 antagonist in these conditions.

To directly test whether RADX could promote fork reversal by decreasing the stability of RAD51 filaments, I examined the ability of SMARCAL1 to catalyze fork reversal on model replication fork substrates in the presence of RAD51, RPA, and RADX (Figure 4.12A). Individually, MBP-RADX or RAD51 inhibited fork reversal when added before SMARCAL1 (Figure 4.12B and 4.12C), but as previously reported, RPA stimulates SMARCAL1 (Figure 4.12B; (Betous et al., 2012).As expected, addition of RPA, RAD51, and MBP-RADX together in the absence of SMARCAL1 did not yield fork reversal (Figure 4.12D). Moreover, adding RPA by itself after RAD51 did not improve SMARCAL1-mediated reversal (Figure 4.12E). In contrast, adding increasing amounts of MBP-RADX in the presence of RPA to a fork substrate with pre-bound RAD51 stimulated fork reversal by SMARCAL1 (Figure 4.12E). Importantly, adding the MBP-RADX QVPK mutant that cannot bind RAD51 or destabilize RAD51 filaments did not stimulate reversal significantly (Figure 4.12F). These data suggest that RADX can promote fork reversal in at least some conditions by destabilizing RAD51.

Discussion

Our findings indicate that RADX regulates replication fork reversal in a context-dependent manner. In the absence of added replication stress, RADX inhibits fork reversal to prevent fork slowing and fork breakage. However, in the presence of added replication stress, RADX helps

generate reversed forks. Therefore, RADX inactivation blocks nascent strand degradation and telomere dysfunction in fork protection-deficient or RTEL1-deficient cells experiencing persistent replication stress, since reversed forks are the substrates for the nuclease processing in these circumstances (Kolinjivadi et al., 2017b; Lemacon et al., 2017; Margalef et al., 2018; Mijic et al., 2017; Taglialatela et al., 2017). Both RADX-dependent inhibition of fork reversal in the absence of stress and generation of reversed forks in the presence of stress depend on its ability to interact directly with RAD51 and ssDNA. On the basis of these findings and our observation that RADX can stimulate fork reversal *in vitro* in conditions in which RAD51 binding a fork substrate is inhibitory, I conclude that RADX likely confines fork reversal to persistently stalled forks by destabilizing RAD51 nucleofilaments. I suggest that the difference in outcome at elongating versus stalled forks is due to the difference in amount and persistence of ssDNA.

Our new data also explain the discrepancies in the literature on the stability of nascent DNA when RADX is inactivated. We reported that silencing RADX with RNAi or knocking out *RADX* with CRISPR-Cas9 caused fork slowing but did not yield nascent strand degradation in the presence of persistent replication stress (Bhat et al., 2018; Dungrawala et al., 2017). Yet (Schubert et al., 2017) reported that RADX siRNA caused nascent strand degradation in HU-treated cells. I now find that inefficient RADX silencing causes nascent strand degradation, indicating that the differences in published results were due to how efficiently RADX was inactivated. In this respect, RADX phenocopies RAD51, as partial silencing of either causes nascent strand degradation, but efficient inactivation yields stable forks in HU-treated cells.

Six observations are consistent with the conclusion that RADX prevents fork reversal in the absence of replication stress: (1) RADX is present at actively elongating replication forks, placing it where it would need to operate to prevent RAD51-dependent reversal (Dungrawala et al., 2017); (2) RADX inactivation causes an increased abundance of RAD51 at replication forks (Dungrawala et al., 2017); (3) RADX inactivation slows replication elongation and increases fork collapse; (4) both fork slowing and fork collapse in the absence of RADX can be rescued by inactivating the fork reversal enzyme HLTF, ZRANB3, or SMARCAL1 or by silencing RAD51; (5) replication elongation rates in RADX-deficient cells are also rescued by addition of PARP inhibitor, which inhibits fork reversal; and (6) direct visualization of replication intermediates by EM shows an accumulation of reversed forks in RADX-deficient cells that are not treated with any replication stress agent.

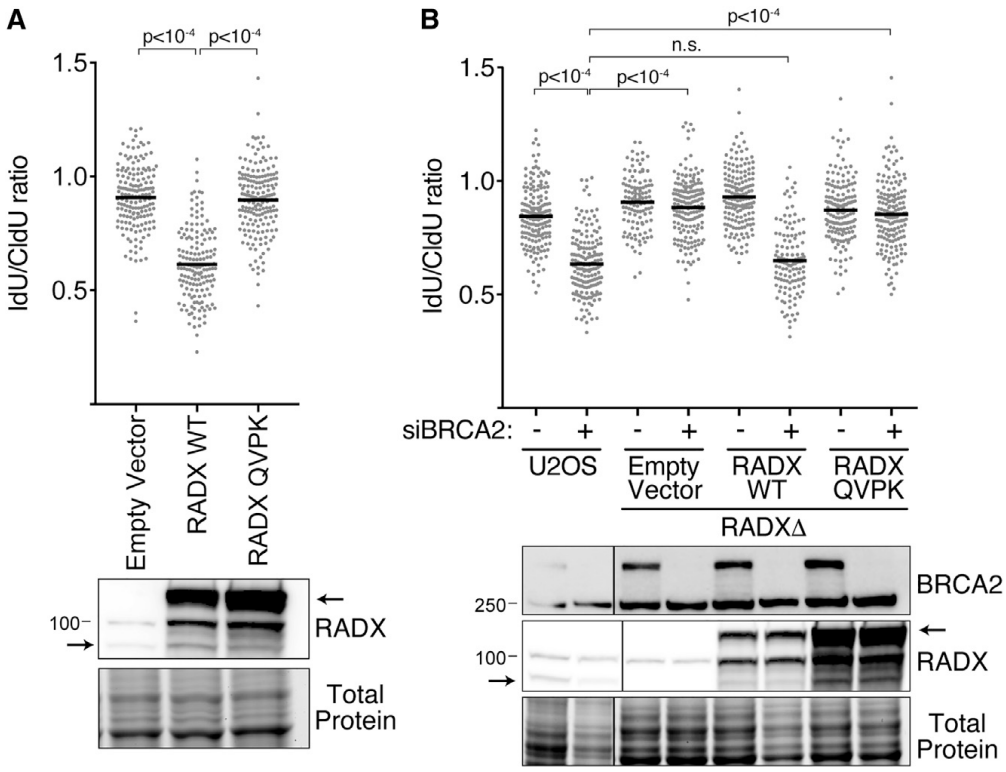

Figure 4.9. A direct interaction of RADX and RAD51 is required to maintain fork stability in cells experiencing persistent replication stress

(A) Fork protection assays with 3 mM HU were performed in U2OS cells immediately after infection with lentiviruses to overexpress WT RADX or RADX QVPK. Arrows in the immunoblot indicate the endogenous and GFP-tagged RADX proteins. (B) Wild-type or RADXΔ U2OS cells complemented with WT RADX or RADX QVPK were transfected with non-targeting or BRCA2 siRNA and examined for fork protection. Note that the WT RADX but not the RADX QVPK mutant expression in the RADXΔ complemented cells decreases after a few passages as previously reported (Adolph et al., 2021). A one-way ANOVA with Tukey's multiple-comparison test was used to calculate all p values. All experiments were completed at least three times. Extra lanes were removed. Taha Mohamed helped generate some data. Dr. David Cortez performed the western blots.

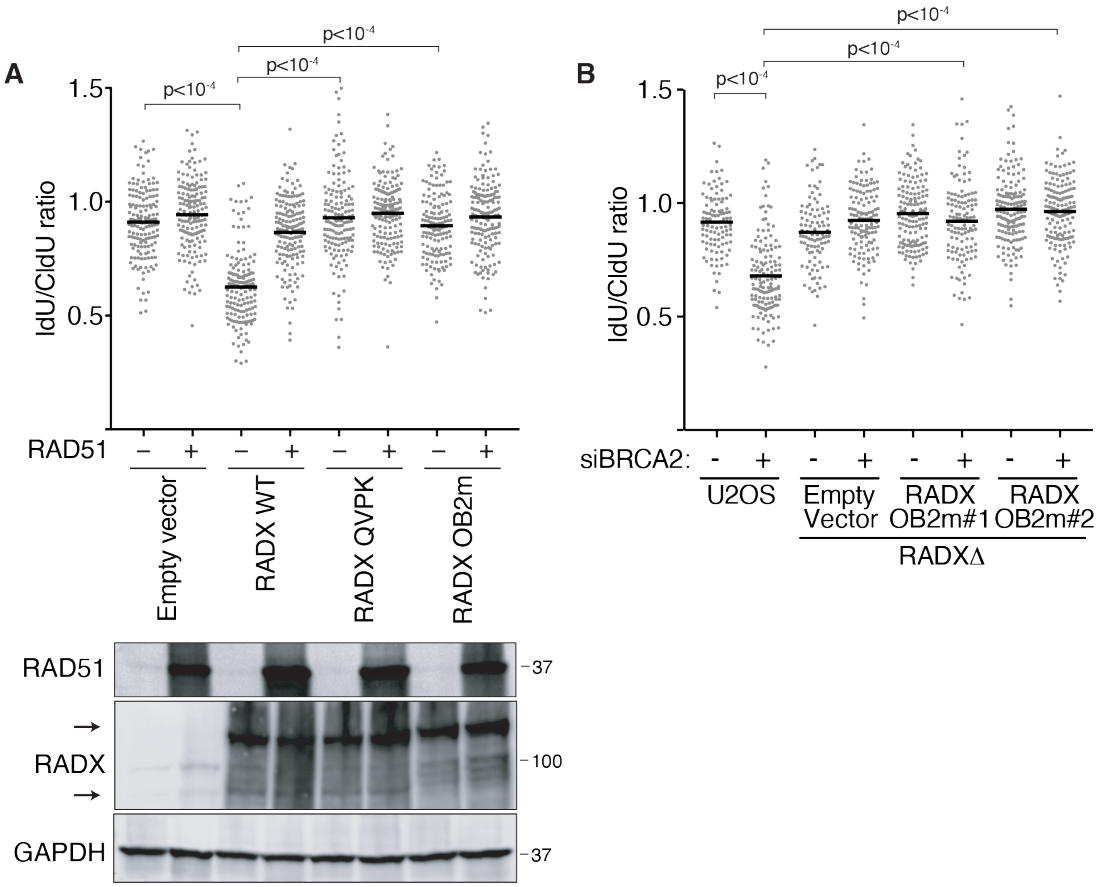

Figure 4.10. Interaction of RADX with single strand DNA and RAD51 is required for nascent strand degradation in cells treated with HU. (A) Fork protection assays were performed in HU-treated cells transiently overexpressing either wild- type RADX, QVPK RADX, or OB2m RADX and wild-type RAD51 as indicated. (B) Wild-type U2OS, RADXD U2OS cells (empty vector), or two clones of RADXD cells complemented with RADX OB2m (Dungrawala et al., 2017), were transfected with non-targeting or BRCA2 siRNA as indicated. Fork protection assays were completed. Arrows in the immunoblot indicate the endogenous and GFP-FLAG-tagged RADX proteins. A one-way ANOVA with Tukey's multiple comparison test was used to calculate all p values. All experiments were completed at least two times.

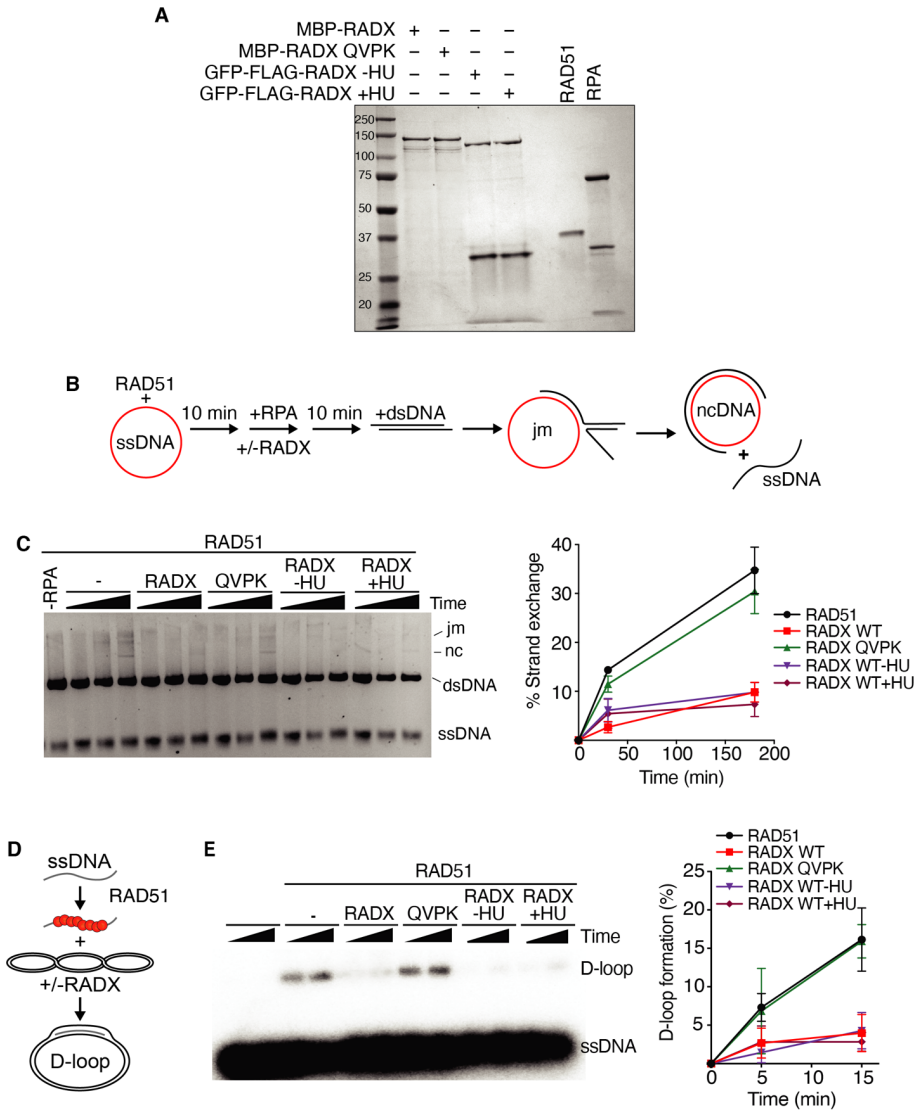

Figure 4.11. RADX purified from unstressed and HU-treated cells inhibits strand exchange and D-loop formation. (A) Coomassie stained SDS- PAGE gel showing purified proteins used in this study. Each lane contains ~200 nM of purified protein. Actual amounts used is specified in each experiment. MBP-RADX and MBP-RADX QVPK were purified from insect cells while FLAG-GFP-RADX -HU and FLAG-GFP-RADX +HU were purified from 293T cells that were synchronized in S-phase and either harvested immediately or treated with 3mM HU for 5 hours before harvesting. (B) Schematic of strand exchange experiment (jm, joint molecules; nc, nicked circular dsDNA). (C) A representative gel and quantitation of n=3 strand exchange assays are shown. Error bars are SD. (D) Schematic of displacement loop assay. (E) Representative gel of the D-loop assay and quantitation of n=3 (mean+/-SD). Dr. Madison Adolph generated all the data in this figure.

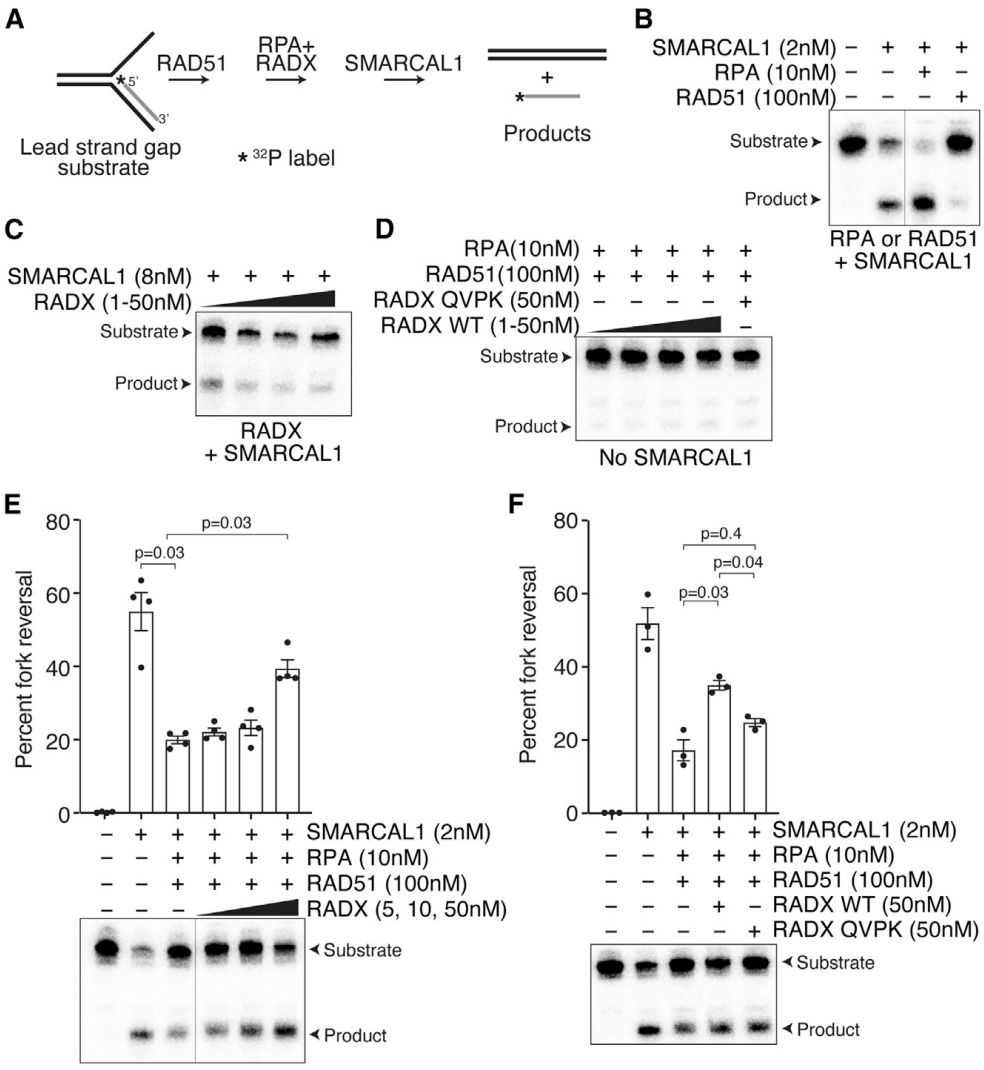

Figure 4.12. RADX promotes fork reversal by destabilizing RAD51 filaments *in vitro*
(A) Schematic of the fork reversal assay. (B) Addition of RPA stimulates SMARCAL1-dependent fork reversal, while addition of RAD51 inhibits fork reversal. (C) Increasing concentrations of RADX by itself inhibits fork reversal by SMARCAL1. (D) Addition of RPA, RADX, and RAD51 does not catalyze fork reversal in the absence of SMARCAL1. (E) Addition of increasing concentrations of RADX in the presence of RPA and SMARCAL1 overcomes the fork reversal inhibition caused by RAD51. Top: quantifications (n = 4; mean ± SEM). Bottom: representative experiment. (G) Unlike WT RADX, RADX QVPK does not stimulate fork reversal in the presence of RAD51, RPA, and SMARCAL1. Top: quantifications (n = 3; mean ± SEM). A representative experiment is shown. A repeated-measures one-way ANOVA with Sidak's multiple-comparison test was used to calculate p values. The line in blots indicate lanes were removed.

Six additional observations support the conclusion that RADX helps generate reversed forks in the presence of replication stress: (1) RADX accumulates at stalled replication forks, where it would need to operate to promote RAD51-dependent reversal (Dungrawala et al., 2017; Schubert et al., 2017); (2) RADX silencing or deletion prevents nascent strand degradation when protection factors, including BRCA2, BRCA1, BOD1L, ABRO1, Fanconi anemia proteins, and DCAF14, are inactivated, similar to the rescue observed by inactivating fork reversal enzymes percentage of reversed forks observed by EM in HU-treated cells is decreased when RADX is inactivated.

I envision two models to explain the apparent difference in RADX functions in the absence or presence of replication stress (Figure 4.13). First, RADX could switch functions from a RAD51 antagonist to a RAD51 activator in response to replication stress. A post-translational modification or change in protein binding partners could mediate this change. Second, RADX could retain the same biochemical activity (reducing RAD51 nucleofilament stability) in both stressed and unstressed cells; however, the reduction in RAD51 nucleofilament stability induced by RADX generates the metastable filaments needed for fork reversal in stressed cells, while it prevents inappropriate RAD51 access to elongating forks in unstressed conditions. In this second model, other changes in the replication fork proteome or DNA structures when cells are treated with HU would be needed to yield the apparent difference in outcome. I hypothesize that the difference may be the amount of ssDNA at active versus stalled forks (Figure 4.13; discussed in Chapter V).

Inactivating RADX in HU-treated cells reduces the percentage of reversed forks visualized by EM, but it does not fully prevent reversal, suggesting that either it is only important at a subset of stalled forks or it reduces the time that all stalled forks reside in the reversed state. Fork reversal is a dynamic process, with reversed forks being “reset” by fork restoration reactions catalyzed by RECQ1 or by the limited action of nucleases such as DNA2 (Berti et al., 2013; Hu et al., 2012; Thangavel et al., 2015). The fork reversal enzymes, such as SMARCAL1, can also catalyze fork restoration reactions (Betous et al., 2013a). Moreover, other fork protection proteins, such as RAD52, can prevent excessive RAD51 function and engagement of translocases at replication forks to limit fork reversal upon stalling (Malacaria et al., 2019). The stability of the RAD51 filament and whether it is formed on gaps in the template DNA strands, on the nascent DNA of a reversed replication fork, or even its binding to double-strand DNA at the fork will also determine the dynamics of the conversion between a three-way to four-way junction. The persistence of the replication block, amount of ssDNA, recruitment of other RAD51 regulators, and activity of competing pathways all likely combine to yield the static snapshot of reversed fork frequency that

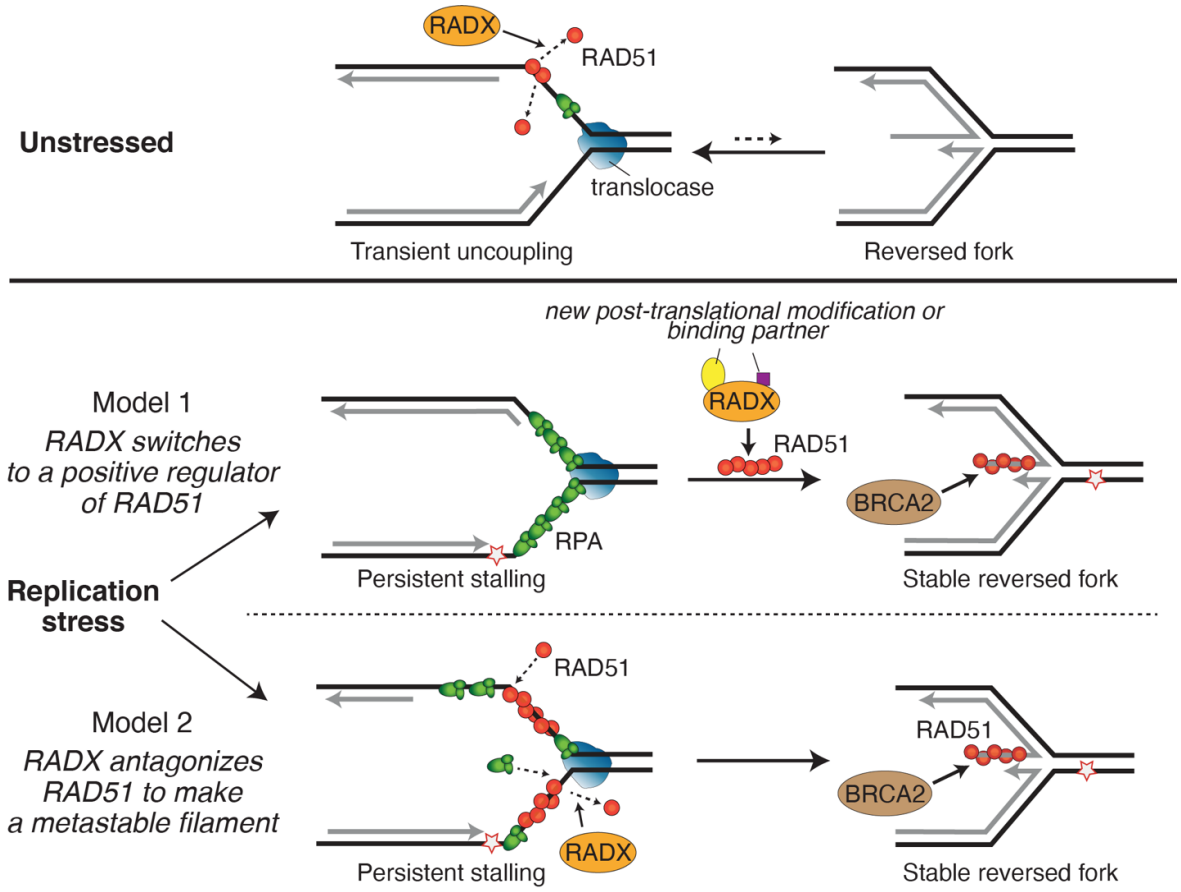

Figure 4.13. Models for RADX function in the absence and presence of added replication stress. RADX directly binds to ssDNA and RAD51, increases RAD51 ATP hydrolysis rates, and destabilizes RAD51 filaments (Adolph et al., 2021). In unstressed cells, RADX may displace RAD51 bound to ssDNA that is exposed on the lagging strand or during transient uncoupling of leading and lagging strand polymerization. This activity prevents fork reversal. Upon addition of replication stress, more extensive ssDNA is generated, and RADX is required to promote fork reversal. In model 1, RADX may gain a post-translational modification or binding partner to switch from an antagonist to an activator of RAD51. Alternatively, in model 2, RADX may be required to displace RAD51 from ssDNA to promote the formation of a metastable RAD51 filament for fork reversal.

is observed by EM. RADX may change the dynamics of RAD51 at HU-stalled forks enough to shift the equilibrium between the three- and four- way junctions toward reversal, but not be absolutely essential explaining why some reversed forks remain visible by EM.

In summary, RADX antagonizes RAD51 in unstressed cells to prevent aberrant fork reversal. However, in stressed cells with persistently stalled forks, RADX interacts with RAD51 to promote reversal. In both cases, RADX may operate by destabilizing RAD51 filaments. By confining fork reversal to stalled forks, RADX prevents aberrant processing by nucleases that can generate genome instability.

Limitations of the study

Although I used more than one cell line in many experiments, it is possible that the some of the effects I observe by inactivating RADX could be cell type dependent. The *in vitro* fork reversal assay results are dependent on protein and DNA concentrations. Furthermore, they do not fully mimic the reaction *in vivo*, as only a few proteins are added to simple DNA substrates in these experiments. Recombinant RADX purified from unstressed and HU-treated cells may not retain the appropriate post-translational modifications, or the biochemical assays may fail to contain the needed components to visualize a shift in function. Furthermore, RPA and RAD51 are also post-translationally modified in response to replication stress, and the *in vitro* reactions do not capture the effects of those modifications. Additional biochemical assays using different DNA substrates and additional proteins including other RAD51 regulators will be needed to fully understand how RADX acts.

CHAPTER V

DISCUSSION AND FUTURE DIRECTIONS

Summary of dissertation work

Errors during replication can drive mutations and cause diseases like cancer. Proteins involved in replication-coupled repair pathways thus represent an important class of chemotherapeutic targets. Examining the mechanisms that regulate replication fidelity is critical for understanding the etiology of cancers and identifying novel therapies.

In response to replication fork stalling lesions, exposure of ssDNA followed by dynamic changes in DNA structure facilitate fork stabilization, repair and restart. ssDNA binding proteins like RPA and RAD51 constitute the first line of response to replication stress and are required for many essential DNA transactions including replication, transcription, repair, and recombination. Thus, regulation of ssDNA binding proteins is critical to overcome replication challenges.

One mechanism for stalled fork repair is replication fork reversal. Fork reversal refers to the remodeling of a three-way junction to a four-way junction through reannealing and extrusion of nascent DNA. Fork reversal is catalyzed by the combined actions of ATP-dependent translocases and helicases such as SMARCAL1, ZRANB3, HLTF, FBH1 and ssDNA binding protein, RAD51 (Bansbach et al., 2009; Betous et al., 2012; Ciccia et al., 2012; Couch et al., 2013; Kile et al., 2015; Zellweger et al., 2015). Proteins that promote fork remodeling are important for genome maintenance (Bansbach et al., 2009; Ciccia et al., 2012; Kile et al., 2015), providing evidence that fork remodeling is a physiological stress response pathway in mammalian cells. The functions of ssDNA binding proteins in regulating replication fork remodeling and resolution of stalled fork intermediates are less well understood.

In this dissertation, I have further examined the functions of ssDNA binding proteins in regulating fork reversal and fork protection. Specifically, in Chapter III, I further characterized the functions of a newly identified RPA-like ssDNA binding protein, RADX, in modulating fork protection. In

Chapter IV, contrary to a previous model, I found that RADX has opposing functions on fork reversal in the presence or absence of replication stress in correlation with the amount of ssDNA. Both of these functions require a direct interaction of RADX with RAD51 and ssDNA. To explain these results, I propose a model in which RADX regulates RAD51 to generate a metastable filament that is required to promote fork reversal.

Discussion

In this section, I will review my current model for the functions of RADX at elongating and stalled replication forks, discuss some observations that do not fit my model, and provide perspective on outstanding questions.

Functions of RADX at replication forks

I discovered that in the absence of added replication stress, RADX inhibits fork reversal to prevent fork slowing and fork breakage. However, in the presence of added replication stress, RADX helps generate reversed forks. Importantly, this context-dependent function of RADX depends on its ability to directly interact with ssDNA and RAD51.

RADX inactivation causes aberrantly reversed forks to accumulate which slows replication fork elongation and promotes fork breakage in the absence of exogenous stress. Indeed, both fork slowing and fork collapse in the absence of RADX can be rescued by inactivating fork reversal enzymes HLTF, ZRANB3, SMARCAL1 or silencing RAD51. Additionally, inactivation of MUS81 rescues fork collapse in RADX-deficient cells. Direct visualization of replication fork intermediates by EM shows an accumulation of reversed forks in the absence of RADX without any added replication stress (Dungrawala et al., 2017; Krishnamoorthy et al., 2021). These observations led me to conclude that RADX inhibits aberrant fork reversal in unstressed cells.

In the presence of replication stress, RADX loss prevents nascent strand degradation when fork protection factors, including BRCA2, BRCA1, and Fanconi anemia proteins, are inactivated,

similar to the rescue observed by inactivating fork reversal enzymes. Our lab initially proposed that the fork protection phenotype upon RADX loss was due to inhibition of nuclease-mediated fork degradation by improving the stability of RAD51 filaments on the reversed arm (Bhat et al., 2018; Dungrawala et al., 2017). However, I found that rescue of fork protection in the absence of RADX occurs without restoration of RAD51 foci. This led me to propose that RADX may promote the formation of reversed forks upon stalling. Indeed, EM and biochemical data support a model where RADX "switches" function from inhibiting fork reversal in the absence of stress to promoting formation of reversed fork structures upon persistent stress (Krishnamoorthy et al., 2021).

Two models can explain the apparent difference in RADX function in the absence or presence of stress. First, RADX could switch from a RAD51 antagonist in the absence of stress to a RAD51 activator in response to stress. A change in binding partner or a post-translational modification could mediate this change. Second, RADX could retain the same biochemical activity in both stressed and unstressed cells; however, by making the RAD51 nucleofilament more dynamic, RADX could generate metastable filaments needed for fork reversal in stressed cells, while it prevents inappropriate RAD51 access to elongating forks in unstressed conditions.

I speculate that the amount of ssDNA determines the phenotypic outcome for reversal at active versus stalled forks. For example, when there is limited ssDNA for short times, such as what would be present on the lagging template strand at active replication forks or what would be generated by stochastic polymerase speed changes (Graham et al., 2017), RADX destabilization could prevent RAD51 from accessing the forks to promote reversal. However, when there is persistent fork stalling yielding more ssDNA, then destabilization of RAD51 filaments that form on the template DNA strands could be needed to allow the fork reversal enzymes to reanneal the parental DNA and catalyze fork reversal. In other words, accumulation of RADX at stalled forks could help the reannealing of the parental DNA strands by making the RAD51 nucleofilament more dynamic so it does not act as a roadblock to reversal and possibly to allow RPA to remain present where it can stimulate SMARCAL1 (Figure 5.1).

While I cannot fully rule out the first model, my current data (as shown in Chapter IV) support the second model for several reasons. First, RADX function in both stressed and unstressed cells

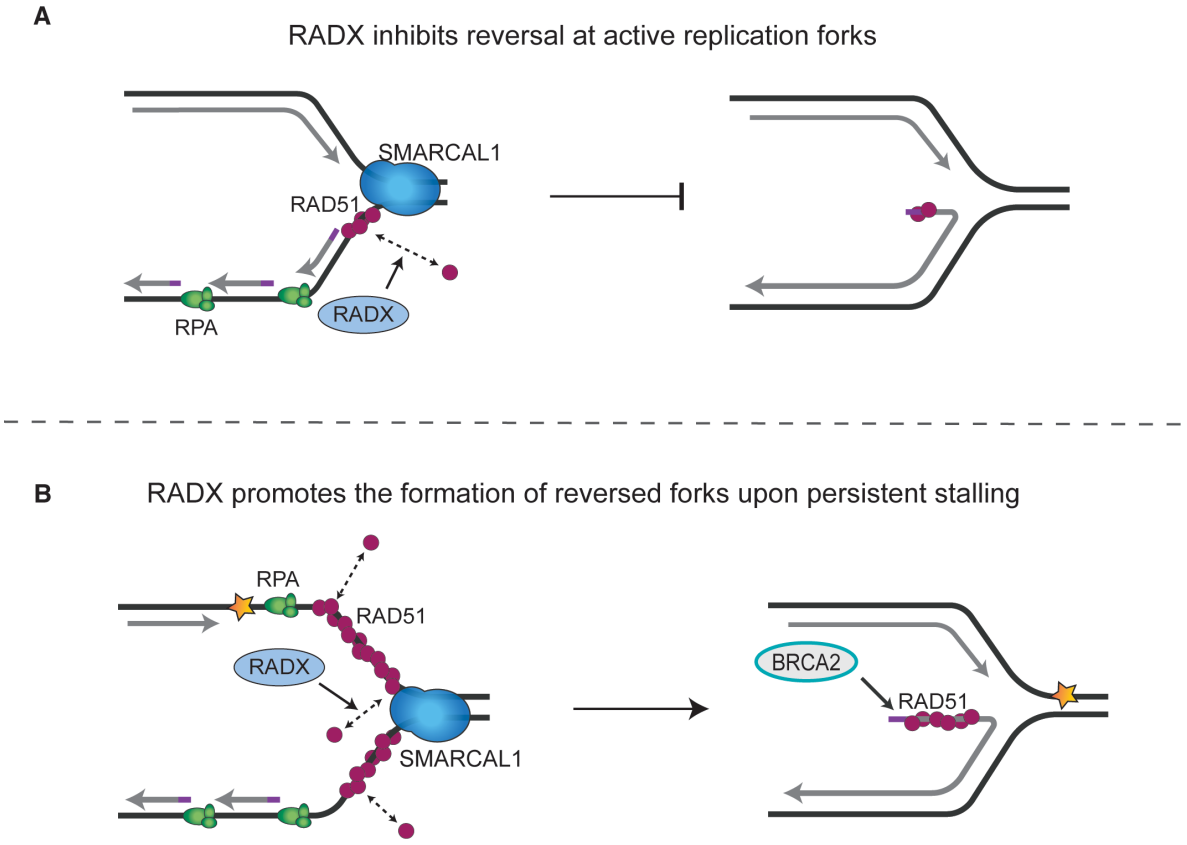

Figure 5.1. Model for RADX functions at replication forks. See text for details. A. RADX prevents fork reversal in the absence of added stress by displacing RAD51 bound to ssDNA. B. Upon addition of replication stress, RADX may promote destabilization of RAD51 from ssDNA to form a metastable filament for fork reversal. In both cases, RADX functions by directly binding to RAD51 and ssDNA.

requires a direct interaction with RAD51 and ssDNA. Second, loss of RADX increases RAD51 chromatin localization both in the absence and presence of stress. Third, RADX purified from unstressed or HU-treated cells inhibits RAD51-mediated strand exchange and D-loop activity. Fourth, overexpressing RAD51 overcomes the fork destabilization caused by overexpressing RADX suggesting they retain an antagonistic relationship in the presence of HU. Fifth, RAD51 added to fork reversal assays can inhibit SMARCAL1, presumably by acting as a steric block to enzyme translocation. Adding RADX to these reactions (but not RADX that cannot interact with RAD51) overcomes the RAD51-dependent inhibition when RPA is also present. The same purified RADX protein inhibits RAD51-dependent strand exchange and destabilizes RAD51 nucleofilaments (Adolph et al., 2021). Finally, a "less is more" model for RAD51 activity has precedence in the bacterial literature, where the *N. gonorrhoeae* RecX protein biochemically inhibits *N. gonorrhoeae* RecA but actually promotes its function *in vivo* (Gruenig et al., 2010). Although RADX has no sequence similarity to RecX, the RecA and RAD51 proteins are orthologs that likely require similar regulatory mechanisms.

In summary, RADX antagonizes RAD51 in unstressed cells to prevent aberrant fork reversal. However, in stressed cells with persistently stalled forks, RADX interacts with RAD51 to generate a "metastable" RAD51 filament proposed to be needed for reversal (Berti et al., 2020a). Future experiments to determine protein interactions and post-translational modifications will be important to identify the mechanism(s) of RADX regulation.

Observations that do not easily fit my current model

My proposed model does not fit several of my observations. I have highlighted a few below and speculated on possible explanations:

- Rescue of fork protection – While there is a partial rescue in the number of reversed forks in HU-treated cells using EM upon RADX inactivation, a complete rescue of nascent strand degradation is observed in cases where fork protection factors are inactivated. Thus, whatever reversal happens in these circumstances is not enough to yield extensive nascent strand degradation. RADX, like RAD51, may be acting in two steps of the fork protection pathway at persistently stalled forks: promoting fork reversal and destabilizing RAD51 filaments on the reversed fork, making it more susceptible to nucleases. Alternatively, nascent strand degradation may require multiple cycles of reversal and degradation. If RADX inactivation reduces this dynamic cycling, that would also explain

why fork degradation is completely dependent on RADX, but fork reversal is only partially dependent on RADX.

- Fork degradation upon prolonged HU treatment – Replication forks undergo nascent strand degradation by DNA2 upon treatment with HU for long periods of time. This degradation occurs even in cells with wild-type levels of RAD51 and BRCA2 (Thangavel et al., 2015). Intriguingly, this degradation is dependent on FBH1-dependent reversal (Mason et al., 2019) but not SMARCAL1, ZRANB3, or HLTF mediated remodeling (my data; Figure 5.2A) . In agreement with reversed forks being degraded, depletion of RAD51 rescues the degradation with prolonged HU treatment (Thangavel et al., 2015)(Figure 5.2B). In Chapter III, I showed that unlike RAD51, depletion of RADX does not rescue the degradation after prolonged HU treatment (Figure 5.2B). However, my model posits that upon stalling, loss of RADX prevents fork reversal by stabilizing RAD51 on parental ssDNA; if this model were correct, then loss of RADX should rescue the fork degradation by preventing the formation of reversed fork structure – the substrate for degradation. One possibility, as explained previously, is that nascent strand degradation may require many cycles of fork reversal followed by nuclease processing; if RADX inactivation reduces this cycling, it might slow degradation but not prevent it. Thus, degradation may still occur but more slowly with prolonged stalling even in the absence of RADX. Alternatively, prolonged HU treatment may promote fork collapse which converts stalled replication forks to DSBs further processed by DNA2. This hypothesis does not explain why degradation is rescued by silencing RAD51 or FBH1 – unless these enzymes are also required to generate the fork collapse substrate. Lastly, Mason et al., showed that exogenous RAD51 overexpression does not rescue fork degradation upon prolonged stalling (Mason et al., 2019) raising the possibility that fork protection in this case is RAD51 independent. This may explain why even though RADX inactivation stabilizes RAD51 nucleofilaments on the regressed arm, it may not be enough to prevent processing by nucleases with extended HU treatment.

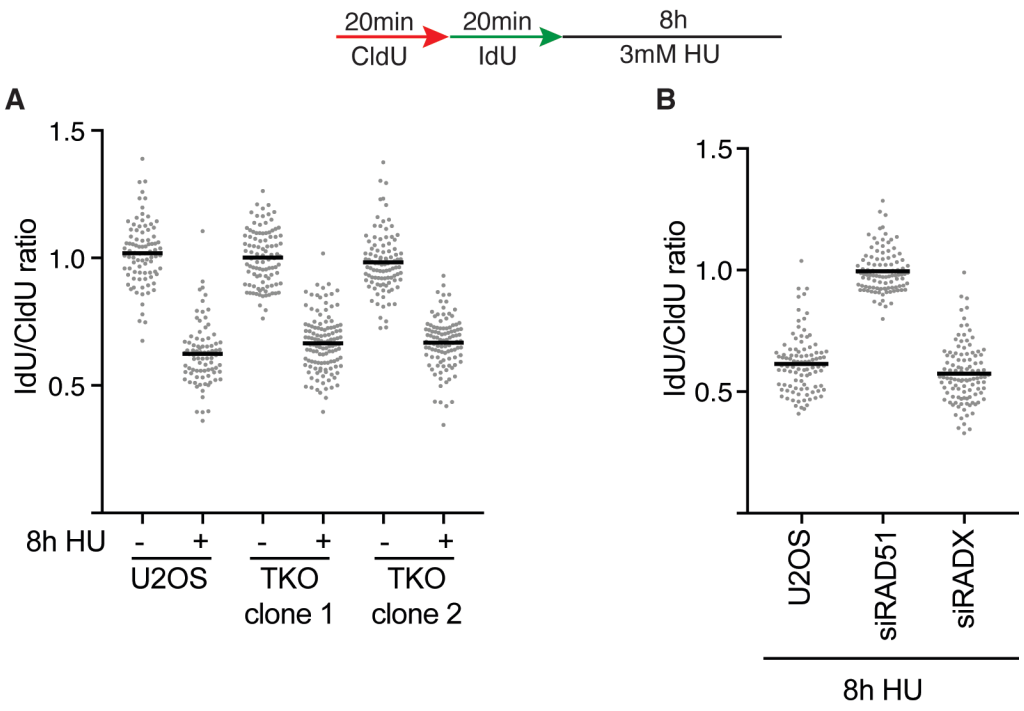

Figure 5.2. Nascent strand degradation upon prolonged HU treatment requires RAD51 but not SMARCAL1, ZRANB3, HLTF, or RADX. A schematic of the DNA fiber experiment is shown. A and B. Fork protection assays with 3mM HU for 8h were performed in triple translocase knockouts (TKO) generated with CRISPR-Cas9 or in cells transfected with siRNA to RAD51 or RADX. Each data point is an individual DNA fiber measurement.

- RAD51 foci – The current model for RADX function proposes that RAD51 stabilized on the exposed parental ssDNA acts as a roadblock to reversal; thus, destabilization of RAD51 filaments by RADX ensures the formation of a metastable filament. In Chapter IV, I observed that inactivating RADX in BRCA2-deficient cells rescues fork protection without restoring RAD51 foci (Figure 4.3, Chapter IV). If RAD51 is stabilized on the parental ssDNA in the absence of RADX, as my model predicts, I should have observed RAD51 foci upon inactivation of BRAC2 and RADX. However, I do not observe RAD51 foci in this case (Figure 5.3). Presumably, the length of ssDNA at a stalled fork is not long enough to establish a RAD51 nucleofilament focus visible by immunofluorescence. More sensitive techniques such as proximity ligation assay (PLA) may help visualize stabilized RAD51 at replication forks.

- Partial depletion of RADX – I previously showed the differential requirements of RAD51 at a stalled fork with more RAD51 required for fork protection than reversal (Bhat et al., 2018). Similarly, partial inactivation of RADX causes nascent strand degradation. The resection substrate in this case is likely a reversed fork since silencing any of the fork reversal enzymes or inhibition of nucleases prevents fork degradation (Krishnamoorthy et al., 2021). It is unclear why partial depletion of RADX promotes nascent strand degradation in otherwise wild type cells. One possibility is that a combination of partly reducing the dynamic cycling between reversal and degradation and destabilization of RAD51 filaments by whatever endogenous RADX is left in cells, may contribute to fork degradation. Regardless, in all of my observations, RADX phenocopies RAD51 with added replication stress. Future experiments to determine the mechanisms by which RADX and RAD51 promote fork reversal will be important to understand partial depletion phenotypes.

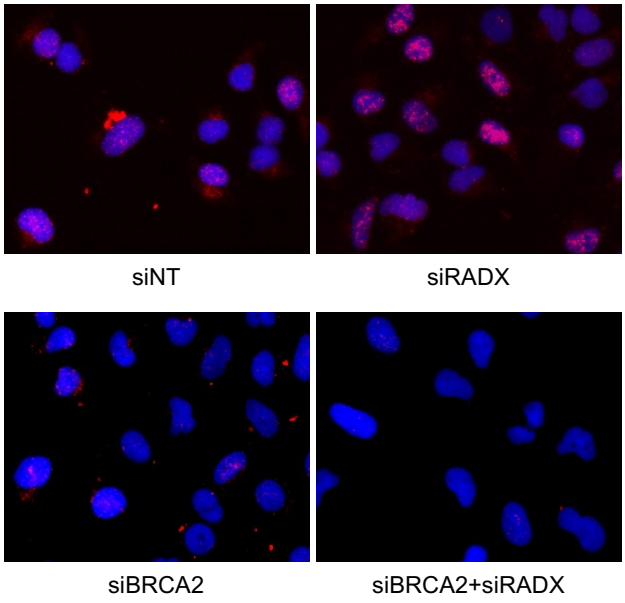

Figure 5.3. Loss of RADX in BRCA2-deficient cells rescues fork protection without restoring RAD51 foci. U2OS cells transfected with indicated siRNA are treated with 3mM HU for 5h. Representative images of chromatin-bound RAD51 are shown. Blue-DAPI, Red- RAD51.

Outstanding questions about RADX

- RADX regulation of DSB repair – While loss of RADX rescues fork degradation when fork protection factors are silenced; inactivation of RADX does not rescue HR defects in BRCA-deficient cells (Dungrawala et al., 2017). This may be due to the amount of ssDNA. For example, HR repair requires extensive resection at the DSB and RAD51 filament formation so, there may not be enough endogenous RADX in cells to destabilize RAD51 at DNA associated with DSBs. In agreement with this hypothesis, cells overexpressing RADX exhibit a modest defect in HR repair (Dungrawala et al., 2017). This indicates that when RADX is highly expressed, it can interfere with DSB repair. Alternatively, since BRCA2 and RADX compete for RAD51 binding, it is possible that BRCA2 excludes RADX from accessing RAD51 at a DSB. This model remains to be tested further.

- RADX regulation of nucleases – One possibility for why RADX depletion causes fork protection at persistently stalled forks would be for RADX to activate or recruit the fork degradation nucleases such as MRE11, DNA2, or EXO1. I do not favor this model for several reasons: First, there is no change in the levels of MRE11 at forks with RADX depletion (Dungrawala et al., 2017). Second, there is no increase in ssDNA or RPA S4/S8 phosphorylation upon RADX inactivation (Dungrawala et al., 2017). Third, no direct interaction is observed between RADX and MRE11. Finally, the percentage of reversed forks decreases upon RADX depletion in the presence of added stress which is the opposite of what would be expected if RADX promoted the activities of MRE11 or DNA2 (Krishnamoorthy et al., 2021).

- RADX regulation of translocases – RADX may regulate the activity or recruitment of translocases. We have not detected a change in the levels of translocases at forks upon RADX depletion nor a direct interaction between RADX and any of the translocases. Moreover, it is difficult to envision a model where RADX regulates all the translocases. Thus, I speculate that RADX indirectly regulates translocase activity by antagonizing RAD51 and modulating ssDNA availability. However, whether RADX directly interacts with the translocases may be an important next question to answer.

- Destabilization of RAD51 bound to dsDNA by RADX – Adolph et al., showed through a combination of single-molecule, negative stain EM, and structure-function mapping that RADX directly binds to and destabilizes RAD51 nucleofilaments on ssDNA (Adolph et al., 2021). Whether RADX is able to destabilize RAD51 bound to dsDNA is unknown. It is possible that dsDNA bound RAD51 has important functions for fork reversal and fork protection which may be regulated by RADX. Additionally, BRCA2 may be important in shifting the balance between RADX and RAD51 on ssDNA and dsDNA. Biochemical experiments using purified proteins will be critical to test these ideas.

Does RADX also regulate RPA?

RADX shares a high degree of structural and sequence similarity with RPA and competes with RAD51 for ssDNA. This raises the question of whether RADX regulates RPA. While we observed no changes in RPA levels at forks or sites of damage upon RADX depletion (Dungrawala et al., 2017), a recent study found that RADX regulates RPA to maintain replication fork integrity (Schubert et al., 2017). Specifically, Schubert and colleagues proposed that RADX may limit excessive RPA association at forks to prevent replication fork instability.

Single molecule and *in vitro* studies indicate that RPA bound to ssDNA cannot be displaced by RADX, possibly highlighting the difference in affinities to ssDNA. Moreover, binding of RADX and/or RPA to DNA prevents RAD51 nucleofilament assembly (Adolph et al., 2021; Ma et al., 2017). Intriguingly, in single-molecule DNA curtain assays, RADX colocalizes with RPA on ssDNA suggesting that RADX may bind to RPA-coated ssDNA (Adolph et al., 2021). It is unclear if RADX-RPA-RAD51 form a trimeric complex to regulate ssDNA availability.

Preliminary data show a direct interaction with RADX and RPA70N/RPA32 using NMR and *in vitro* studies (Remy Le Meur and Madison Adolph, unpublished). Structure-function studies will help map which domains of RADX mediate this interaction with RPA. It will also be important to characterize the function(s) of this interaction.

Fork reversal

In this section, I will discuss the functions of translocases and RAD51 in fork reversal and fork protection. I will conclude by proposing a unified model for how ssDNA binding proteins such as RADX, RPA, RAD51 and translocases coordinate to promote fork reversal.

Why so many fork reversal enzymes?

Fork reversal stabilizes stalled replication forks and promotes genome stability. However, aberrant accumulation of reversed fork structures can have deleterious consequences (Bansbach et al., 2009; Couch et al., 2013). Therefore, identifying mechanisms that regulate fork reversal is important to understand how this process is coordinated with other replication stress tolerance and repair mechanisms to yield stable genomes.

As mentioned in Chapter I, fork reversal occurs by the coordinated action of multiple ATP-dependent motor proteins like SMARCAL1, ZRANB3, HLTF, and FBH1. Three of these enzymes (SMARCAL1, ZRANB3, HLTF) may work in the same pathway since inactivation of any one reduces reversal and restores fork protection to BRCA2-deficient cells. In certain genetic contexts, FBH1 may operate in a separate pathway to remodel forks. RAD51 is required for promoting fork reversal in both pathways since inactivation of RAD51 blocks formation of reversed forks as observed by EM. In addition, other ssDNA binding proteins such as RPA and RADX also regulate fork reversal. *How multiple proteins cooperate across at least two distinct pathways to remodel forks remains unknown. This raises two important question that are addressed below: a) Why are there so many fork reversal enzymes? b) How are fork remodelers regulated to prevent inappropriate reversal?*

Differences in substrate preference

SMARCAL1, ZRANB3, HLTF, and FBH1 can all catalyze fork reversal on model DNA substrates and have been confirmed by EM to promote fork reversal in cells in response to replication stress

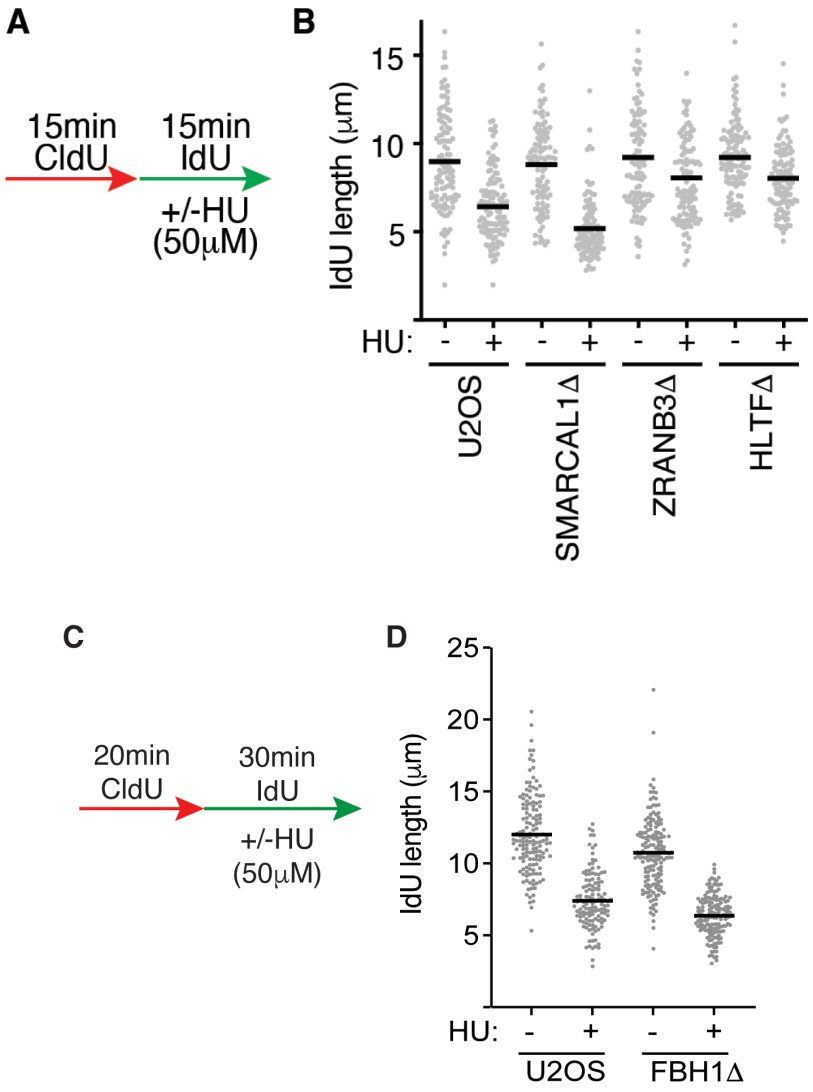

Figure 5.4. Differences in fork speed in the presence of low levels of replication stress after inactivation of fork reversal enzymes. A, C. Schematic of DNA combing experiment. B, D. A representative experiment showing fork speeds in the indicated U2OS-derived cells.

(Bai et al., 2020; Betous et al., 2012; Chavez et al., 2018; Ciccia et al., 2012; Fugger et al., 2015a; Taglialatela et al., 2017). However, these enzymes exhibit differences in substrate specificity *in vitro* (Betous et al., 2013a; Chavez et al., 2018) and have different phenotypic outcomes upon their inactivation suggesting a simple linear pathway may not be sufficient to explain their functions.

One possible explanation for these differences is that each enzyme prefers a specific DNA substrate to remodel upon stalling. I observed one such difference between the translocases in cells treated with low dose HU. While HLTF restrained fork speeds in response to mild levels of replication stress (Bai et al., 2020), I did not observe faster elongation speeds in SMARCAL1-deficient U2OS cells treated with 50 μM HU, although ZRANB3 inactivation did cause faster forks in these conditions (Figures 5.4A and 5.4B). The reason for the difference between translocases is unclear, however, it is possible that the structure generated in response to low dose HU is not preferentially remodeled by SMARCAL1. It has been shown previously that SMARCAL1 is less active on substrates with a lagging strand gap (Betous et al., 2013a). Whether this structure is generated upon low dose HU is yet to be tested. Preliminary data suggests that FBH1, like SMARCAL1, also does not rescue fork elongation defects in these conditions (Figures 5.4C and 5.4D).

Liu *et al*., recently showed that fork protection is restored in BRCA2-deficient cells upon inactivation of either SMARCAL1, ZRANB3 or HLTF individually or together suggesting that they work in the same pathway. Conversely, silencing FBH1 but not SMARCAL1/ZRANB3/HLTF rescued nascent strand degradation when 53BP1, BOD1L, and FANCA are inactivated (Liu et al., 2020). These observations indicate that at least two distinct fork remodeling pathways likely operate to generate resection substrates that require different fork protection proteins for stability. I speculate that differences in DNA structure could determine pathway choice. Alternatively, differences in genomic or chromatin contexts could also necessitate different remodelers. Determining chromatin structures and protein recruitment at individually stalled forks will be important future steps.

Differences in regulation of recruitment and function

Another model to explain the need for multiple fork reversal enzymes could be the different mechanisms of regulation – both in recruitment and context-dependent function. A few examples of such regulation for each translocase are discussed below:

SMARCAL1- As discussed in Chapter I, RPA bound to the leading strand gap mimicking a 'stalled fork' stimulates SMARCAL1 while RPA bound to lagging strand gap inhibits SMARCAL1 (Betous et al., 2012). How RPA achieves this dual function – stimulating on some substrates while inhibiting on others is unknown. The mechanism of RPA stimulation is likely due to the intrinsic polarity with which RPA binds DNA. Specifically, the orientation of the high-affinity DNA binding domains DBD-A and DBD-B of RPA with respect to the fork junction may be critical for regulation of SMARCAL1 (Bhat et al., 2015). In addition, the N-terminus of SMARCAL1 primarily interacts with RPA32C and has a secondary interaction with RPA70N (Bansbach et al., 2009; Ciccia et al., 2009; Yuan et al., 2009; Yusufzai et al., 2009). It is possible that the specific interaction of RPA with SMARCAL1 imposes conformational changes to the fork to facilitate the movement of SMARCAL1. The secondary interaction site on 70N is less well characterized. Structural and single-molecule studies will help map sites of interaction and design mutations. Moreover, SMARCAL1 is regulated by post-translational modifications. Phosphorylation of SMARCAL1 by ATR limits its fork remodeling activity after binding to DNA (Couch et al., 2013). Several other sites of phosphorylation on SMARCAL1 have been reported but their significance remains unknown (Carroll et al., 2014).

ZRANB3- In contrast to SMARCAL1, RPA bound to leading strand gap inhibits ZRANB3 activity. However, ZRANB3 activity remains unchanged when RPA is bound to a lagging strand gap (Betous et al., 2013a). How RPA directs ZRANB3 activity is unclear since there is no direct interaction between RPA and ZRANB3. One possibility is that RPA acts as a steric block to translocation of ZRANB3 on DNA. How this is selective to leading strand remains to be studied. In addition to RPA, ZRANB3 is regulated by PCNA. ZRANB3 contains multiple PCNA interacting domains which are all important for its localization. ZRANB3 also preferentially binds to polyubiquitylated PCNA which is important for fork restart following replication fork stalling (Ciccia et al., 2012). Intriguingly, ZRANB3 contains a nuclease domain whose activity may be regulated

by its interaction with PCNA (Sebesta et al., 2017). The nuclease domain has not been well-studied. Finally, although there are no known post-translational modifications on ZRANB3, ATR or ATM inhibition affects its retention on DNA indicating that phosphorylation of ZRANB3 may be affected (Ciccia et al., 2012). Mapping relevant post translational modifications on ZRANB3 may be a next important step.

HLTF- Unlike SMARCAL1 and ZRANB3, HLTF has no known mechanism of recruitment to replication forks. However, HLTF can polyubiquitylate PCNA at K164 residue which promotes ZRANB3 recruitment (Motegi et al., 2008; Unk et al., 2008). *In vitro*, HLTF shows no preference for remodeling forks with a leading or lagging strand gap and is modestly inhibited by RPA bound to lagging strand gap (Chavez et al., 2018). How RPA regulates HLTF function is unknown. Since HLTF is both a translocase and an E3 ligase, how both of these activities are coordinated is not clear. For example, separation of function mutants that abrogate ubiquitin ligase but not translocation or fork regression activity will be useful to determine how HLTF is regulated in cells. Furthermore, it will be important to map the regulation of HLTF function by post-translational modifications.

FBH1- Similar to HLTF, FBH1 contains a helicase and an E3 ligase domain. *In vitro*, RPA stimulates the helicase activity of yeast FBH1 (Park et al., 1997). Whether the same regulation occurs in mammalian cells is not known. In addition, FBH1 helicase activity is required for early phosphorylation of ATM substrates CHK2 and CtIP and for hyperphosphorylation of RPA (Fugger et al., 2015b), and is part of an SCF^{FBH1} complex that ubiquitylates RAD51 (Chu et al., 2015). If these mechanisms of regulation modulate FBH1 function in cells is yet to be determined. In addition, FBH1 can be post-translationally modified by ubiquitylation through CRL4(CDT2) leading to its degradation; possibly promoting its turnover at replication forks to facilitate repair through translesion (TLS) synthesis (Bacquin et al., 2013; Masuda-Ozawa et al., 2013).

In summary, multiple layers of regulation likely determine the pathway choice for fork remodeling. Future studies using a combination of genetic, biochemical, cell biology, and structural approaches will better define a unified model for fork reversal.

Functions of RAD51 at replication forks

RAD51 has well-defined functions as a recombinase in double strand break (DSB) repair. In addition, RAD51 has at least two functions at replication forks– promoting fork reversal and preventing nascent strand degradation (Kolinjivadi et al., 2017b). By itself, RAD51 cannot promote fork reversal *in vitro* although it can stimulate fork reversal in the presence of other proteins *in vitro* (Bugreev et al., 2011). Below, I discuss a few key questions about the functions and mechanisms of RAD51 at replication forks.

How does RAD51 promote reversal?

There are several possible mechanisms by which RAD51 can promote reversal. First, RAD51 may bind to parental ssDNA to cooperate with the translocases to catalyze fork reversal. While it is unclear how RAD51 cooperates with the translocases to promote reversal, my observations propose that a stable RAD51 filament on the parental DNA could act as a roadblock for translocases. Second, thinking of fork reversal as a dynamic process with the reversed fork in equilibrium with the restored fork suggests that RAD51 binding to the reversed arm could promote reversal through product capture. For example, when the fork reverses because of a leading strand lesion, there will be ssDNA on the reversed arm since the lengths of the nascent leading and lagging strands are different. RAD51 binding to that ssDNA could capture it and shift the equilibrium towards fork reversal, thus explaining the genetic requirement for RAD51 to observe reversed forks. Third, there could be mediator proteins, such as MMS22L-TONSL or RAD51 paralogs that are important for fork reversal functions of RAD51 (Berti et al., 2020b; Duro et al., 2010; O'Donnell et al., 2010; Piwko et al., 2016). Fourth, while RAD51-mediated fork reversal is thought to be BRCA2-independent, recent reports have shown that in cases of reduced RAD51 filament stability, BRCA2 may be required to drive reversal (Liu et al., 2020). How BRCA2 mechanistically mediates reversal and if this is distinct from its functions at DSB repair will require further investigation. Finally, a recent report also showed that the strand exchange activity of RAD51 may not be required for its fork reversal or fork protection function (Mason et al., 2019); whether this is true in all genetic contexts remains to be tested.

Regardless of the mechanism, RAD51 mediated fork reversal may be a highly dynamic process and stable filaments of RAD51 could act as a roadblock for reversal. Thus, I speculate that a 'metastable' filament of RAD51 is required to promote reversal, similar to what has been proposed recently (Berti et al., 2020a; Krishnamoorthy et al., 2021).

In the next section, I will compare and contrast the functions of RAD51 at fork reversal, fork protection, and DSB repair. I would also like to define a few terms:

RAD51 loading– I refer to RAD51 loading as the process by which 3-4 protomers of RAD51 are brought to ssDNA. Loading is typically facilitated by BRC1-4 repeat of BRCA2. These BRC repeats are insufficient for fork protection but sufficient for HR (also reviewed in Chapter I).

RAD51 stabilization– In this process, pre-loaded RAD51 protomers are stabilized and elongated. BRC5-8 and C-terminus are required for stabilization. Intriguingly, BRCA2 C-terminus is dispensable for HR but absolutely required for fork protection (reviewed in Chapter I).

How does RAD51 promote fork protection?

Unlike DSB repair, stabilization of RAD51 is sufficient to protect reversed forks from degradation by nucleases such as MRE11 or DNA2. This was recently demonstrated using a C-terminal mutant of BRCA2. This mutant cannot stabilize RAD51 filaments and is fully functional for HR, but deficient in fork protection (Schlacher et al., 2011). Indeed, recent microscopy-based studies show that cells lacking the BRCA2 C-terminus, do not form extended RAD51 filaments although they can initiate protofilament formation (Haas et al., 2018). This indicates that in HR, BRCA2-mediated stabilization of RAD51 filaments is either not as important, or is mediated by other factors, such as the RAD51 paralogs (Chun et al., 2013; Taylor et al., 2016).

BRCA2 mediated loading of RAD51 is not sufficient for fork protection. This suggests one of two possibilities: a) RAD51 can bind DNA at forks sufficiently without a mediator, complete fork reversal and then has a requirement for BRCA2 mediated stabilization or b) Mediators other than

BRCA2 might load RAD51 at forks, such as the MMS2L-TONSL complex (Piwko et al., 2016). As mentioned above, fork protection requires the C-terminus of BRCA2, implying that a stable RAD51 filament is critical for fork protection. Recent studies also suggest that the BRCA2 N-terminal domain and interaction with PALB2 is required for the recruitment and protection function of BRCA2 at stalled replication forks (Hartford et al., 2016; Murphy et al., 2014). The BRCA2-PALB2 complex is also thought to stabilize RAD51 further highlighting the importance of a stable RAD51 filament for fork protection.

All of the genetic and electron microscopy observations thus far indicate that a reversed fork is the entry point for nascent strand degradation by nucleases. Indeed, blocking fork reversal by depletion of any of the translocases or helicases in BRCA-deficient cells prevents fork degradation. While fork reversal may be a prerequisite for degradation in most cases, whether reversal is mandatory for degradation is unclear (Berti et al., 2020a). EM studies indicate that postreplicative gaps are typically observed in cells treated with sublethal doses of genotoxic agents (Zellweger et al., 2015). Moreover, recent studies show that postreplicative ssDNA gaps behind the fork such as those generated by PRIMPOL, maybe a substrate for fork degradation by nucleases like MRE11 (Quinet et al., 2020). A recent study identified a separation of function BRCA2 mutant that is proficient for gap filling but not fork protection implying that gaps may not be a substrate for degradation in all cases (Panzarino et al., 2021). Regardless, further studies are needed to determine the structures that undergo degradation upon fork stalling.

As discussed above, RAD51 has several functions in cells including fork reversal, fork protection, and HR. *This raises an important question: What are the differences between multiple functions of RAD51?* Several possibilities are discussed below.

Cells treated with a drug that inhibits RAD51-DNA binding, B02, exhibit fork degradation (Kolinjivadi et al., 2017b; Leuzzi et al., 2016). In this case, fork reversal is still presumed to occur since a reversed fork is the entry point for nascent strand degradation. One possible explanation is that RAD51-DNA binding is not required for fork reversal. An alternate hypothesis could be that fork protection is more sensitive to RAD51 inhibition than fork reversal. In other words, less RAD51 may be required to perform reversal than protection. This is consistent with BRCA2 being dispensable for fork reversal but required for fork protection to stabilize RAD51 filaments. In

support of the latter hypothesis, I found that at high concentrations, two potent individual siRNAs to RAD51 prevented fork degradation. However, when the siRNAs were titrated to intermediate concentration, I observed nascent strand degradation (Bhat et al., 2018). This indicates that the amount of functional RAD51 determines the fate of stalled replication forks, with more RAD51 required for fork protection than fork reversal and even more required for HR repair. Additionally, cells harboring a patient mutation (T131P; reviewed in Chapter I) that is defective in fork protection also phenocopies B02 treatment (Wang et al., 2015) implying a similar mechanism of RAD51 function for fork reversal and fork protection.

Conversely, cells treated with B02 or cell lines expressing T131P could form structures other than a reversed fork, such as postreplicative ssDNA gaps, which may be targeted for degradation. It is possible that RAD51 loading or stabilization on ssDNA gaps can protect forks from degradation. Direct visualization of replication intermediates using electron microscopy will be a next important step in understanding the complex mechanisms underlying fork reversal and fork protection.

The model describing differential requirements for RAD51 in fork reversal versus protection accurately depicts the genetic data, however, does not capture the complicated mechanisms of regulation. It is likely that an important determinant of RAD51 requirement is the amount of ssDNA (Figure 5.5). For example, HR involves the generation of long stretches of ssDNA (ranging from a few hundred nucleotides to ~10kb) and thus, the requirement for the highest amount of RAD51. In *E. coli*, RecA filament formation involves several, slow nucleation steps followed by rapid filament extension steps, similar to mammalian RAD51 (Cox, 2007; Hilario et al., 2009; Mine et al., 2007). It is possible that HR requires multiple RAD51 loading events, thus causing a need for the loading function of BRCA2. Recent single molecule studies using purified proteins from *C. elegans* indicate that BRCA2 initiates (likely multiple) RAD51 nucleation events on RPA-coated ssDNA which are then extended by RAD51 paralogs thereby promoting efficient strand invasion (Belan et al., 2021). Similarly, at reversed replication forks, stabilized RAD51 is required to protect from nucleases like MRE11 and DNA2 to prevent nascent strand degradation (Kolinjivadi et al., 2017b; Mijic et al., 2017; Schlacher et al., 2011; Taglialatela et al., 2017; Vujanovic et al., 2017). However, EM studies indicate that the amount of ssDNA on the regressed arm can range from 100-300 nucleotides upon stalling (Zellweger et al., 2015). Thus, the requirement for RAD51 function at reversed forks is lower than that for HR proportional to the amount of ssDNA. There is still a need to stabilize RAD51 bound to the regressed arm to prevent fork degradation as

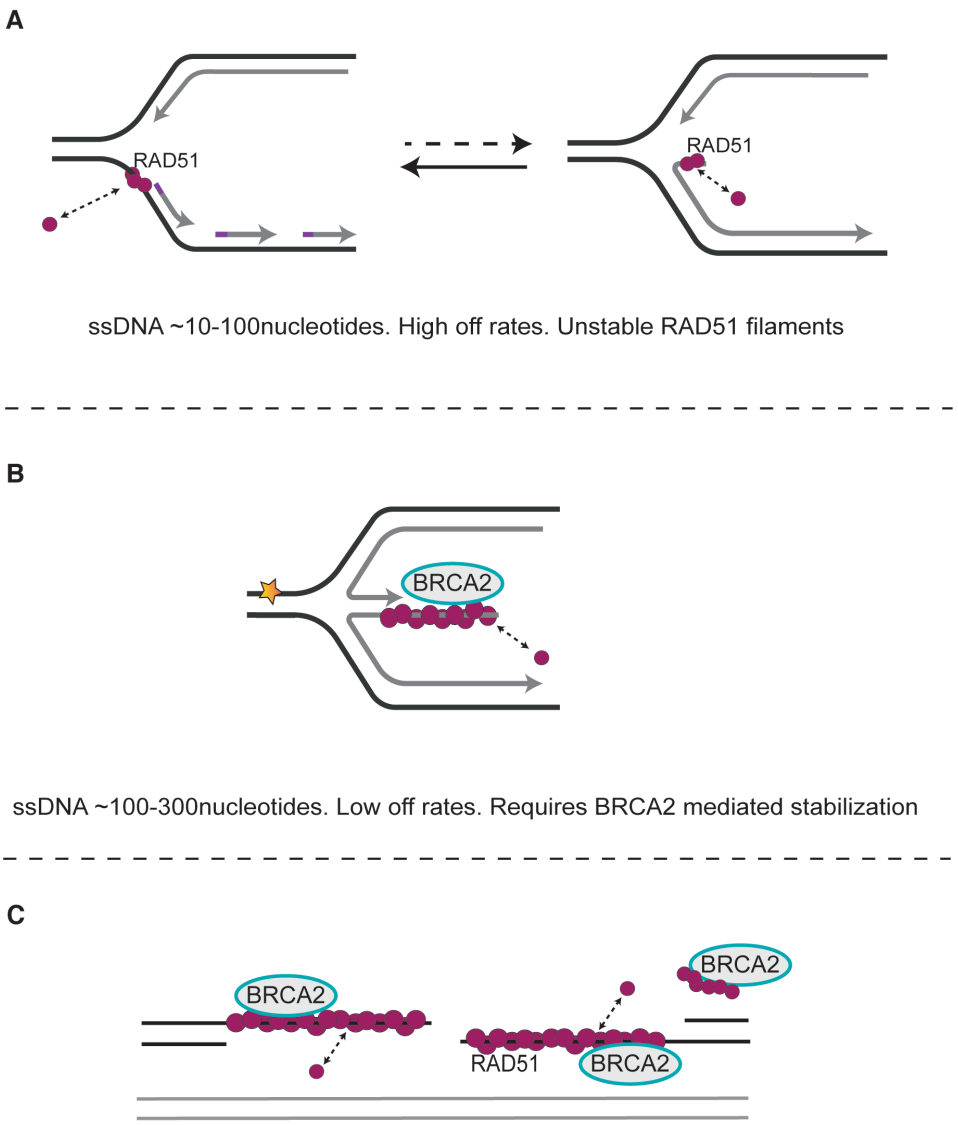

Figure 5.5. Model depicting differential RAD51 and BRCA2 requirements during fork reversal, fork protection, and DSB repair. The amount and availability of ssDNA are important determinants for recruitment and regulation of ssDNA binding proteins. See text for further details.

observed using mutants of BRCA2 that fail to stabilize RAD51 (Schlacher et al., 2011).

Presumably, in the absence of BRCA2-mediated stabilization, transient RAD51 dissociation allows nucleases to access the DNA to promote fork degradation. Finally, upon addition of replication stress, ~10-100 nucleotides of ssDNA is exposed at the fork junction (Neelsen et al., 2014; Zellweger et al., 2015). This is likely bound by RAD51 that are not stabilized since unstable filaments are presumably advantageous for fork remodeling. In agreement, many studies show that BRCA2 is not required for fork reversal (Kolinjivadi et al., 2017b; Mijic et al., 2017). It is possible that mediators are involved in loading RAD51 which promote reversal (reviewed in Chapter I).

Despite a lot of recent work on fork reversal and protection, how RAD51 promotes fork reversal is unknown. Specifically, it is unclear what activities of RAD51 are required for fork remodeling. One strategy would be to perform *in vitro* fork reversal and EM assays with RAD51 mutants (described in Chapter I and future directions) to help define the basis for substrate preference and mechanisms of fork reversal/branch migration.

While RAD51 has important functions at replication forks, excessive RAD51 activity can be detrimental. Indeed, RAD51 is frequently overexpressed in cancers and RAD51 overexpression causes genome instability (Hansen et al., 2003; Klein, 2008; Parplys et al., 2015; Richardson et al., 2004; Tennstedt et al., 2013; Vispe et al., 1998). Thus, tight regulation of RAD51 function by a multitude of RAD51 mediators and antagonists is essential to prevent inappropriate RAD51 activity and maintain genome stability (Marians, 2018).

RPA, RAD51, RADX, and translocases: how do they coordinate?

In the absence of added stress, inherent asymmetry in leading and lagging strand polymerase rates exposes short stretches of ssDNA (Graham et al., 2017). Limited ssDNA for short times may not be able to engage fork reversal proteins. However, overexpression of RAD51 or depletion of RADX promotes aberrant fork reversal even in the absence of replication stress (Dungrawala et al., 2017; Krishnamoorthy et al., 2021; Parplys et al., 2015). Additionally, overexpression of

SMARCAL1 or ATR inhibition are detrimental to genome stability likely due to unregulated fork reversal (Bansbach et al., 2009; Couch et al., 2013).

Upon replication fork stalling, functional uncoupling of helicase from polymerase generates a platform for the recruitment of ssDNA binding proteins. RPA, a highly-abundant protein with high affinity for ssDNA, is the first responder. As reviewed earlier, RPA recruits and directs the activities of SMARCAL1 (Betous et al., 2013a). In certain contexts, RPA may regulate the functions of other translocases. In addition to translocases, RAD51 is also required for fork reversal. Intriguingly, RAD51-mediated fork reversal is independent of BRCA2. RAD51 has a modest binding affinity to ssDNA; so, how RAD51 gains access to RPA-coated ssDNA without a mediator is unclear. Perhaps, the interaction between RPA-ssDNA is dynamic with frequent binding and dissociation events which may provide access to other ssDNA binding proteins. Additionally, *in vitro*, RAD51 does not have any fork remodeling activity on its own (Bugreev et al., 2011). Therefore, how RAD51 mechanistically coordinates with RPA and translocases to promote fork reversal remains to be studied. I have speculated a few possibilities below:

Whether RAD51 binds to the parental ssDNA to catalyze reversal or if it binds to the extruded regressed arm is unknown (Figures 5.6A and 5.6B). Regardless, many studies have found that the fork reversal function of RAD51 is BRCA2-independent (Kolinjivadi et al., 2017b; Mijic et al., 2017). Perhaps the initial extruded ssDNA tail is too small (<20nts) for RPA to bind in its high affinity DNA binding mode precluding the need for displacement by BRCA2. It is also possible that mediators such as MMS22L-TONSL complex or even BRCA2 may promote the fork reversal activities of RAD51 in some genetic contexts (Figure 5.6C). Additionally, RAD51 bound to dsDNA may also be involved in fork reversal. Biochemical reconstitution studies will be required to test these ideas. Nonetheless, stabilized RAD51 nucleofilaments (either on ssDNA or dsDNA) may inhibit fork reversal. An antagonist of RAD51 like RADX may be required to destabilize RAD51 to generate a discontinuous filament. Short stretches of RAD51, separated by RPA, may aid fork remodeling by yet unknown mechanisms. Finally, Berti et al., also recently proposed that a dynamic ‘metastable’ filament of RAD51 may be required for fork reversal (Berti et al., 2020a) in agreement with my hypothesis.

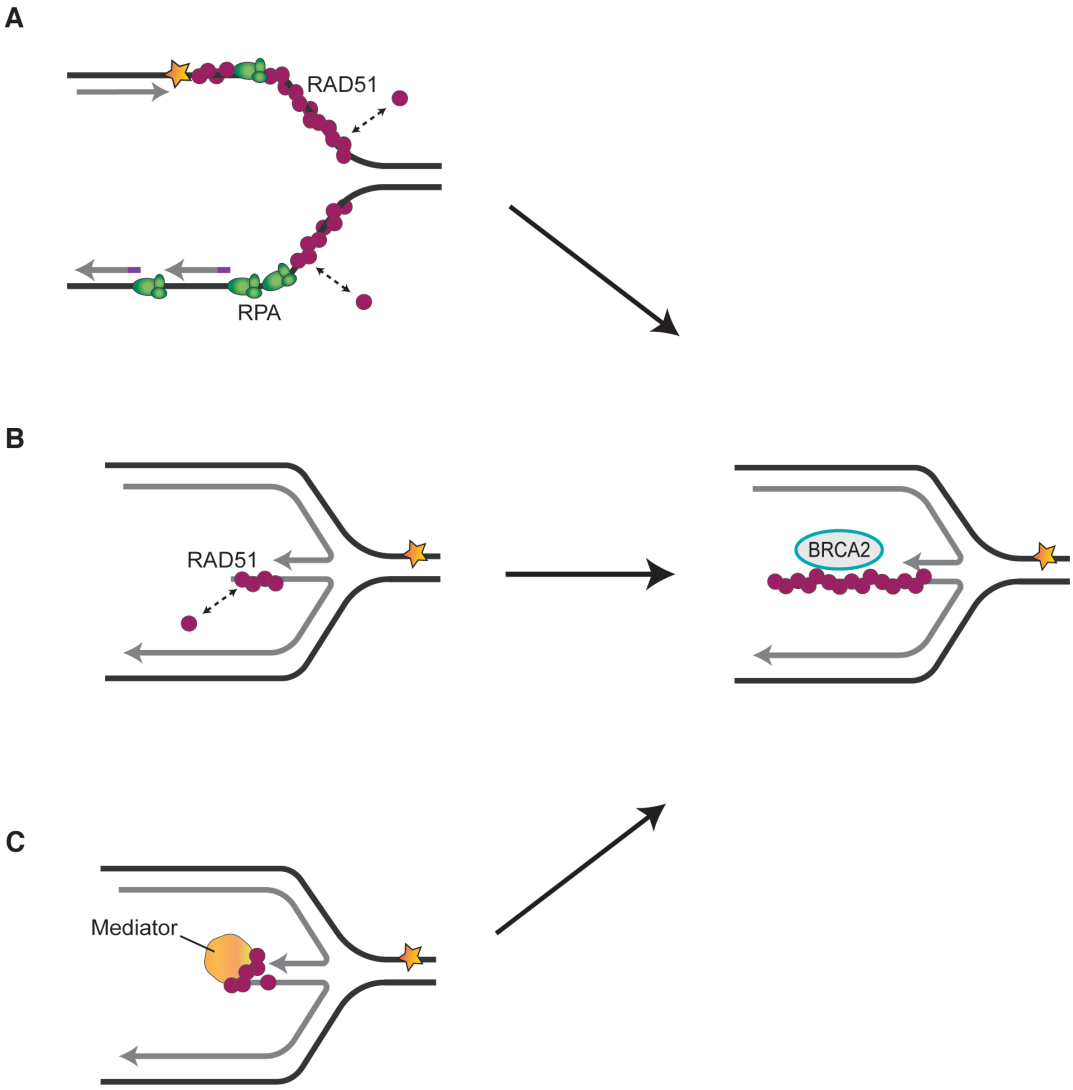

Figure 5.6. Possible mechanisms of RAD51 mediated fork reversal. A. RAD51 bound to parental ssDNA may coordinate with translocases to promote reversal. B. RAD51 may capture an already reversed fork to drive the equilibrium towards reversal. C. Mediator proteins could help load RAD51 to promote fork reversal.

Fork reversal is likely a highly dynamic process with the reversed fork in equilibrium with a restored fork during active replication. If the replication stress is persistent, however, the equilibrium shifts in favor of fork reversal. To remodel the stalled fork, RPA and/or RAD51 must be removed from the parental DNA as the template DNA is reannealed. SMARCAL1 is recruited by RPA and can promote fork reversal, suggesting that this could be a first step for remodeling. Moreover, single molecule studies show that SMARCAL1 works in repetitive annealing bursts where fork reversal is followed by pausing events (Betous et al., 2013a). Pausing presumably allows for dissociation, regulation, strand-switching, or 'hand-off' to another enzyme. The regressed arm may then be captured by RAD51. HLTF and ZRANB3 could 'complete' fork reversal by recognizing different substrates in coordination with ssDNA binding proteins such as RPA, RAD51, and RADX.

Another fork reversal pathway genetically distinct from SMARCAL1/ZRANB3/HLTF is mediated by FBH1 (Liu et al., 2020). How the helicase activity of FBH1 cooperates with RAD51 to promote reversal is unclear. Differences in stalled fork structure, nature of replication stress, localization and recruitment of reversal enzymes could influence the pathway choice. Future studies to describe where, when, and how translocases and helicases mechanistically coordinate with ssDNA binding proteins to maintain genome stability will require a combination of structure, solution and single-molecule biochemistry, model organism genetics and human cell experiments.

To add to the complexity, limited MRE11 or DNA2 mediated nuclease processing could yield alternative DNA structures to allow for translocase mediated reversal. For example, MRE11 nuclease is able to utilize its endonuclease activity and subsequently catalyze an exonucleolytic 3′-5′ resection which primes the activity of 5'-3' long-range nuclease EXO1 (Paull and Gellert, 1998). However, DNA2 is only able to catalyze 5′-3′ resection and has been shown to have activity against 5′ ssDNA flaps arising during Okazaki fragment maturation (Ayyagari et al., 2003; Rossi et al., 2018). This difference in substrate end recognition could promote degradation/processing of diverse structures. Thus, controlled degradation can also participate in fork remodeling in addition to translocases, raising the possibility that fork reversal involves multiple regulatory processes.

Future directions

Protein interactions for RADX

So far, we have identified that RADX directly interacts with ssDNA and RAD51. Preliminary experiments indicate that RADX may interact with itself to form higher order structures and with RPA (Madison Adolph and Taha Mohamed, unpublished). Previously, Drs. Kami Bhat and Huzefa Dungrawala attempted IP-MS experiments with endogenous RADX but did not observe any strong enrichment of proteins. Upon RADX overexpression, however, some weak interactors such as MCM2-6 complex, BRCA1, BLM and HLTF were observed (Kami Bhat, unpublished). These interactions were verified with a FLAG-IP followed by immunoblotting but have not been followed up. It will be important to identify RADX interaction partners to help understand the mechanisms by which RADX maintains genome stability.

In Appendix I, I describe my attempts to design an unbiased proximity labeling screen to identify RADX interactors.

Structure-function analysis of RADX

Structural modeling predicts that RADX has five structured domains, three OB-folds (OB-1, OB-2, OB-3) and two C-terminal domains (D4 and D5; Figure 1.12A). D4 and D5 are predicted to share structural similarity with the oligomerization domains of bacterial transcription factors DasR and NtrR, respectively (Remy Le Meur, unpublished). OB-2 domain interacts with ssDNA while OB-3 mediates interaction with RAD51. Preliminary data indicate that D4 and D5 may promote oligomerization of RADX (Taha Mohamed, unpublished). More recently, Alphafold software predicts a four OB-fold structure for RADX with the fourth OB-fold composed of part of OB-3 and D4 (unpublished). It is possible that the fourth OB-fold is important for secondary ssDNA binding and oligomerization.

Mutations in the OB-2 domain (OB2m) show reduced affinity to ssDNA and exhibit modest inhibition of some RAD51 functions *in vitro* (Adolph et al., 2021; Dungrawala et al., 2017). A recent report suggested that RADX inhibits RAD51 binding by condensing ssDNA and the OB2m

inactivates this function (Zhang et al., 2020). However, our lab found that the OB2m still retains some activity suggesting a few possibilities: First, RADX may have more than one site for ssDNA binding. Further experiments to map ssDNA binding sites will be important to test this idea. Second, other functions of RADX such as oligomerization may be important for ssDNA binding. Third, post-translational modifications could affect RADX binding to ssDNA. Understanding the regulation of RADX (described in the next section) will provide insights into its mechanisms of function at replication forks.

Regulation of RADX

Very little is understood about the regulation of RADX. It is possible that RADX is regulated on multiple levels including transcription, post-translational modifications that regulate its protein interactions, affinity for ssDNA, or oligomerization. Indeed, RAD51, RPA, and BRCA2 are all phosphorylated, SUMOylated, or ubiquitylated in response to DNA damage (Dou et al., 2010; Esashi et al., 2005; Luo et al., 2016; Schoenfeld et al., 2004; Shima et al., 2013). It will be important to identify the post-translational modifications on RADX to determine its mechanisms of regulation.

Localization/recruitment of RADX

In agreement with iPOND experiments, proximity ligation assays with endogenously tagged RADX indicate that RADX localizes to active and stalled replication forks. RADX OB2m shows a reduction in localization to forks however RADX QVPK does not, suggesting that direct interaction with ssDNA is sufficient for recruitment to forks (Adolph et al., 2021; Schubert et al., 2017). It will be interesting to test the localization of an RPA interaction mutant of RADX.

Conversely, upon overexpression of tagged RADX protein, RADX puncta are visible within the nucleus that do not co-localize with markers of DNA replication and do not change in response to replication stress. Intriguingly, none of the RADX mutants (OB2m, QVPK, or oligomerization mutant) form these aggregates (unpublished observations). It is currently unclear if these are functional oligomeric units or non-functional protein aggregates.

RAD51 functions for fork reversal

It is unknown how RAD51 promotes fork reversal. Specifically, it is unknown which activities of RAD51– strand exchange/D-loop activity, ssDNA/dsDNA binding, or ATPase is/are required for fork reversal. In addition, how RAD51 protein interactions affect fork reversal has not been characterized.

To address these questions, it will be important to utilize separation of function mutants to test fork reversal both biochemically and in cells. For example, my model predicts that hyperstable RAD51 nucleofilaments (in the case for ATPase deficient RAD51 mutant; K133R) should prevent reversal by acting as a roadblock to translocases when bound to parental ssDNA. Indeed, overexpression of RAD51 K133R in BRCA-deficient cells restores fork protection but it is unknown if this is due to stabilization of RAD51 on the reversed arm or if it is due to lack of fork reversal (Schlacher et al., 2011). Preliminary experiments with purified proteins indicate that K133R blocks SMARCAL1 mediated fork reversal on model substrates (Figure 5.7A). In contrast, another RAD51 mutant defective for ATP binding, K133A, unable to form active nucleofilaments, has a modest inhibitory effect on SMARCAL1 mediated reversal (Figure 5.7B). These observations are consistent with the model that a metastable RAD51 filament is required for fork reversal. It will be interesting to expand these studies to other mutants outlined in Chapter I (Table 1.1).

Concluding remarks

In summary, I have examined the functions of ssDNA binding proteins like RAD51 and RADX in replication fork reversal and fork protection. In Chapter III, I outlined the functions of a newly characterized RPA-like ssDNA binding protein, RADX, and further characterized its mechanisms in fork protection. In Chapter IV, I identified the differential regulation of fork reversal by RADX in the presence and absence of exogenous stress. Importantly, I identified that RADX antagonizes RAD51 at unstressed and stalled replication forks to favor different phenotypic outcomes depending on the amount of ssDNA. Overall, my thesis project has changed the way we think about fork reversal and provides a mechanistic explanation for the requirement of a ‘metastable’ RAD51 filament to promote fork reversal. In addition, I have made two important contributions

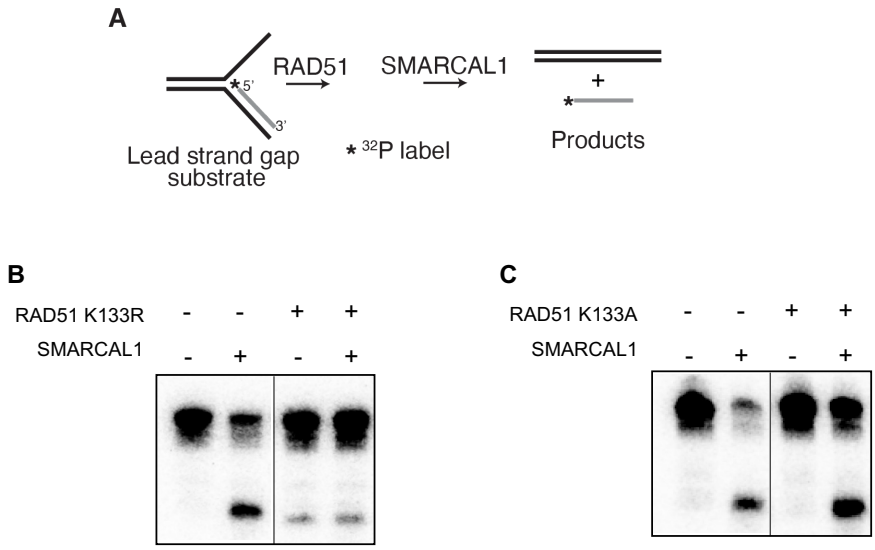

Figure 5.7 Hyperstable RAD51 filaments may inhibit fork reversal on model substrates. A. Schematic of the fork reversal assay. B. Addition of a hyperstable RAD51 mutant prevents SMARCAL1-mediated fork reversal. C. Addition of a constitutively unstable RAD51 mutant modestly inhibits SMARCAL1- mediated reversal. Extra lanes were removed.

toward understanding fork reversal. First, I showed the differential requirements of RAD51 in fork reversal and fork protection. Second, I showed that BRCA2 may promote RAD51-mediated fork reversal in certain genetic contexts.

Fork reversal and fork protection are common responses to DNA damaging chemotherapies. Moreover, mutations in fork remodeling and fork protection proteins promote developmental disorders and cancers. Thus, these replication stress responses not only determine mutation rates and contribute to tumorigenesis; they also are important determinants of therapeutic response (Ray Chaudhuri et al., 2016). Future studies to determine how mechanistic differences in fork processing contribute to cancer cell viability and chemotherapeutic response will be critical to understand cancer etiology and identify novel therapies.

APPENDIX A

DESIGNING A BioID SCREEN TO IDENTIFY THE RADX INTERACTOME

In this section, I describe my attempts to design an unbiased, proximity ligation-based screen to identify interaction partners of RADX.

Introduction and cloning

Proximity dependent biotin identification (BioID) is a tool to identify proximal protein associations within the cell (Roux et al., 2012). BioID conventionally uses a mutant of biotin ligase (BirA*; R118G) originally derived from *E. coli* to biotinylate proteins within a 10nm radius. This mutation allows premature release of a biotin intermediate which allows for promiscuous labeling of proximate proteins. Another mutant of biotin ligase from *A. aeolicus*, BioID2 (R40G), was recently shown to be more sensitive to lower concentrations of biotin and have improved localization in cells thus alleviating some concerns with BirA* (Kim et al., 2016). Both BirA* and BioID2 covalently link exogenously supplemented biotin to proximal surface-exposed ε-lysines on a protein thereby allowing for the modification to remain through the life of the protein. Fusing BirA* or BioID2 to a protein of interest thus allows for biotin labeling of proximate proteins and subsequent identification of the protein interactome by mass spectrometry (Figure AA.1) (Sears et al., 2019).

BioID/BioID2 has several advantages. First, this method has the ability to detect weak/transient interactions in cells that cannot be detected by yeast two hybrid or affinity purification (Roux et al., 2012). Second, the covalent addition of biotin allows the proteins to withstand stringent lysis and wash conditions, maximizing the purity of proteins identified by mass spectrometry (Choi-Rhee et al., 2004; Kim and Roux, 2016). Third, this method is biotin inducible which allows for temporal control and makes it amenable to drug treatments. Finally, BioID can be used to identify protein interactors in various subcellular compartments (Birendra et al., 2017). Disadvantages of this system include its inability to differentiate between true interactors and proteins in physical proximity, and potential inactivation of the protein of interest due to biotinylation.

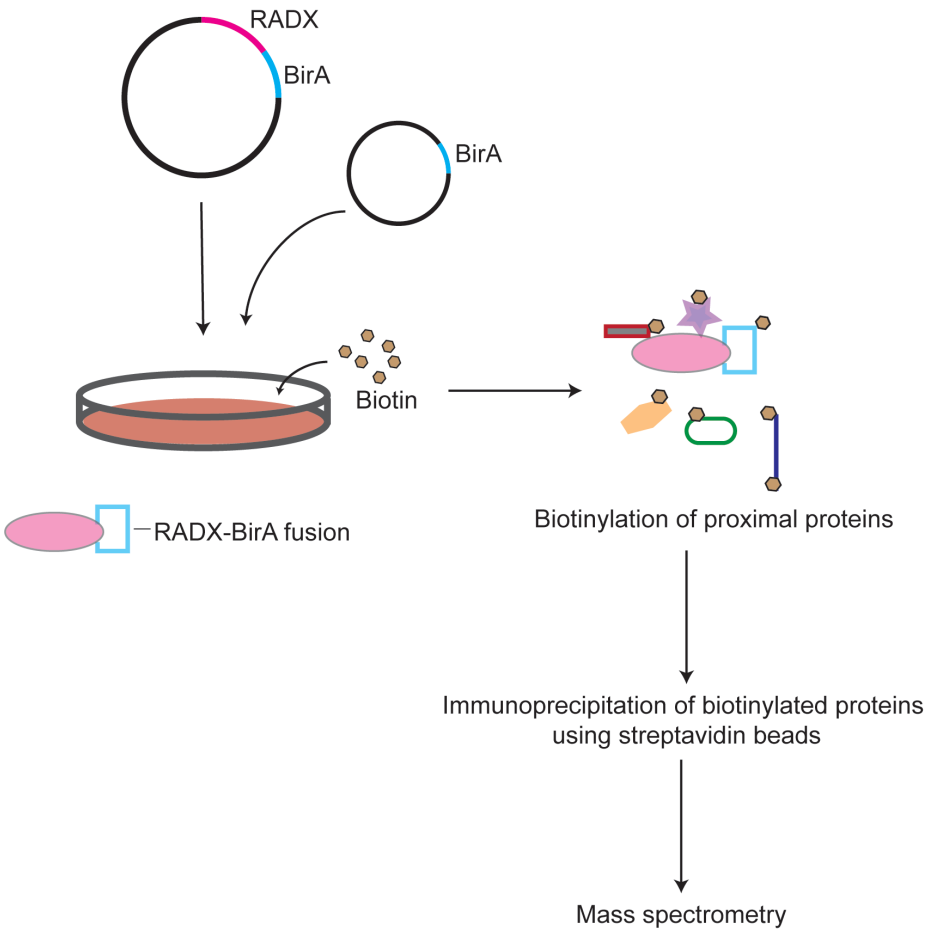

Figure AA.1. Schematic of BioID protocol. Expression of BioID-RADX fusion protein or BioID alone will result in biotinylation of interacting or proximal proteins upon addition of exogenous biotin. After lysis under denaturing conditions, the biotinylated proteins are immunoprecipitated with streptavidin beads and sent to mass spectrometry for further analysis.

iPOND data from our lab indicates RADX is not part of a single, stable complex since its abundance in these datasets does not correlate strongly with any other protein (data not shown). RADX likely has transient or weak interactions that may be important for its mechanism of action. Therefore, I attempted to establish a BioID/BioID2 system with RADX as detailed below.

I tagged RADX at the C-terminus with HA-BioID and HA-BioID2 (backbone expression vectors from Addgene# 36047 and 74224). Empty and RADX tagged vectors were transiently overexpressed in HeLa cells and biotin was added at a final concentration of 50μM for 18 hours prior to fixation and staining. Since overexpression of tagged RADX generates aggregates that do not form with non-functional RADX (as described in Chapter V), I used this method as a proxy to identify if a C-terminal tag on RADX is still functional. Indeed, I found that RADX-HA-BioID and RADX-HA-BioID2 form puncta similar to what is observed with GFP-tagged RADX (Figure AA.2A and data not shown) (Dungrawala et al., 2017). Next, I confirmed that addition of biotin does not disrupt localization of RADX by immunostaining with fluorophore conjugated streptavidin antibody (Figure AA.2B). It should be noted that I observed some cytoplasmic biotinylation in cells transfected with RADX-BirA.

Preliminary attempts at BioID

As a proof-of-concept, I transiently overexpressed the RADX-HA-BioID/BioID2 construct in 293T cells, supplemented media with biotin for 18h prior to harvesting, followed by lysis and immunoblotting. As expected, biotinylation was observed in cells expressing RADX tagged BioID while some background signal was obtained with empty BioID vector alone (Figure AA.3). It should be noted that these are whole cell lysates and are not pull downs.

Next, I attempted pull downs with a streptavidin Myone dynabeads. Substantial biotinylation is detected in samples without exogenous biotin (data not shown). Similarly, more RADX signal is observed in the RADX-BioID transfected sample in the absence of biotin. It is unclear why I detect more biotinylation in the absence of biotin upon pull-down while I observe the opposite in whole cell lysates. I am currently troubleshooting the protocol. I suspect that the dynabeads may be contributing to erroneous signal. Alternatively, it would be worthwhile to stably transfect to avoid mislocalization of proteins and maintain similar levels of expression across conditions.

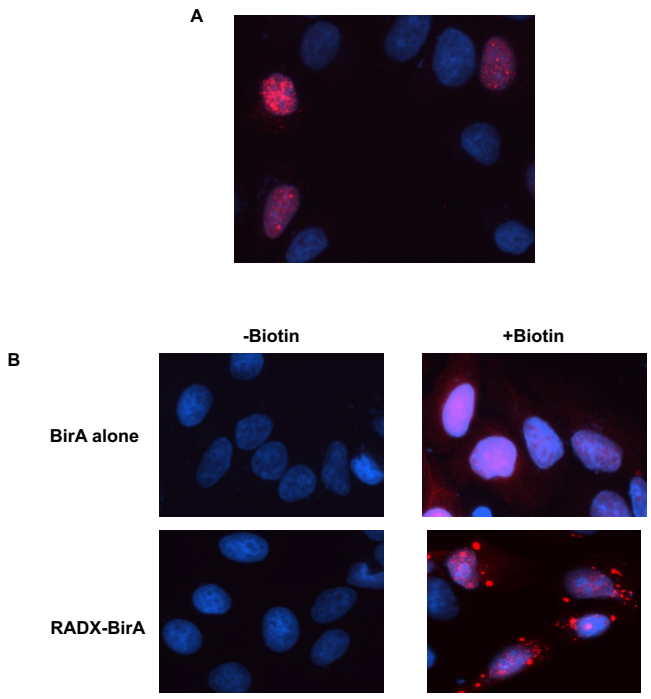

Figure AA.2. Expression of BioID fusion protein does not alter localization. A. Representative images of cells transiently overexpressing RADX-BirA are shown. Overexpression results in punctate localization of RADX. DAPI-Blue, RADX-BirA-Red. B. Using fluorescent microscopy, biotinylation was detected in cells expressing the indicated constructs with streptavidin-594 (red) antibody.

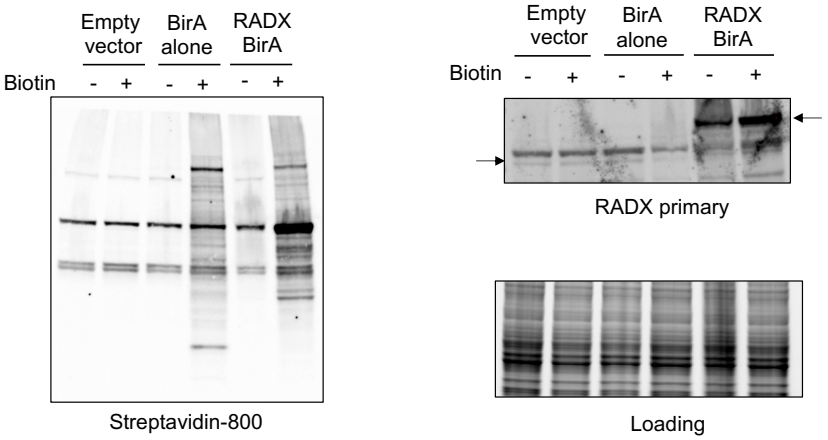

Figure AA.3. Biotinylation is detected in whole cell lysates. Cells expressing the indicated constructs were immunoblotted for biotinylation with Streptavidin-800 antibody. To check fusion protein expression, lysates were immunoblotted with RADX antibody. Arrows indicate endogenous and BioID-tagged RADX proteins.

APPENDIX B

DESIGNING AN ASSAY TO DETECT FORK REVERSAL

In this appendix, I discuss my attempts to develop an assay to detect fork reversal.

Introduction

Electron microscopy (EM) is the current standard tool for direct visualization of replication intermediates. Very few labs in the country have the capability of performing EM and analyzing electron micrographs thus necessitating the requirement for alternative assays to detect fork reversal. Recent papers have proposed proximity ligation assays (PLA) (Malacaria et al., 2019; Nieminuszczy et al., 2019) to indirectly test reversal. Additionally, Margalef et al., examined fork reversal in the context of telomeres. In this section, however, I describe my attempts to develop a more direct approach to visualize replication fork reversal at single-molecule level.

Xia et al., recently described an engineered mutant of the Holliday junction resolvase RuvC, known as RuvCmut, which traps it on DNA and inhibits its nuclease activity. Specifically, they express a GFP-tagged RuvCmut in *E.coli* to label and quantify Holliday junctions using live cell imaging. They further map the sites of Holliday junctions in genomes by performing Chromatin Immunoprecipitation sequencing (ChIP-seq) to assess whether these are intermediates formed during Homologous Recombination (HR) or fork reversal (Xia et al., 2016).

I attempted to utilize the RuvCmut to trap and detect reversed forks on purified genomic DNA using the techniques described below.

Design of the assay

To detect reversed forks with purified RuvC, I utilized two techniques – slot blot and DNA combing assay.

Slot blot – The principle of this assay is similar to a RADAR (Rapid approach to DNA adduct recovery) assay with the exception that purified protein is used to probe a specific DNA structure. Genomic DNA is harvested from cells treated with different genotoxic agents known to promote fork reversal (Zellweger et al., 2015). Native DNA is then transferred to a nitrocellulose membrane using vacuum. Next, the membrane is incubated with purified RuvC, washed, and probed with specific primary and secondary antibodies to the protein.

DNA combing – Cells are labeled with a nucleoside analog, EdU, are combed onto silanized coverslips. The advantage of using EdU over other nucleoside analogs, such as IdU or CldU, is that EdU incorporation can be detected in native conditions by using click chemistry. This will likely preserve the reversed fork structure that would otherwise be destroyed by denaturation. The coverslips are incubated with biotin azide to click biotin to EdU, probed with purified RuvC, and subsequently incubated with primary and secondary antibodies. Lastly, since this is single molecule assay, every instance of fork reversal can be technically detected using this technique.

Preliminary results

In initial experiments with purified RuvCmut, I observed that the protein does not cleave or bind to synthetic HJs in contrast to wild-type RuvC (Figures AB.1A and AB.1B) thus making the mutant protein incapable of detecting fork reversal events in my assays. Wild-type, active RuvC, sold commercially, is only active in the presence of Mg^{2+}. However, I found that wild type RuvC, in the presence of a different salt, like KCl, mimics a RuvC trap. Specifically, wild-type RuvC binds to but does not cleave HJs in a buffer containing KCl (Figure AB.2). From here on, I use wild-type RuvC in KCl buffer for all the assays described below.

Slot blot

Asynchronous U2OS cells were either harvested without addition of any replication stress or after treatment with 3mM HU for 5h. After washing with PBS, DNA was crosslinked by incubating with psoralen followed by exposure to UV. This step ensures that reversed forks do not undergo spontaneous branch migration to restore the replication fork. I extracted genomic DNA using chloroform-isoamylalcohol extraction. Next, I purified genomic DNA by isopropanol precipitation followed by digestion with PvuII. I reasoned that restriction digest will fragment the DNA and allow

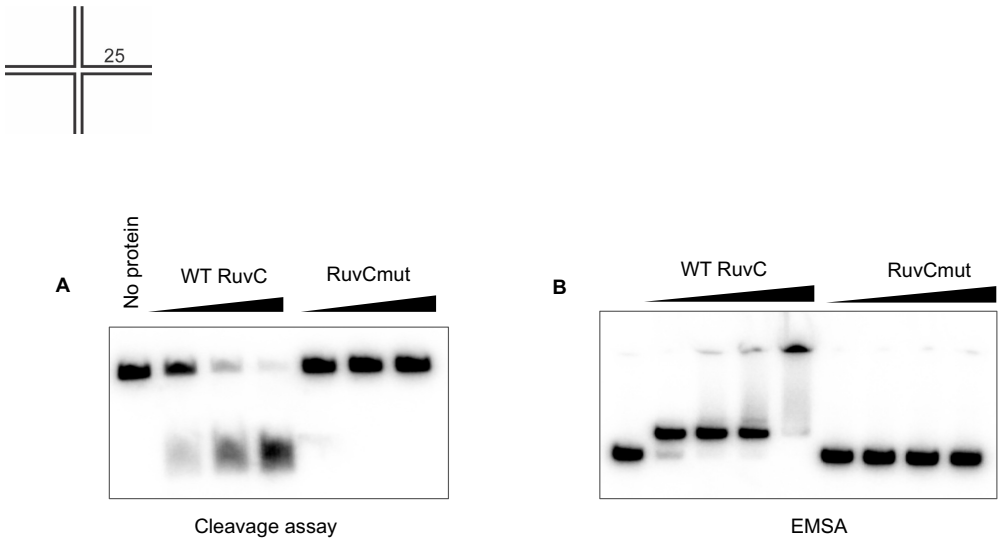

Figure AB.1. RuvCmut does not cleave or bind model Holliday junctions. Synthetic Holliday junction used in the assays is shown. A. Increasing concentrations of Wild type (WT) RuvC but not RuvCmut cleaves model Holliday junctions in solution. It should be noted that the buffer used in this assay contains $MgCl_2$. B. Representative gel showing an Electrophoretic Mobility Shift Assay (EMSA) with RuvCmut and WT RuvC. This assay was performed in KCl buffer.

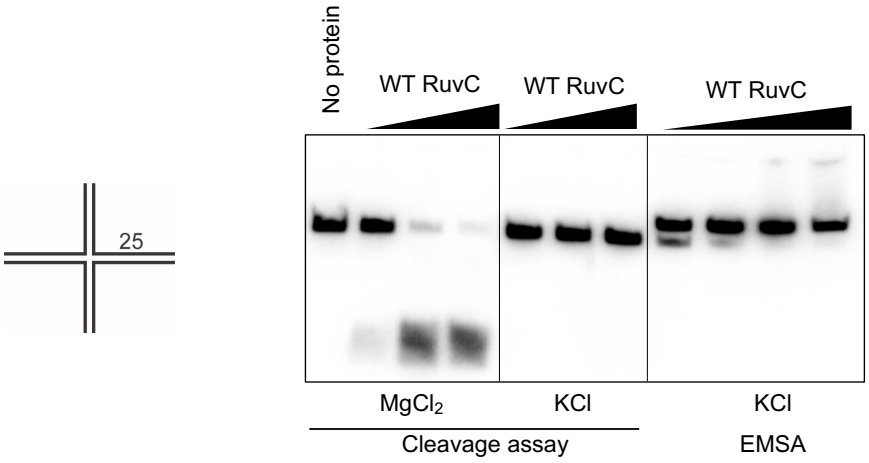

Figure AB.2. Wild-type (WT) RuvC binds, does not cleave, model Holliday junctions in KCl buffer. Increasing concentrations of WT RuvC does not cleave, yet binds to Holliday junctions in KCl buffer. In contrast, WT RuvC cleaves Holliday junctions in $MgCl_2$ buffer.

for RuvC to easily access a reversed fork structure. I also included an uncut sample for comparison. Then, I transferred the DNA samples in duplicate on to a nitrocellulose membrane with a slot blot apparatus. To determine even loading, the membrane was denatured with NaOH and probed with anti-ssDNA (Figure AB.3A). When probing for reversal events, the membrane was directly blocked with milk/PBST. Next, I incubated the membrane with different concentrations of purified RuvC in a buffer containing 25mM HEPES (pH 7.9), 10mM KCl, and 0.1% Triton-X overnight. The membrane was then immunoblotted for RuvC (Figure AB.3A).

Preliminary analyses show a moderate increase in RuvC signal with HU (Figure AB.3B). The small increase in the presence of HU may be a true readout of reversed forks or simply variation in the signal. Further validation with conditions known to reduce fork reversal, such as depletion of RAD51, treatment with PARPi or triple translocase knockout cell line is required.

DNA combing with RuvC

HCT116 cells were pulsed with 25μM EdU for 25 minutes and harvested right after or treated with 3mM HU for 5h before harvesting. To test if DNA combing is compatible with crosslinked DNA, I psoralen treated the cells as outlined above and combed the DNA on silanized coverslips using a standard protocol (See chapter II). Strikingly, I observed that incubating cells with psoralen followed by exposure to UV sheared the DNA. The DNA fibers were shorter and appeared more fragmented in contrast to non-crosslinked samples (Figure AB.4).

Coverslips were incubated with purified RuvC protein overnight in the same buffer described above, and immunostained with appropriate primary and secondary antibodies. As controls, I performed the same assay in the absence of purified RuvC or without primary antibody (data not shown). Ideally, in cells treated with HU, the DNA fiber may have a reversed fork at the end and so I reasoned that I would see a RuvC signal at the end of a fiber. Indeed, in most cases, I see RuvC signal as a single focus at the end of a fiber (Figure AB.5A). In some cases, however, I also see RuvC signal in the middle of a DNA fiber tract suggesting either background localization or fork reversal during termination/origin firing (Figure AB.5B). Visually, there seems to be a higher incidence of RuvC localization at the end of a DNA fiber with HU than in the absence of any added replication stress (Figure AB. 5C). Regardless, it will be important to quantitate the frequency of

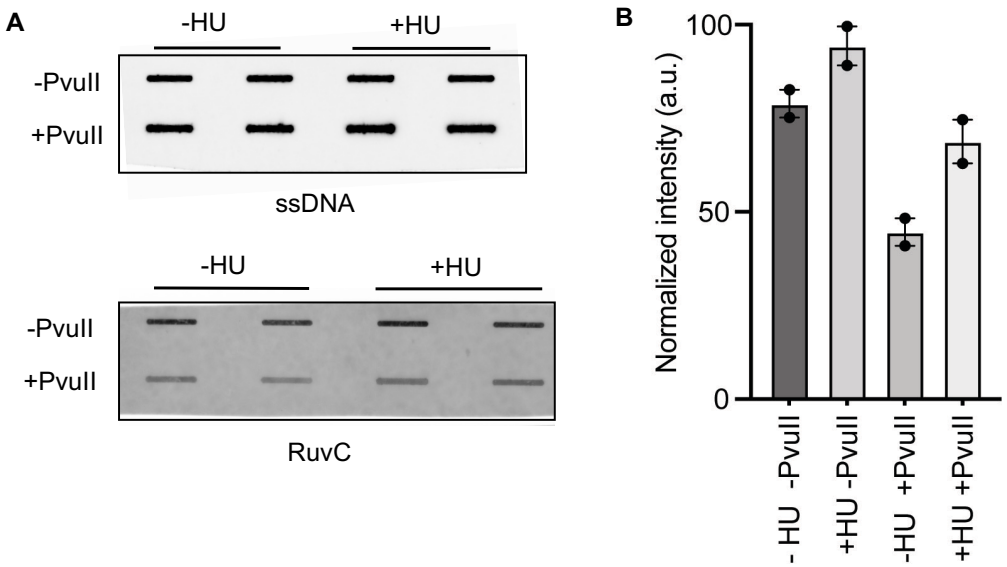

Figure AB.3. Analysis of RuvC binding to genomic DNA. A. Cells were either treated with 3mM HU for 5h or left untreated and genomic DNA was harvested. After harvesting, DNA was digested with PvuII as indicated and probed with ssDNA antibody or purified RuvC. B. Quantification of A. Mean +/- SEM.

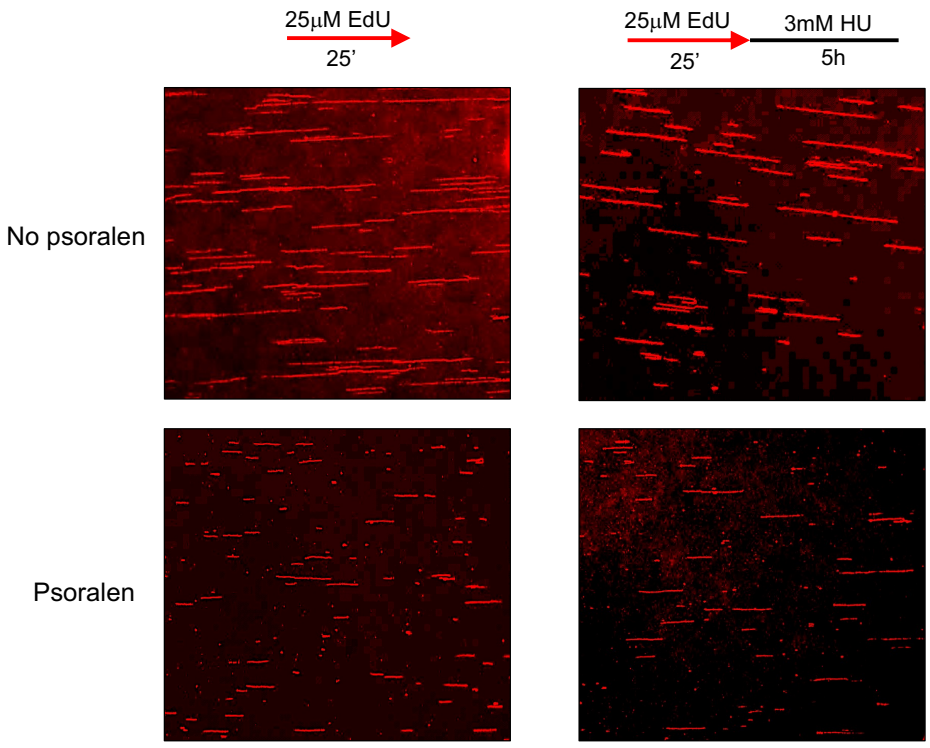

Figure AB.4. DNA combing with psoralen crosslinking. Representative images showing EdU-labeled DNA fibers (red) crosslinked by incubating with psoralen followed by UV treatment.

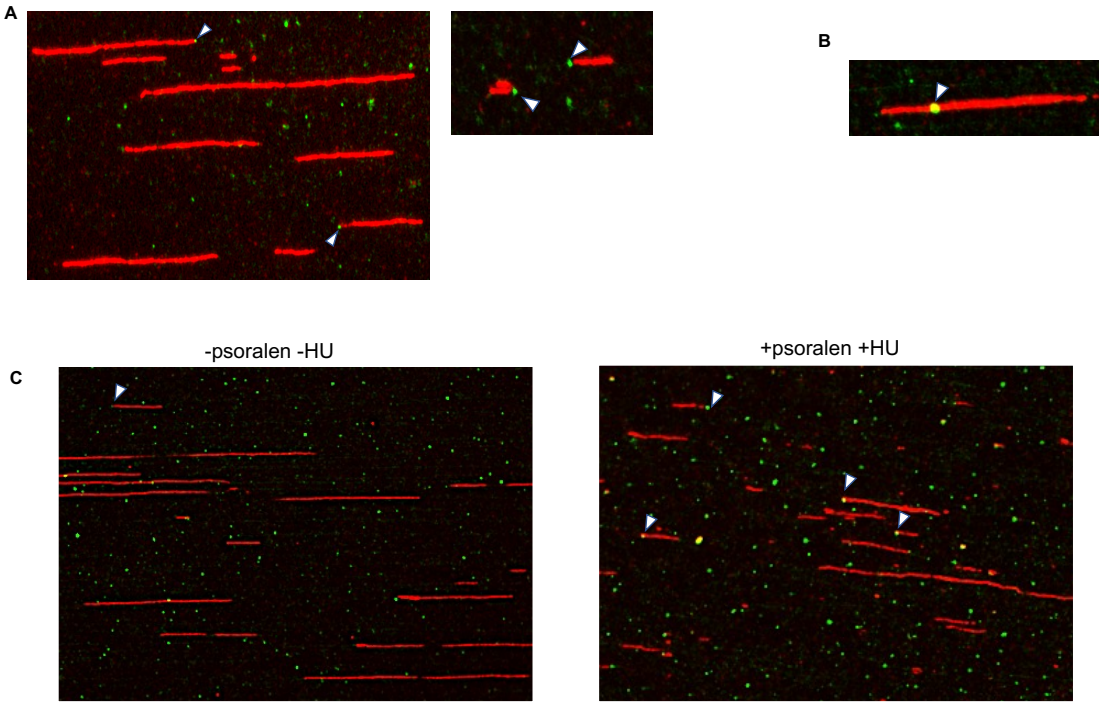

Figure AB.5. DNA combing with RuvC. A and B. Representative images with EdU-labeled DNA fibers (red) probed with purified RuvC (green) and immunostained with biotin and RuvC antibodies. C. Images showing frequency of RuvC (green) colocalization at the end of a DNA fiber (red) obtained from cells treated as indicated. White triangles indicate localization events.

colocalization events. Additionally, as described previously, validation of this assay will require testing genetic contexts with reduced fork reversal.

It is hard to envision how a dimer of RuvC bound to a reversed fork on a DNA fiber can generate a signal strong enough to be visualized by immunofluorescence. Therefore, I attempted to boost the signal by performing a proximity ligation assay (PLA) with biotin and RuvC. Unfortunately, preliminary experiments show poor immunofluorescence signal of the DNA fiber in many conditions (Figure AB.6). I am currently optimizing the PLA protocol.

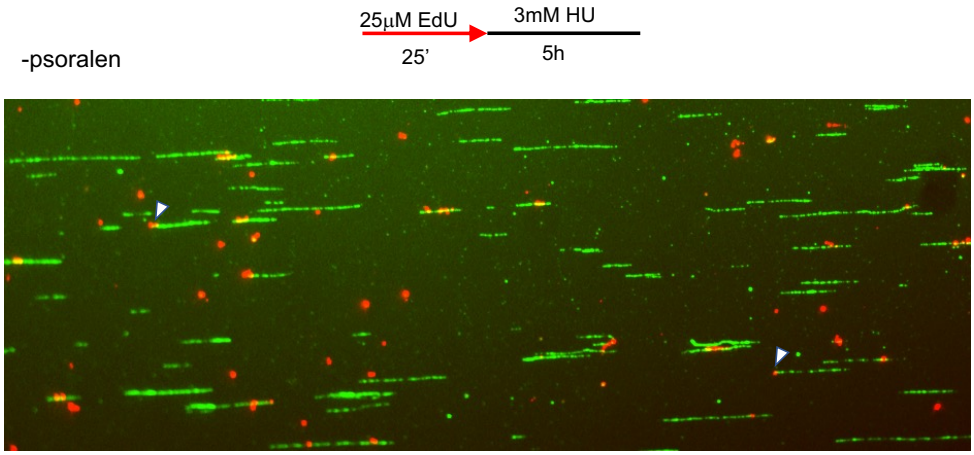

Figure AB.6. Proximity ligation assay (PLA) combined with DNA combing to detect RuvC localization. Representative image of PLA with RuvC and biotin (red) on DNA fibers (green). White triangles indicate localization.

REFERENCES

Abe, T., Kawasumi, R., Giannattasio, M., Dusi, S., Yoshimoto, Y., Miyata, K., Umemura, K., Hirota, K., and Branzei, D. (2018). AND-1 fork protection function prevents fork resection and is essential for proliferation. Nat Commun *9*, 3091.

Adolph, M.B., Mohamed, T.M., Balakrishnan, S., Xue, C., Morati, F., Modesti, M., Greene, E.C., Chazin, W.J., and Cortez, D. (2021). RADX controls RAD51 filament dynamics to regulate replication fork stability. Mol Cell *81*, 1074-1083 e1075.

Atkinson, J., and McGlynn, P. (2009). Replication fork reversal and the maintenance of genome stability. Nucleic Acids Res *37*, 3475-3492.

Ayoub, N., Rajendra, E., Su, X., Jeyasekharan, A.D., Mahen, R., and Venkitaraman, A.R. (2009). The carboxyl terminus of Brca2 links the disassembly of Rad51 complexes to mitotic entry. Curr Biol *19*, 1075-1085.

Ayyagari, R., Gomes, X.V., Gordenin, D.A., and Burgers, P.M. (2003). Okazaki fragment maturation in yeast. I. Distribution of functions between FEN1 AND DNA2. J Biol Chem *278*, 1618-1625.

Bacquin, A., Pouvelle, C., Siaud, N., Perderiset, M., Salome-Desnoulez, S., Tellier-Lebegue, C., Lopez, B., Charbonnier, J.B., and Kannouche, P.L. (2013). The helicase FBH1 is tightly regulated by PCNA via CRL4(Cdt2)-mediated proteolysis in human cells. Nucleic Acids Res *41*, 6501-6513.

Bai, G., Kermi, C., Stoy, H., Schiltz, C.J., Bacal, J., Zaino, A.M., Hadden, M.K., Eichman, B.F., Lopes, M., and Cimprich, K.A. (2020). HLTF Promotes Fork Reversal, Limiting Replication Stress Resistance and Preventing Multiple Mechanisms of Unrestrained DNA Synthesis. Mol Cell *78*, 1237-1251 e1237.

Bansbach, C.E., Betous, R., Lovejoy, C.A., Glick, G.G., and Cortez, D. (2009). The annealing helicase SMARCAL1 maintains genome integrity at stalled replication forks. Genes Dev *23*, 2405-2414.

Belan, O., Barroso, C., Kaczmarczyk, A., Anand, R., Federico, S., O'Reilly, N., Newton, M.D., Maeots, E., Enchev, R.I., Martinez-Perez, E.*, et al.* (2021). Single-molecule analysis reveals cooperative stimulation of Rad51 filament nucleation and growth by mediator proteins. Mol Cell *81*, 1058-1073 e1057.

Bell, J.C., Plank, J.L., Dombrowski, C.C., and Kowalczykowski, S.C. (2012). Direct imaging of RecA nucleation and growth on single molecules of SSB-coated ssDNA. Nature *491*, 274-278.

Berti, M., Cortez, D., and Lopes, M. (2020a). The plasticity of DNA replication forks in response to clinically relevant genotoxic stress. Nat Rev Mol Cell Biol *21*, 633-651.

Berti, M., Ray Chaudhuri, A., Thangavel, S., Gomathinayagam, S., Kenig, S., Vujanovic, M., Odreman, F., Glatter, T., Graziano, S., Mendoza-Maldonado, R.*, et al.* (2013). Human RECQ1 promotes restart of replication forks reversed by DNA topoisomerase I inhibition. Nat Struct Mol Biol *20*, 347-354.

Berti, M., Teloni, F., Mijic, S., Ursich, S., Fuchs, J., Palumbieri, M.D., Krietsch, J., Schmid, J.A., Garcin, E.B., Gon, S.*, et al.* (2020b). Sequential role of RAD51 paralog complexes in replication fork remodeling and restart. Nat Commun *11*, 3531.

Betous, R., Couch, F.B., Mason, A.C., Eichman, B.F., Manosas, M., and Cortez, D. (2013a). Substrate-selective repair and restart of replication forks by DNA translocases. Cell Rep *3*, 1958-1969.

Betous, R., Glick, G.G., Zhao, R., and Cortez, D. (2013b). Identification and Characterization of SMARCAL1 Protein Complexes. PLoS One *8*, e63149.

Betous, R., Mason, A.C., Rambo, R.P., Bansbach, C.E., Badu-Nkansah, A., Sirbu, B.M., Eichman, B.F., and Cortez, D. (2012). SMARCAL1 catalyzes fork regression and Holliday junction migration to maintain genome stability during DNA replication. Genes & development *26*, 151-162.

Bhat, K.P., Betous, R., and Cortez, D. (2015). High-affinity DNA-binding domains of replication protein A (RPA) direct SMARCAL1-dependent replication fork remodeling. J Biol Chem *290*, 4110-4117.

Bhat, K.P., and Cortez, D. (2018). RPA and RAD51: fork reversal, fork protection, and genome stability. Nat Struct Mol Biol *25*, 446-453.

Bhat, K.P., Krishnamoorthy, A., Dungrawala, H., Garcin, E.B., Modesti, M., and Cortez, D. (2018). RADX Modulates RAD51 Activity to Control Replication Fork Protection. Cell Rep *24*, 538-545.

Bignell, G., Micklem, G., Stratton, M.R., Ashworth, A., and Wooster, R. (1997). The BRC repeats are conserved in mammalian BRCA2 proteins. Hum Mol Genet *6*, 53-58.

Birendra, K., May, D.G., Benson, B.V., Kim, D.I., Shivega, W.G., Ali, M.H., Faustino, R.S., Campos, A.R., and Roux, K.J. (2017). VRK2A is an A-type lamin-dependent nuclear envelope kinase that phosphorylates BAF. Mol Biol Cell *28*, 2241-2250.

Blastyak, A., Hajdu, I., Unk, I., and Haracska, L. (2010). Role of double-stranded DNA translocase activity of human HLTF in replication of damaged DNA. Mol Cell Biol *30*, 684-693.

Bochkarev, A., and Bochkareva, E. (2004). From RPA to BRCA2: lessons from single-stranded DNA binding by the OB-fold. Curr Opin Struct Biol *14*, 36-42.

Bonilla, B., Hengel, S.R., Grundy, M.K., and Bernstein, K.A. (2020). RAD51 Gene Family Structure and Function. Annu Rev Genet *54*, 25-46.

Brouwer, I., Moschetti, T., Candelli, A., Garcin, E.B., Modesti, M., Pellegrini, L., Wuite, G.J., and Peterman, E.J. (2018). Two distinct conformational states define the interaction of human RAD51-ATP with single-stranded DNA. EMBO J *37*.

Bryant, H.E., Schultz, N., Thomas, H.D., Parker, K.M., Flower, D., Lopez, E., Kyle, S., Meuth, M., Curtin, N.J., and Helleday, T. (2005). Specific killing of BRCA2-deficient tumours with inhibitors of poly(ADP-ribose) polymerase. Nature *434*, 913-917.

Bugreev, D.V., and Mazin, A.V. (2004). Ca2+ activates human homologous recombination protein Rad51 by modulating its ATPase activity. Proc Natl Acad Sci U S A *101*, 9988-9993.

Bugreev, D.V., Rossi, M.J., and Mazin, A.V. (2011). Cooperation of RAD51 and RAD54 in regression of a model replication fork. Nucleic Acids Res *39*, 2153-2164.

Bugreev, D.V., Yu, X., Egelman, E.H., and Mazin, A.V. (2007). Novel pro- and anti-recombination activities of the Bloom's syndrome helicase. Genes Dev *21*, 3085-3094.

Burgers, P.M.J., and Kunkel, T.A. (2017). Eukaryotic DNA Replication Fork. Annu Rev Biochem *86*, 417-438.

Buss, J.A., Kimura, Y., and Bianco, P.R. (2008). RecG interacts directly with SSB: implications for stalled replication fork regression. Nucleic Acids Res *36*, 7029-7042.

Candelli, A., Holthausen, J.T., Depken, M., Brouwer, I., Franker, M.A., Marchetti, M., Heller, I., Bernard, S., Garcin, E.B., Modesti, M*., et al.* (2014). Visualization and quantification of nascent RAD51 filament formation at single-monomer resolution. Proc Natl Acad Sci U S A *111*, 15090-15095.

Cardenas, P.P., Carrasco, B., Defeu Soufo, C., Cesar, C.E., Herr, K., Kaufenstein, M., Graumann, P.L., and Alonso, J.C. (2012). RecX facilitates homologous recombination by modulating RecA activities. PLoS Genet *8*, e1003126.

Carreira, A., Hilario, J., Amitani, I., Baskin, R.J., Shivji, M.K., Venkitaraman, A.R., and Kowalczykowski, S.C. (2009). The BRC repeats of BRCA2 modulate the DNA-binding selectivity of RAD51. Cell *136*, 1032-1043.

Carreira, A., and Kowalczykowski, S.C. (2011). Two classes of BRC repeats in BRCA2 promote RAD51 nucleoprotein filament function by distinct mechanisms. Proc Natl Acad Sci U S A *108*, 10448-10453.

Carroll, C., Bansbach, C.E., Zhao, R., Jung, S.Y., Qin, J., and Cortez, D. (2014). Phosphorylation of a C-terminal auto-inhibitory domain increases SMARCAL1 activity. Nucleic Acids Res *42*, 918-925.

Celli, G.B., and de Lange, T. (2005). DNA processing is not required for ATM-mediated telomere damage response after TRF2 deletion. Nat Cell Biol *7*, 712-718.

Chavez, D.A., Greer, B.H., and Eichman, B.F. (2018). The HIRAN domain of helicase-like transcription factor positions the DNA translocase motor to drive efficient DNA fork regression. J Biol Chem *293*, 8484-8494.

Chen, P.L., Chen, C.F., Chen, Y., Xiao, J., Sharp, Z.D., and Lee, W.H. (1998). The BRC repeats in BRCA2 are critical for RAD51 binding and resistance to methyl methanesulfonate treatment. Proc Natl Acad Sci U S A *95*, 5287-5292.

Chi, P., San Filippo, J., Sehorn, M.G., Petukhova, G.V., and Sung, P. (2007). Bipartite stimulatory action of the Hop2-Mnd1 complex on the Rad51 recombinase. Genes Dev *21*, 1747-1757.

Chi, P., Van Komen, S., Sehorn, M.G., Sigurdsson, S., and Sung, P. (2006). Roles of ATP binding and ATP hydrolysis in human Rad51 recombinase function. DNA Repair (Amst) *5*, 381-391.

Choi-Rhee, E., Schulman, H., and Cronan, J.E. (2004). Promiscuous protein biotinylation by Escherichia coli biotin protein ligase. Protein Sci *13*, 3043-3050.

Chu, W.K., Payne, M.J., Beli, P., Hanada, K., Choudhary, C., and Hickson, I.D. (2015). FBH1 influences DNA replication fork stability and homologous recombination through ubiquitylation of RAD51. Nat Commun *6*, 5931.

Chun, J., Buechelmaier, E.S., and Powell, S.N. (2013). Rad51 paralog complexes BCDX2 and CX3 act at different stages in the BRCA1-BRCA2-dependent homologous recombination pathway. Mol Cell Biol *33*, 387-395.

Ciccia, A., Bredemeyer, A.L., Sowa, M.E., Terret, M.E., Jallepalli, P.V., Harper, J.W., and Elledge, S.J. (2009). The SIOD disorder protein SMARCAL1 is an RPA-interacting protein involved in replication fork restart. Genes Dev *23*, 2415-2425.

Ciccia, A., Nimonkar, A.V., Hu, Y., Hajdu, I., Achar, Y.J., Izhar, L., Petit, S.A., Adamson, B., Yoon, J.C., Kowalczykowski, S.C*., et al.* (2012). Polyubiquitinated PCNA Recruits the ZRANB3 Translocase to Maintain Genomic Integrity after Replication Stress. Mol Cell *47*, 396-409.

Cloud, V., Chan, Y.L., Grubb, J., Budke, B., and Bishop, D.K. (2012). Rad51 is an accessory factor for Dmc1-mediated joint molecule formation during meiosis. Science *337*, 1222-1225.

Cong, K., Peng, M., Kousholt, A.N., Lee, W.T.C., Lee, S., Nayak, S., Krais, J., VanderVere-Carozza, P.S., Pawelczak, K.S., Calvo, J*., et al.* (2021). Replication gaps are a key determinant of PARP inhibitor synthetic lethality with BRCA deficiency. Mol Cell *81*, 3128-3144 e3127.

Cortez, D. (2019). Replication-Coupled DNA Repair. Mol Cell *74*, 866-876.

Couch, F.B., Bansbach, C.E., Driscoll, R., Luzwick, J.W., Glick, G.G., Betous, R., Carroll, C.M., Jung, S.Y., Qin, J., Cimprich, K.A*., et al.* (2013). ATR phosphorylates SMARCAL1 to prevent replication fork collapse. Genes Dev *27*, 1610-1623.

Courcelle, J., Donaldson, J.R., Chow, K.H., and Courcelle, C.T. (2003). DNA damage-induced replication fork regression and processing in Escherichia coli. Science *299*, 1064-1067.

Cox, K.E., Marechal, A., and Flynn, R.L. (2016). SMARCAL1 Resolves Replication Stress at ALT Telomeres. Cell Rep *14*, 1032-1040.

Cox, M.M. (2007). Regulation of bacterial RecA protein function. Crit Rev Biochem Mol Biol *42*, 41-63.

Davies, A.A., Masson, J.Y., McIlwraith, M.J., Stasiak, A.Z., Stasiak, A., Venkitaraman, A.R., and West, S.C. (2001). Role of BRCA2 in control of the RAD51 recombination and DNA repair protein. Mol Cell *7*, 273-282.

Davies, O.R., and Pellegrini, L. (2007). Interaction with the BRCA2 C terminus protects RAD51-DNA filaments from disassembly by BRC repeats. Nat Struct Mol Biol *14*, 475-483.

Dhont, L., Mascaux, C., and Belayew, A. (2016). The helicase-like transcription factor (HLTF) in cancer: loss of function or oncomorphic conversion of a tumor suppressor? Cell Mol Life Sci *73*, 129-147.

Ding, X., Ray Chaudhuri, A., Callen, E., Pang, Y., Biswas, K., Klarmann, K.D., Martin, B.K., Burkett, S., Cleveland, L., Stauffer, S.*, et al.* (2016). Synthetic viability by BRCA2 and PARP1/ARTD1 deficiencies. Nat Commun *7*, 12425.

Dou, H., Huang, C., Singh, M., Carpenter, P.B., and Yeh, E.T. (2010). Regulation of DNA repair through deSUMOylation and SUMOylation of replication protein A complex. Mol Cell *39*, 333-345.
Drees, J.C., Lusetti, S.L., Chitteni-Pattu, S., Inman, R.B., and Cox, M.M. (2004). A RecA filament capping mechanism for RecX protein. Mol Cell *15*, 789-798.

Dungrawala, H., Bhat, K.P., Le Meur, R., Chazin, W.J., Ding, X., Sharan, S.K., Wessel, S.R., Sathe, A.A., Zhao, R., and Cortez, D. (2017). RADX Promotes Genome Stability and Modulates Chemosensitivity by Regulating RAD51 at Replication Forks. Mol Cell *67*, 374-386 e375.

Dupre, A., Boyer-Chatenet, L., Sattler, R.M., Modi, A.P., Lee, J.H., Nicolette, M.L., Kopelovich, L., Jasin, M., Baer, R., Paull, T.T.*, et al.* (2008). A forward chemical genetic screen reveals an inhibitor of the Mre11-Rad50-Nbs1 complex. Nat Chem Biol *4*, 119-125.

Duro, E., Lundin, C., Ask, K., Sanchez-Pulido, L., MacArtney, T.J., Toth, R., Ponting, C.P., Groth, A., Helleday, T., and Rouse, J. (2010). Identification of the MMS22L-TONSL complex that promotes homologous recombination. Mol Cell *40*, 632-644.

Esashi, F., Christ, N., Gannon, J., Liu, Y., Hunt, T., Jasin, M., and West, S.C. (2005). CDK-dependent phosphorylation of BRCA2 as a regulatory mechanism for recombinational repair. Nature *434*, 598-604.

Esashi, F., Galkin, V.E., Yu, X., Egelman, E.H., and West, S.C. (2007). Stabilization of RAD51 nucleoprotein filaments by the C-terminal region of BRCA2. Nat Struct Mol Biol *14*, 468-474.

Farmer, H., McCabe, N., Lord, C.J., Tutt, A.N., Johnson, D.A., Richardson, T.B., Santarosa, M., Dillon, K.J., Hickson, I., Knights, C.*, et al.* (2005). Targeting the DNA repair defect in BRCA mutant cells as a therapeutic strategy. Nature *434*, 917-921.

Feng, W., and Jasin, M. (2017). BRCA2 suppresses replication stress-induced mitotic and G1 abnormalities through homologous recombination. Nat Commun *8*, 525.

Forget, A.L., Loftus, M.S., McGrew, D.A., Bennett, B.T., and Knight, K.L. (2007). The human Rad51 K133A mutant is functional for DNA double-strand break repair in human cells. Biochemistry *46*, 3566-3575.

Fortin, G.S., and Symington, L.S. (2002). Mutations in yeast Rad51 that partially bypass the requirement for Rad55 and Rad57 in DNA repair by increasing the stability of Rad51-DNA complexes. EMBO J *21*, 3160-3170.

Fugger, K., Mistrik, M., Danielsen, J.R., Dinant, C., Falck, J., Bartek, J., Lukas, J., and Mailand, N. (2009). Human Fbh1 helicase contributes to genome maintenance via pro- and anti-recombinase activities. J Cell Biol *186*, 655-663.

Fugger, K., Mistrik, M., Neelsen, K.J., Yao, Q., Zellweger, R., Kousholt, A.N., Haahr, P., Chu, W.K., Bartek, J., Lopes, M.*, et al.* (2015a). FBH1 Catalyzes Regression of Stalled Replication Forks. Cell Rep.

Fugger, K., Mistrik, M., Neelsen, K.J., Yao, Q., Zellweger, R., Kousholt, A.N., Haahr, P., Chu, W.K., Bartek, J., Lopes, M.*, et al.* (2015b). FBH1 Catalyzes Regression of Stalled Replication Forks. Cell Rep *10*, 1749-1757.

Garcia-Gomez, S., Reyes, A., Martinez-Jimenez, M.I., Chocron, E.S., Mouron, S., Terrados, G., Powell, C., Salido, E., Mendez, J., Holt, I.J.*, et al.* (2013). PrimPol, an archaic primase/polymerase operating in human cells. Mol Cell *52*, 541-553.

Garcin, E.B., Gon, S., Sullivan, M.R., Brunette, G.J., Cian, A., Concordet, J.P., Giovannangeli, C., Dirks, W.G., Eberth, S., Bernstein, K.A.*, et al.* (2019). Differential Requirements for the RAD51 Paralogs in Genome Repair and Maintenance in Human Cells. PLoS Genet *15*, e1008355.

Graham, J.E., Marians, K.J., and Kowalczykowski, S.C. (2017). Independent and Stochastic Action of DNA Polymerases in the Replisome. Cell *169*, 1201-1213 e1217.

Gruenig, M.C., Stohl, E.A., Chitteni-Pattu, S., Seifert, H.S., and Cox, M.M. (2010). Less is more: Neisseria gonorrhoeae RecX protein stimulates recombination by inhibiting RecA. J Biol Chem *285*, 37188-37197.

Grundy, M.K., Buckanovich, R.J., and Bernstein, K.A. (2020). Regulation and pharmacological targeting of RAD51 in cancer. NAR Cancer *2*, zcaa024.

Haas, K.T., Lee, M., Esposito, A., and Venkitaraman, A.R. (2018). Single-molecule localization microscopy reveals molecular transactions during RAD51 filament assembly at cellular DNA damage sites. Nucleic Acids Res *46*, 2398-2416.

Hansen, L.T., Lundin, C., Spang-Thomsen, M., Petersen, L.N., and Helleday, T. (2003). The role of RAD51 in etoposide (VP16) resistance in small cell lung cancer. Int J Cancer *105*, 472-479.

Hartford, S.A., Chittela, R., Ding, X., Vyas, A., Martin, B., Burkett, S., Haines, D.C., Southon, E., Tessarollo, L., and Sharan, S.K. (2016). Interaction with PALB2 Is Essential for Maintenance of Genomic Integrity by BRCA2. PLoS Genet *12*, e1006236.

Hashimoto, Y., Ray Chaudhuri, A., Lopes, M., and Costanzo, V. (2010). Rad51 protects nascent DNA from Mre11-dependent degradation and promotes continuous DNA synthesis. Nat Struct Mol Biol *17*, 1305-1311.

Helleday, T., Bryant, H.E., and Schultz, N. (2005). Poly(ADP-ribose) polymerase (PARP-1) in homologous recombination and as a target for cancer therapy. Cell Cycle *4*, 1176-1178.

Higgins, N.P., Kato, K., and Strauss, B. (1976). A model for replication repair in mammalian cells. J Mol Biol *101*, 417-425.

Higgs, M.R., Reynolds, J.J., Winczura, A., Blackford, A.N., Borel, V., Miller, E.S., Zlatanou, A., Nieminuszczy, J., Ryan, E.L., Davies, N.J.*, et al.* (2015). BOD1L Is Required to Suppress Deleterious Resection of Stressed Replication Forks. Mol Cell *59*, 462-477.

Higgs, M.R., Sato, K., Reynolds, J.J., Begum, S., Bayley, R., Goula, A., Vernet, A., Paquin, K.L., Skalnik, D.G., Kobayashi, W.*, et al.* (2018). Histone Methylation by SETD1A Protects Nascent DNA through the Nucleosome Chaperone Activity of FANCD2. Mol Cell *71*, 25-41 e26.

Hilario, J., Amitani, I., Baskin, R.J., and Kowalczykowski, S.C. (2009). Direct imaging of human Rad51 nucleoprotein dynamics on individual DNA molecules. Proc Natl Acad Sci U S A *106*, 361-368.

Hu, J., Sun, L., Shen, F., Chen, Y., Hua, Y., Liu, Y., Zhang, M., Hu, Y., Wang, Q., Xu, W.*, et al.* (2012). The intra-s phase checkpoint targets dna2 to prevent stalled replication forks from reversing. Cell *149*, 1221-1232.

Hu, Y., Raynard, S., Sehorn, M.G., Lu, X., Bussen, W., Zheng, L., Stark, J.M., Barnes, E.L., Chi, P., Janscak, P.*, et al.* (2007). RECQL5/Recql5 helicase regulates homologous recombination and suppresses tumor formation via disruption of Rad51 presynaptic filaments. Genes Dev *21*, 3073-3084.

Jasin, M., and Rothstein, R. (2013). Repair of strand breaks by homologous recombination. Cold Spring Harb Perspect Biol *5*, a012740.

Jensen, R.B., Carreira, A., and Kowalczykowski, S.C. (2010). Purified human BRCA2 stimulates RAD51-mediated recombination. Nature *467*, 678-683.

Jeong, Y.T., Cermak, L., Guijarro, M.V., Hernando, E., and Pagano, M. (2013). FBH1 protects melanocytes from transformation and is deregulated in melanomas. Cell Cycle *12*, 1128-1132.

Kile, A.C., Chavez, D.A., Bacal, J., Eldirany, S., Korzhnev, D.M., Bezsonova, I., Eichman, B.F., and Cimprich, K.A. (2015). HLTF's Ancient HIRAN Domain Binds 3' DNA Ends to Drive Replication Fork Reversal. Mol Cell *58*, 1090-1100.

Kim, D.I., Jensen, S.C., Noble, K.A., Kc, B., Roux, K.H., Motamedchaboki, K., and Roux, K.J. (2016). An improved smaller biotin ligase for BioID proximity labeling. Mol Biol Cell *27*, 1188-1196.

Kim, D.I., and Roux, K.J. (2016). Filling the Void: Proximity-Based Labeling of Proteins in Living Cells. Trends Cell Biol *26*, 804-817.

Kim, J., Kim, J.H., Lee, S.H., Kim, D.H., Kang, H.Y., Bae, S.H., Pan, Z.Q., and Seo, Y.S. (2002). The novel human DNA helicase hFBH1 is an F-box protein. J Biol Chem *277*, 24530-24537.

Klein, H.L. (2008). The consequences of Rad51 overexpression for normal and tumor cells. DNA Repair (Amst) *7*, 686-693.

Kolinjivadi, A.M., Sannino, V., de Antoni, A., Techer, H., Baldi, G., and Costanzo, V. (2017a). Moonlighting at replication forks - a new life for homologous recombination proteins BRCA1, BRCA2 and RAD51. FEBS Lett *591*, 1083-1100.

Kolinjivadi, A.M., Sannino, V., De Antoni, A., Zadorozhny, K., Kilkenny, M., Techer, H., Baldi, G., Shen, R., Ciccia, A., Pellegrini, L.*, et al.* (2017b). Smarcal1-Mediated Fork Reversal Triggers Mre11-Dependent Degradation of Nascent DNA in the Absence of Brca2 and Stable Rad51 Nucleofilaments. Mol Cell.

Kowalczykowski, S.C. (2015). An Overview of the Molecular Mechanisms of Recombinational DNA Repair. Cold Spring Harb Perspect Biol *7*.

Kraakman-van der Zwet, M., Overkamp, W.J., van Lange, R.E., Essers, J., van Duijn-Goedhart, A., Wiggers, I., Swaminathan, S., van Buul, P.P., Errami, A., Tan, R.T.*, et al.* (2002). Brca2 (XRCC11) deficiency results in radioresistant DNA synthesis and a higher frequency of spontaneous deletions. Mol Cell Biol *22*, 669-679.

Kreuzer, K.N. (2013). DNA damage responses in prokaryotes: regulating gene expression, modulating growth patterns, and manipulating replication forks. Cold Spring Harbor perspectives in biology *5*, a012674.

Krishnamoorthy, A., Jackson, J., Mohamed, T., Adolph, M., Vindigni, A., and Cortez, D. (2021). RADX prevents genome instability by confining replication fork reversal to stalled forks. Mol Cell *81*, 3007-3017 e3005.

Lawrence, M.S., Stojanov, P., Mermel, C.H., Robinson, J.T., Garraway, L.A., Golub, T.R., Meyerson, M., Gabriel, S.B., Lander, E.S., and Getz, G. (2014). Discovery and saturation analysis of cancer genes across 21 tumour types. Nature *505*, 495-501.

Lemacon, D., Jackson, J., Quinet, A., Brickner, J.R., Li, S., Yazinski, S., You, Z., Ira, G., Zou, L., Mosammaparast, N.*, et al.* (2017). MRE11 and EXO1 nucleases degrade reversed forks and elicit MUS81-dependent fork rescue in BRCA2-deficient cells. Nat Commun *8*, 860.

Leuzzi, G., Marabitti, V., Pichierri, P., and Franchitto, A. (2016). WRNIP1 protects stalled forks from degradation and promotes fork restart after replication stress. EMBO J *35*, 1437-1451.

Lim, D.S., and Hasty, P. (1996). A mutation in mouse rad51 results in an early embryonic lethal that is suppressed by a mutation in p53. Mol Cell Biol *16*, 7133-7143.

Lin, J.R., Zeman, M.K., Chen, J.Y., Yee, M.C., and Cimprich, K.A. (2011). SHPRH and HLTF act in a damage-specific manner to coordinate different forms of postreplication repair and prevent mutagenesis. Mol Cell *42*, 237-249.

Liu, J., Sneeden, J., and Heyer, W.D. (2011). In vitro assays for DNA pairing and recombination-associated DNA synthesis. Methods Mol Biol *745*, 363-383.

Liu, W., Krishnamoorthy, A., Zhao, R., and Cortez, D. (2020). Two replication fork remodeling pathways generate nuclease substrates for distinct fork protection factors. Science Advances *6*, eabc3598.

Liu, W., Zhou, M., Li, Z., Li, H., Polaczek, P., Dai, H., Wu, Q., Liu, C., Karanja, K.K., Popuri, V.*, et al.* (2016). A Selective Small Molecule DNA2 Inhibitor for Sensitization of Human Cancer Cells to Chemotherapy. EBioMedicine *6*, 73-86.

Lo, T., Pellegrini, L., Venkitaraman, A.R., and Blundell, T.L. (2003). Sequence fingerprints in BRCA2 and RAD51: implications for DNA repair and cancer. DNA Repair (Amst) *2*, 1015-1028.
Lord, C.J., and Ashworth, A. (2017). PARP inhibitors: Synthetic lethality in the clinic. Science *355*, 1152-1158.

Lorenz, A., Osman, F., Folkyte, V., Sofueva, S., and Whitby, M.C. (2009). Fbh1 limits Rad51-dependent recombination at blocked replication forks. Mol Cell Biol *29*, 4742-4756.

Luo, K., Li, L., Li, Y., Wu, C., Yin, Y., Chen, Y., Deng, M., Nowsheen, S., Yuan, J., and Lou, Z. (2016). A phosphorylation-deubiquitination cascade regulates the BRCA2-RAD51 axis in homologous recombination. Genes Dev *30*, 2581-2595.

Lusetti, S.L., and Cox, M.M. (2002). The bacterial RecA protein and the recombinational DNA repair of stalled replication forks. Annu Rev Biochem *71*, 71-100.

Ma, C.J., Gibb, B., Kwon, Y., Sung, P., and Greene, E.C. (2017). Protein dynamics of human RPA and RAD51 on ssDNA during assembly and disassembly of the RAD51 filament. Nucleic Acids Res *45*, 749-761.

Malacaria, E., Pugliese, G.M., Honda, M., Marabitti, V., Aiello, F.A., Spies, M., Franchitto, A., and Pichierri, P. (2019). Rad52 prevents excessive replication fork reversal and protects from nascent strand degradation. Nat Commun *10*, 1412.

Manosas, M., Perumal, S.K., Bianco, P., Ritort, F., Benkovic, S.J., and Croquette, V. (2013). RecG and UvsW catalyse robust DNA rewinding critical for stalled DNA replication fork rescue. Nat Commun *4*, 2368.

Manosas, M., Perumal, S.K., Croquette, V., and Benkovic, S.J. (2012). Direct observation of stalled fork restart via fork regression in the T4 replication system. Science *338*, 1217-1220.

Margalef, P., Kotsantis, P., Borel, V., Bellelli, R., Panier, S., and Boulton, S.J. (2018). Stabilization of Reversed Replication Forks by Telomerase Drives Telomere Catastrophe. Cell *172*, 439-453 e414.

Marians, K.J. (2018). Lesion Bypass and the Reactivation of Stalled Replication Forks. Annu Rev Biochem *87*, 217-238.

Mason, A.C., Rambo, R.P., Greer, B., Pritchett, M., Tainer, J.A., Cortez, D., and Eichman, B.F. (2014). A structure-specific nucleic acid-binding domain conserved among DNA repair proteins. Proc Natl Acad Sci U S A.

Mason, J.M., Chan, Y.L., Weichselbaum, R.W., and Bishop, D.K. (2019). Non-enzymatic roles of human RAD51 at stalled replication forks. Nat Commun *10*, 4410.

Masson, J.Y., Tarsounas, M.C., Stasiak, A.Z., Stasiak, A., Shah, R., McIlwraith, M.J., Benson, F.E., and West, S.C. (2001). Identification and purification of two distinct complexes containing the five RAD51 paralogs. Genes Dev *15*, 3296-3307.

Masuda, Y., Suzuki, M., Kawai, H., Hishiki, A., Hashimoto, H., Masutani, C., Hishida, T., Suzuki, F., and Kamiya, K. (2012). En bloc transfer of polyubiquitin chains to PCNA in vitro is mediated by two different human E2-E3 pairs. Nucleic Acids Res *40*, 10394-10407.

Masuda-Ozawa, T., Hoang, T., Seo, Y.S., Chen, L.F., and Spies, M. (2013). Single-molecule sorting reveals how ubiquitylation affects substrate recognition and activities of FBH1 helicase. Nucleic Acids Res *41*, 3576-3587.

Matsuzaki, K., Kondo, S., Ishikawa, T., and Shinohara, A. (2019). Human RAD51 paralogue SWSAP1 fosters RAD51 filament by regulating the anti-recombinase FIGNL1 AAA+ ATPase. Nat Commun *10*, 1407.

McGlynn, P., and Lloyd, R.G. (2000). Modulation of RNA polymerase by (p)ppGpp reveals a RecG-dependent mechanism for replication fork progression. Cell *101*, 35-45.

Mijic, S., Zellweger, R., Chappidi, N., Berti, M., Jacobs, K., Mutreja, K., Ursich, S., Ray Chaudhuri, A., Nussenzweig, A., Janscak, P*., et al.* (2017). Replication fork reversal triggers fork degradation in BRCA2-defective cells. Nat Commun *8*, 859.

Mine, J., Disseau, L., Takahashi, M., Cappello, G., Dutreix, M., and Viovy, J.L. (2007). Real-time measurements of the nucleation, growth and dissociation of single Rad51-DNA nucleoprotein filaments. Nucleic Acids Res *35*, 7171-7187.

Moinova, H.R., Chen, W.D., Shen, L., Smiraglia, D., Olechnowicz, J., Ravi, L., Kasturi, L., Myeroff, L., Plass, C., Parsons, R*., et al.* (2002). HLTF gene silencing in human colon cancer. Proc Natl Acad Sci U S A *99*, 4562-4567.

Moldovan, G.L., Dejsuphong, D., Petalcorin, M.I., Hofmann, K., Takeda, S., Boulton, S.J., and D'Andrea, A.D. (2012). Inhibition of Homologous Recombination by the PCNA-Interacting Protein PARI. Molecular cell *45*, 75-86.

Morrison, C., Shinohara, A., Sonoda, E., Yamaguchi-Iwai, Y., Takata, M., Weichselbaum, R.R., and Takeda, S. (1999). The essential functions of human Rad51 are independent of ATP hydrolysis. Mol Cell Biol *19*, 6891-6897.

Motegi, A., Liaw, H.J., Lee, K.Y., Roest, H.P., Maas, A., Wu, X., Moinova, H., Markowitz, S.D., Ding, H., Hoeijmakers, J.H*., et al.* (2008). Polyubiquitination of proliferating cell nuclear antigen by HLTF and SHPRH prevents genomic instability from stalled replication forks. Proc Natl Acad Sci U S A *105*, 12411-12416.

Mouron, S., Rodriguez-Acebes, S., Martinez-Jimenez, M.I., Garcia-Gomez, S., Chocron, S., Blanco, L., and Mendez, J. (2013). Repriming of DNA synthesis at stalled replication forks by human PrimPol. Nat Struct Mol Biol *20*, 1383-1389.

Mukherjee, C., Tripathi, V., Manolika, E.M., Heijink, A.M., Ricci, G., Merzouk, S., de Boer, H.R., Demmers, J., van Vugt, M., and Ray Chaudhuri, A. (2019). RIF1 promotes replication fork protection and efficient restart to maintain genome stability. Nat Commun *10*, 3287.

Murphy, A.K., Fitzgerald, M., Ro, T., Kim, J.H., Rabinowitsch, A.I., Chowdhury, D., Schildkraut, C.L., and Borowiec, J.A. (2014). Phosphorylated RPA recruits PALB2 to stalled DNA replication forks to facilitate fork recovery. J Cell Biol *206*, 493-507.

Neelsen, K.J., Chaudhuri, A.R., Follonier, C., Herrador, R., and Lopes, M. (2014). Visualization and interpretation of eukaryotic DNA replication intermediates in vivo by electron microscopy. Methods Mol Biol *1094*, 177-208.

Neelsen, K.J., and Lopes, M. (2015). Replication fork reversal in eukaryotes: from dead end to dynamic response. Nat Rev Mol Cell Biol *16*, 207-220.

Nieminuszczy, J., Broderick, R., Bellani, M.A., Smethurst, E., Schwab, R.A., Cherdyntseva, V., Evmorfopoulou, T., Lin, Y.L., Minczuk, M., Pasero, P.*, et al.* (2019). EXD2 Protects Stressed Replication Forks and Is Required for Cell Viability in the Absence of BRCA1/2. Mol Cell *75*, 605-619 e606.

Nomme, J., Takizawa, Y., Martinez, S.F., Renodon-Corniere, A., Fleury, F., Weigel, P., Yamamoto, K., Kurumizaka, H., and Takahashi, M. (2008). Inhibition of filament formation of human Rad51 protein by a small peptide derived from the BRC-motif of the BRCA2 protein. Genes Cells *13*, 471-481.

O'Connor, M.J. (2015). Targeting the DNA Damage Response in Cancer. Mol Cell *60*, 547-560.

O'Donnell, L., Panier, S., Wildenhain, J., Tkach, J.M., Al-Hakim, A., Landry, M.C., Escribano-Diaz, C., Szilard, R.K., Young, J.T., Munro, M.*, et al.* (2010). The MMS22L-TONSL complex mediates recovery from replication stress and homologous recombination. Mol Cell *40*, 619-631.

Ozcelik, H., Schmocker, B., Di Nicola, N., Shi, X.H., Langer, B., Moore, M., Taylor, B.R., Narod, S.A., Darlington, G., Andrulis, I.L.*, et al.* (1997). Germline BRCA2 6174delT mutations in Ashkenazi Jewish pancreatic cancer patients [letter]. Nat Genet *16*, 17-18.

Panzarino, N.J., Krais, J.J., Cong, K., Peng, M., Mosqueda, M., Nayak, S.U., Bond, S.M., Calvo, J.A., Doshi, M.B., Bere, M.*, et al.* (2021). Replication Gaps Underlie BRCA Deficiency and Therapy Response. Cancer Res *81*, 1388-1397.

Paoletti, F., El-Sagheer, A.H., Allard, J., Brown, T., Dushek, O., and Esashi, F. (2020). Molecular flexibility of DNA as a key determinant of RAD51 recruitment. EMBO J *39*, e103002.

Park, J.S., Choi, E., Lee, S.H., Lee, C., and Seo, Y.S. (1997). A DNA helicase from Schizosaccharomyces pombe stimulated by single-stranded DNA-binding protein at low ATP concentration. J Biol Chem *272*, 18910-18919.

Parplys, A.C., Seelbach, J.I., Becker, S., Behr, M., Wrona, A., Jend, C., Mansour, W.Y., Joosse, S.A., Stuerzbecher, H.W., Pospiech, H.*, et al.* (2015). High levels of RAD51 perturb DNA replication elongation and cause unscheduled origin firing due to impaired CHK1 activation. Cell Cycle *14*, 3190-3202.

Paull, T.T., and Gellert, M. (1998). The 3' to 5' exonuclease activity of Mre 11 facilitates repair of DNA double-strand breaks. Mol Cell *1*, 969-979.

Pazin, M.J., and Kadonaga, J.T. (1997). SWI2/SNF2 and related proteins: ATP-driven motors that disrupt protein-DNA interactions? Cell *88*, 737-740.

Piwko, W., Mlejnkova, L.J., Mutreja, K., Ranjha, L., Stafa, D., Smirnov, A., Brodersen, M.M., Zellweger, R., Sturzenegger, A., Janscak, P.*, et al.* (2016). The MMS22L-TONSL heterodimer directly promotes RAD51-dependent recombination upon replication stress. EMBO J *35*, 2584-2601.

Poole, L.A., Zhao, R., Glick, G.G., Lovejoy, C.A., Eischen, C.M., and Cortez, D. (2015). SMARCAL1 maintains telomere integrity during DNA replication. Proc Natl Acad Sci U S A *112*, 14864-14869.

Prakash, S., Johnson, R.E., and Prakash, L. (2005). Eukaryotic translesion synthesis DNA polymerases: specificity of structure and function. Annu Rev Biochem *74*, 317-353.

Qi, Z., Redding, S., Lee, J.Y., Gibb, B., Kwon, Y., Niu, H., Gaines, W.A., Sung, P., and Greene, E.C. (2015). DNA sequence alignment by microhomology sampling during homologous recombination. Cell *160*, 856-869.

Qiu, Y., Antony, E., Doganay, S., Koh, H.R., Lohman, T.M., and Myong, S. (2013). Srs2 prevents Rad51 filament formation by repetitive motion on DNA. Nat Commun *4*, 2281.

Quinet, A., Lemacon, D., and Vindigni, A. (2017). Replication Fork Reversal: Players and Guardians. Mol Cell *68*, 830-833.

Quinet, A., Tirman, S., Jackson, J., Svikovic, S., Lemacon, D., Carvajal-Maldonado, D., Gonzalez-Acosta, D., Vessoni, A.T., Cybulla, E., Wood, M.*, et al.* (2020). PRIMPOL-Mediated Adaptive Response Suppresses Replication Fork Reversal in BRCA-Deficient Cells. Mol Cell *77*, 461-474 e469.

Raderschall, E., Stout, K., Freier, S., Suckow, V., Schweiger, S., and Haaf, T. (2002). Elevated levels of Rad51 recombination protein in tumor cells. Cancer Res *62*, 219-225.

Ragone, S., Maman, J.D., Furnham, N., and Pellegrini, L. (2008). Structural basis for inhibition of homologous recombination by the RecX protein. EMBO J *27*, 2259-2269.

Ray Chaudhuri, A., Callen, E., Ding, X., Gogola, E., Duarte, A.A., Lee, J.E., Wong, N., Lafarga, V., Calvo, J.A., Panzarino, N.J.*, et al.* (2016). Replication fork stability confers chemoresistance in BRCA-deficient cells. Nature *535*, 382-387.

Richardson, C., Stark, J.M., Ommundsen, M., and Jasin, M. (2004). Rad51 overexpression promotes alternative double-strand break repair pathways and genome instability. Oncogene *23*, 546-553.

Ristic, D., Modesti, M., van der Heijden, T., van Noort, J., Dekker, C., Kanaar, R., and Wyman, C. (2005). Human Rad51 filaments on double- and single-stranded DNA: correlating regular and irregular forms with recombination function. Nucleic Acids Res *33*, 3292-3302.

Rondinelli, B., Gogola, E., Yucel, H., Duarte, A.A., van de Ven, M., van der Sluijs, R., Konstantinopoulos, P.A., Jonkers, J., Ceccaldi, R., Rottenberg, S.*, et al.* (2017). EZH2 promotes degradation of stalled replication forks by recruiting MUS81 through histone H3 trimethylation. Nat Cell Biol *19*, 1371-1378.

Rossi, S.E., Foiani, M., and Giannattasio, M. (2018). Dna2 processes behind the fork long ssDNA flaps generated by Pif1 and replication-dependent strand displacement. Nat Commun *9*, 4830.

Roux, K.J., Kim, D.I., Raida, M., and Burke, B. (2012). A promiscuous biotin ligase fusion protein identifies proximal and interacting proteins in mammalian cells. J Cell Biol *196*, 801-810.

Roy, U., Kwon, Y., Marie, L., Symington, L., Sung, P., Lisby, M., and Greene, E.C. (2021). The Rad51 paralog complex Rad55-Rad57 acts as a molecular chaperone during homologous recombination. Mol Cell *81*, 1043-1057 e1048.

Saeki, H., Siaud, N., Christ, N., Wiegant, W.W., van Buul, P.P., Han, M., Zdzienicka, M.Z., Stark, J.M., and Jasin, M. (2006). Suppression of the DNA repair defects of BRCA2-deficient cells with heterologous protein fusions. Proc Natl Acad Sci U S A *103*, 8768-8773.

Sakofsky, C.J., and Malkova, A. (2017). Break induced replication in eukaryotes: mechanisms, functions, and consequences. Crit Rev Biochem Mol Biol *52*, 395-413.

Saldivar, J.C., Cortez, D., and Cimprich, K.A. (2017). The essential kinase ATR: ensuring faithful duplication of a challenging genome. Nat Rev Mol Cell Biol *18*, 622-636.

Sarbajna, S., and West, S.C. (2014). Holliday junction processing enzymes as guardians of genome stability. Trends Biochem Sci *39*, 409-419.

Schlacher, K., Christ, N., Siaud, N., Egashira, A., Wu, H., and Jasin, M. (2011). Double-Strand Break Repair-Independent Role for BRCA2 in Blocking Stalled Replication Fork Degradation by MRE11. Cell *145*, 529-542.

Schlacher, K., Wu, H., and Jasin, M. (2012). A distinct replication fork protection pathway connects Fanconi anemia tumor suppressors to RAD51-BRCA1/2. Cancer Cell *22*, 106-116.

Schoenfeld, A.R., Apgar, S., Dolios, G., Wang, R., and Aaronson, S.A. (2004). BRCA2 is ubiquitinated in vivo and interacts with USP11, a deubiquitinating enzyme that exhibits prosurvival function in the cellular response to DNA damage. Mol Cell Biol *24*, 7444-7455.

Schubert, L., Ho, T., Hoffmann, S., Haahr, P., Guerillon, C., and Mailand, N. (2017). RADX interacts with single-stranded DNA to promote replication fork stability. EMBO Rep *18*, 1991-2003.

Sears, R.M., May, D.G., and Roux, K.J. (2019). BioID as a Tool for Protein-Proximity Labeling in Living Cells. Methods Mol Biol *2012*, 299-313.

Sebesta, M., Cooper, C.D.O., Ariza, A., Carnie, C.J., and Ahel, D. (2017). Structural insights into the function of ZRANB3 in replication stress response. Nat Commun *8*, 15847.

Sharan, S.K., Morimatsu, M., Albrecht, U., Lim, D.S., Regel, E., Dinh, C., Sands, A., Eichele, G., Hasty, P., and Bradley, A. (1997). Embryonic lethality and radiation hypersensitivity mediated by Rad51 in mice lacking Brca2. Nature *386*, 804-810.

Shima, H., Suzuki, H., Sun, J., Kono, K., Shi, L., Kinomura, A., Horikoshi, Y., Ikura, T., Ikura, M., Kanaar, R*., et al.* (2013). Activation of the SUMO modification system is required for the accumulation of RAD51 at sites of DNA damage. J Cell Sci *126*, 5284-5292.

Shin, D.S., Pellegrini, L., Daniels, D.S., Yelent, B., Craig, L., Bates, D., Yu, D.S., Shivji, M.K., Hitomi, C., Arvai, A.S*., et al.* (2003). Full-length archaeal Rad51 structure and mutants: mechanisms for RAD51 assembly and control by BRCA2. EMBO J *22*, 4566-4576.

Shivji, M.K., Davies, O.R., Savill, J.M., Bates, D.L., Pellegrini, L., and Venkitaraman, A.R. (2006). A region of human BRCA2 containing multiple BRC repeats promotes RAD51-mediated strand exchange. Nucleic Acids Res *34*, 4000-4011.

Short, J.M., Liu, Y., Chen, S., Soni, N., Madhusudhan, M.S., Shivji, M.K., and Venkitaraman, A.R. (2016). High-resolution structure of the presynaptic RAD51 filament on single-stranded DNA by electron cryo-microscopy. Nucleic Acids Res *44*, 9017-9030.

Siaud, N., Barbera, M.A., Egashira, A., Lam, I., Christ, N., Schlacher, K., Xia, B., and Jasin, M. (2011). Plasticity of BRCA2 function in homologous recombination: genetic interactions of the PALB2 and DNA binding domains. PLoS Genet *7*, e1002409.

Simandlova, J., Zagelbaum, J., Payne, M.J., Chu, W.K., Shevelev, I., Hanada, K., Chatterjee, S., Reid, D.A., Liu, Y., Janscak, P.*, et al.* (2013). FBH1 helicase disrupts RAD51 filaments in vitro and modulates homologous recombination in mammalian cells. J Biol Chem *288*, 34168-34180.

Sogo, J.M., Lopes, M., and Foiani, M. (2002). Fork reversal and ssDNA accumulation at stalled replication forks owing to checkpoint defects. Science *297*, 599-602.

Spirek, M., Mlcouskova, J., Belan, O., Gyimesi, M., Harami, G.M., Molnar, E., Novacek, J., Kovacs, M., and Krejci, L. (2018). Human RAD51 rapidly forms intrinsically dynamic nucleoprotein filaments modulated by nucleotide binding state. Nucleic Acids Res *46*, 3967-3980.

Stark, J.M., Hu, P., Pierce, A.J., Moynahan, M.E., Ellis, N., and Jasin, M. (2002). ATP hydrolysis by mammalian RAD51 has a key role during homology-directed DNA repair. J Biol Chem *277*, 20185-20194.

Su, F., Mukherjee, S., Yang, Y., Mori, E., Bhattacharya, S., Kobayashi, J., Yannone, S.M., Chen, D.J., and Asaithamby, A. (2014). Nonenzymatic role for WRN in preserving nascent DNA strands after replication stress. Cell Rep *9*, 1387-1401.

Subramanyam, S., Ismail, M., Bhattacharya, I., and Spies, M. (2016). Tyrosine phosphorylation stimulates activity of human RAD51 recombinase through altered nucleoprotein filament dynamics. Proc Natl Acad Sci U S A *113*, E6045-E6054.

Symington, L.S. (2014). End resection at double-strand breaks: mechanism and regulation. Cold Spring Harb Perspect Biol *6*.

Taglialatela, A., Alvarez, S., Leuzzi, G., Sannino, V., Ranjha, L., Huang, J.W., Madubata, C., Anand, R., Levy, B., Rabadan, R.*, et al.* (2017). Restoration of Replication Fork Stability in BRCA1- and BRCA2-Deficient Cells by Inactivation of SNF2-Family Fork Remodelers. Mol Cell *68*, 414-430 e418.

Taylor, M.R.G., Spirek, M., Jian Ma, C., Carzaniga, R., Takaki, T., Collinson, L.M., Greene, E.C., Krejci, L., and Boulton, S.J. (2016). A Polar and Nucleotide-Dependent Mechanism of Action for RAD51 Paralogs in RAD51 Filament Remodeling. Mol Cell *64*, 926-939.

Taylor, M.R.G., and Yeeles, J.T.P. (2018). The Initial Response of a Eukaryotic Replisome to DNA Damage. Mol Cell *70*, 1067-1080 e1012.

Tennstedt, P., Fresow, R., Simon, R., Marx, A., Terracciano, L., Petersen, C., Sauter, G., Dikomey, E., and Borgmann, K. (2013). RAD51 overexpression is a negative prognostic marker for colorectal adenocarcinoma. Int J Cancer *132*, 2118-2126.

Thada, V., and Cortez, D. (2019). Common motifs in ETAA1 and TOPBP1 required for ATR kinase activation. J Biol Chem *294*, 8395-8402.

Thakar, T., Leung, W., Nicolae, C.M., Clements, K.E., Shen, B., Bielinsky, A.K., and Moldovan, G.L. (2020). Ubiquitinated-PCNA protects replication forks from DNA2-mediated degradation by regulating Okazaki fragment maturation and chromatin assembly. Nat Commun *11*, 2147.

Thangavel, S., Berti, M., Levikova, M., Pinto, C., Gomathinayagam, S., Vujanovic, M., Zellweger, R., Moore, H., Lee, E.H., Hendrickson, E.A.*, et al.* (2015). DNA2 drives processing and restart of reversed replication forks in human cells. J Cell Biol *208*, 545-562.

Thorslund, T., McIlwraith, M.J., Compton, S.A., Lekomtsev, S., Petronczki, M., Griffith, J.D., and West, S.C. (2010). The breast cancer tumor suppressor BRCA2 promotes the specific targeting of RAD51 to single-stranded DNA. Nat Struct Mol Biol *17*, 1263-1265.

Toledo, L.I., Altmeyer, M., Rask, M.B., Lukas, C., Larsen, D.H., Povlsen, L.K., Bekker-Jensen, S., Mailand, N., Bartek, J., and Lukas, J. (2013). ATR prohibits replication catastrophe by preventing global exhaustion of RPA. Cell *155*, 1088-1103.

Tombline, G., and Fishel, R. (2002). Biochemical characterization of the human RAD51 protein. I. ATP hydrolysis. J Biol Chem *277*, 14417-14425.

Tonzi, P., Yin, Y., Lee, C.W.T., Rothenberg, E., and Huang, T.T. (2018). Translesion polymerase kappa-dependent DNA synthesis underlies replication fork recovery. Elife *7*.

Unk, I., Hajdu, I., Blastyak, A., and Haracska, L. (2010). Role of yeast Rad5 and its human orthologs, HLTF and SHPRH in DNA damage tolerance. DNA Repair (Amst) *9*, 257-267.

Unk, I., Hajdu, I., Fatyol, K., Hurwitz, J., Yoon, J.H., Prakash, L., Prakash, S., and Haracska, L. (2008). Human HLTF functions as a ubiquitin ligase for proliferating cell nuclear antigen polyubiquitination. Proc Natl Acad Sci U S A *105*, 3768-3773.

Vasianovich, Y., Altmannova, V., Kotenko, O., Newton, M.D., Krejci, L., and Makovets, S. (2017). Unloading of homologous recombination factors is required for restoring double-stranded DNA at damage repair loci. EMBO J *36*, 213-231.

Vispe, S., Cazaux, C., Lesca, C., and Defais, M. (1998). Overexpression of Rad51 protein stimulates homologous recombination and increases resistance of mammalian cells to ionizing radiation. Nucleic Acids Res *26*, 2859-2864.

Vujanovic, M., Krietsch, J., Raso, M.C., Terraneo, N., Zellweger, R., Schmid, J.A., Taglialatela, A., Huang, J.W., Holland, C.L., Zwicky, K.*, et al.* (2017). Replication Fork Slowing and Reversal upon DNA Damage Require PCNA Polyubiquitination and ZRANB3 DNA Translocase Activity. Mol Cell *67*, 882-890 e885.

Waddell, N., Arnold, J., Cocciardi, S., da Silva, L., Marsh, A., Riley, J., Johnstone, C.N., Orloff, M., Assie, G., Eng, C.*, et al.* (2010). Subtypes of familial breast tumours revealed by expression and copy number profiling. Breast Cancer Res Treat *123*, 661-677.

Wang, A.T., Kim, T., Wagner, J.E., Conti, B.A., Lach, F.P., Huang, A.L., Molina, H., Sanborn, E.M., Zierhut, H., Cornes, B.K.*, et al.* (2015). A Dominant Mutation in Human RAD51 Reveals Its

Function in DNA Interstrand Crosslink Repair Independent of Homologous Recombination. Mol Cell *59*, 478-490.

Waters, L.S., Minesinger, B.K., Wiltrout, M.E., D'Souza, S., Woodruff, R.V., and Walker, G.C. (2009). Eukaryotic translesion polymerases and their roles and regulation in DNA damage tolerance. Microbiol Mol Biol Rev *73*, 134-154.

Weston, R., Peeters, H., and Ahel, D. (2012). ZRANB3 is a structure-specific ATP-dependent endonuclease involved in replication stress response. Genes Dev *26*, 1558-1572.

Wright, W.D., Shah, S.S., and Heyer, W.D. (2018). Homologous recombination and the repair of DNA double-strand breaks. J Biol Chem *293*, 10524-10535.

Xia, J., Chen, L.T., Mei, Q., Ma, C.H., Halliday, J.A., Lin, H.Y., Magnan, D., Pribis, J.P., Fitzgerald, D.M., Hamilton, H.M.*, et al.* (2016). Holliday junction trap shows how cells use recombination and a junction-guardian role of RecQ helicase. Sci Adv *2*, e1601605.

Xia, J., Mei, Q., and Rosenberg, S.M. (2019). Tools To Live By: Bacterial DNA Structures Illuminate Cancer. Trends in genetics : TIG *35*, 383-395.

Xu, J., Zhao, L., Xu, Y., Zhao, W., Sung, P., and Wang, H.W. (2017a). Cryo-EM structures of human RAD51 recombinase filaments during catalysis of DNA-strand exchange. Nat Struct Mol Biol *24*, 40-46.

Xu, S., Wu, X., Wu, L., Castillo, A., Liu, J., Atkinson, E., Paul, A., Su, D., Schlacher, K., Komatsu, Y.*, et al.* (2017b). Abro1 maintains genome stability and limits replication stress by protecting replication fork stability. Genes Dev *31*, 1469-1482.

Xue, C., Molnarova, L., Steinfeld, J.B., Zhao, W., Ma, C., Spirek, M., Kaniecki, K., Kwon, Y., Belan, O., Krejci, K.*, et al.* (2021). Single-molecule visualization of human RECQ5 interactions with single-stranded DNA recombination intermediates. Nucleic Acids Res *49*, 285-305.

Yazinski, S.A., Comaills, V., Buisson, R., Genois, M.M., Nguyen, H.D., Ho, C.K., Todorova Kwan, T., Morris, R., Lauffer, S., Nussenzweig, A.*, et al.* (2017). ATR inhibition disrupts rewired homologous recombination and fork protection pathways in PARP inhibitor-resistant BRCA-deficient cancer cells. Genes Dev *31*, 318-332.

Yoshioka, K., Yumoto-Yoshioka, Y., Fleury, F., and Takahashi, M. (2003). pH- and salt-dependent self-assembly of human Rad51 protein analyzed as fluorescence resonance energy transfer between labeled proteins. J Biochem *133*, 593-597.

Yuan, J., Ghosal, G., and Chen, J. (2009). The annealing helicase HARP protects stalled replication forks. Genes Dev *23*, 2394-2399.

Yuan, J., Ghosal, G., and Chen, J. (2012). The HARP-like domain-containing protein AH2/ZRANB3 binds to PCNA and participates in cellular response to replication stress. Mol Cell *47*, 410-421.

Yusufzai, T., and Kadonaga, J.T. (2008). HARP is an ATP-driven annealing helicase. Science *322*, 748-750.

Yusufzai, T., and Kadonaga, J.T. (2010). Annealing helicase 2 (AH2), a DNA-rewinding motor with an HNH motif. Proc Natl Acad Sci U S A *107*, 20970-20973.

Yusufzai, T., Kong, X., Yokomori, K., and Kadonaga, J.T. (2009). The annealing helicase HARP is recruited to DNA repair sites via an interaction with RPA. Genes Dev *23*, 2400-2404.

Zadorozhny, K., Sannino, V., Belan, O., Mlcouskova, J., Spirek, M., Costanzo, V., and Krejci, L. (2017). Fanconi-Anemia-Associated Mutations Destabilize RAD51 Filaments and Impair Replication Fork Protection. Cell Rep *21*, 333-340.

Zellweger, R., Dalcher, D., Mutreja, K., Berti, M., Schmid, J.A., Herrador, R., Vindigni, A., and Lopes, M. (2015). Rad51-mediated replication fork reversal is a global response to genotoxic treatments in human cells. J Cell Biol *208*, 563-579.

Zeman, M.K., and Cimprich, K.A. (2014). Causes and consequences of replication stress. Nat Cell Biol *16*, 2-9.

Zhang, H., Schaub, J.M., and Finkelstein, I.J. (2020). RADX condenses single-stranded DNA to antagonize RAD51 loading. Nucleic Acids Res *48*, 7834-7843.